Simon Benjamin Hollweger, BSc

Optimizing Interface Polymorph Growth Using Optimal Control Theory

MASTER'S THESIS

to achieve the university degree of

Diplom-Ingenieur

Master's degree programme:
Technical Physics

submitted to

Graz University of Technology

Supervisor

Assoc. Prof. Dipl.-Ing. Dr.techn. Oliver T. Hofmann
Institute of Solid State Physics

Co-Supervisor

Dipl.-Ing. Anna Werkovits, BSc

Graz, January 2023

AFFIDAVIT

I declare that I have authored this thesis independently, that I have not used other than the declared sources/resources, and that I have explicitly indicated all material which has been quoted either literally or by content from the sources used. The text document uploaded to TUGRAZonline is identical to the present master's thesis.

Date, Signature

Abstract

Physical properties of organic-inorganic interfaces are mainly determined by the formed structure of the organic molecules on the surface of an inorganic material. Dependent on the arrangement of the molecules physical properties can change quite a lot, for example, the work function of the interface. Organic-inorganic interfaces can form a huge number of different polymorphs. For technical applications, usually specific interface structures are more desirable than others because of some superior properties. But it can happen that those high-performance polymorphs are not the energetically most favorable ones. To be able to form structures that are unfavorable in a thermodynamic picture we need to bring the system out of thermodynamic equilibrium by changing temperature and pressure in the system. At these new thermodynamic conditions, the system starts to equilibrate to a new structure with the lowest Gibbs free energy. During this equilibration process the system can form new metastable interface structures which we then can try to trap by bringing the thermodynamic conditions in to a region where the new structure is more stable. This leads to the idea that we can control the structure of an interface system with time dependent temperature and pressure protocols. If we know the kinetic transition network of such an interface polymorph system we can use Optimal Control theory to find optimal temperature and pressure curves to maximize the concentration of a specific interface polymorph.

Kurzfassung

Physikalische Eigenschaften von organisch-anorganischen Grenzflächen werden hauptsächlich durch die gebildete Struktur der organischen Moleküle auf der Oberfläche eines anorganischen Materials bestimmt. Abhängig von der Anordnung der Moleküle können sich physikalische Eigenschaften stark ändern, beispielsweise die Austrittsarbeit eines Elektrons an der Grenzfläche. Organisch-anorganische Grenzflächen können eine Vielzahl unterschiedlicher Polymorphe bilden. Für technische Anwendungen sind bestimmte Grenzflächenstrukturen normalerweise besser geeignet als andere. Normalerweise sind diese Hochleistungspolymorphe aber nicht die energetisch günstigsten. Um thermodynamisch ungünstige Strukturen bilden zu können, müssen wir das System aus dem thermodynamischen Gleichgewicht bringen, indem wir Temperatur und Druck im System verändern. Bei diesen neuen thermodynamischen Bedingungen beginnt das System, sich zu einer neuen Struktur mit der niedrigsten freien Gibbs-Energie umzuformen. Während dieses Umformungssprozesses kann das System neue metastabile Grenzflächenstrukturen bilden, die wir dann versuchen können zu stabilisieren, indem wir die thermodynamischen Bedingungen in einen Bereich bringen, in der die neue Struktur stabiler ist. Dies führt zu der Idee, dass wir die Struktur einer Grenzfläche mit zeitabhängigen Temperatur- und Druckprotokollen steuern können. Wenn wir das kinetische Übergangsnetzwerk eines solchen polymorphen Grenzflächensystems kennen, können wir die Theorie der optimalen Steuerung verwenden, um optimale Temperatur- und Druckkurven zu finden, um die Konzentration eines speziellen Grenzflächenpolymorphs zu maximieren.

Acknowledgements

I would like to acknowledge all the people who helped me and guided me through the process of writing this thesis. First and foremost, I want to thank my supervisor Oliver T. Hofmann, for all the guidance, support and feedback he gave me.
The same holds for my co-supervisor Anna Werkovits. Thank you for all the enlightening discussions, the help you provided and for prove reading this thesis.
I also want to give my deepest appreciation to all members of the OTH group. Thank you, Lukas, Johannes, Fabio, Anna, Bernhard, Elias and Richard for all the fruitful discussions and advice you gave me. There was never a boring day at university with you guys. Special thanks to Richard for prove reading the math sections.
Thanks of course to my parents Susanne and Franz for their great support.
Finally, thank you Maria for all the times you motivated me, told me to take a break when I needed one badly, and for your caring support in general.

Contents

1. Introduction **1**
- 1.1. Motivation . . . 1
- 1.2. Interface Polymorphism . . . 1
- 1.3. Ab-initio thermodynamics . . . 2
  - 1.3.1. Chemical potential . . . 5
- 1.4. Transition rates . . . 6

2. Kinetics of a polymorph system **9**
- 2.1. Polymorph transition system . . . 9
  - 2.1.1. State equation . . . 9
  - 2.1.2. Accuracy of the state equation . . . 12
  - 2.1.3. Example system . . . 13
- 2.2. Accessibility of polymorphs . . . 15

3. Optimal control theory **19**
- 3.1. Mathematical framework . . . 19
  - 3.1.1. Performance measure . . . 19
  - 3.1.2. Augmented functional . . . 20
  - 3.1.3. Necessary conditions for optimality . . . 21
  - 3.1.4. Performance measure with a control derivative . . . 25
- 3.2. Numerical solution technique . . . 26
- 3.3. Optimization algorithms . . . 28
  - 3.3.1. Gradient descent . . . 28
  - 3.3.2. BFGS optimization . . . 29

4. Optimal control of a polymorph transition system **33**
- 4.1. Unconstrained optimal control . . . 33
  - 4.1.1. Analytical discussion . . . 34
  - 4.1.2. Analytical discussion: Two control variables . . . 38
- 4.2. Constrained optimal control . . . 41

5. Results **45**
- 5.1. Two polymorph system unconstrained . . . 46
  - 5.1.1. Analytical solution . . . 48
  - 5.1.2. Numerical solution with gradient descent . . . 51
- 5.2. Two polymorph system constrained . . . 54
- 5.3. Three polymorph system . . . 56
- 5.4. Three-polymorph system - "Elevator polymorph" problem . . . 66

6. Conclusions and Outlook **71**

References **75**

A. Appendix **77**
A.1. Chemical potential of tetracyanoethylene TCNE 77
A.2. BFGS update formula 78
A.3. Two state example: Sufficient condition for a minimum 81

1. Introduction

1.1. Motivation

Properties of materials are usually characterized by the spatial geometry of the individual atoms of the material. For example, a material with only one chemical compound can have very different physical properties based on its structure. A very famous example of this are the different phases of pure carbon. Carbon can occur in solid form as graphite or diamond. These two materials have very different mechanical, thermal, optical and electronic properties. For technical applications, some phases or polymorphs of a material are of more interest because of their superior properties compared to others. For example the hardness of diamond is much bigger than the one of graphite. The challenge is how we can force a system to form a specific structure with the desired properties for a technical application. In a thermodynamic picture, usually the structure with the lowest energy is formed. A requirement for this is thermodynamic equilibrium. This is not necessarily the case for many systems. For example, diamond would not be observed at room temperature and atmospheric pressure if solid carbon would be in thermodynamic equilibrium. The energy of the graphite structure is lower than the one of diamond at normal conditions. Diamond is actually a metastable phase of carbon at normal conditions but the transition rate to form graphite is so slow that this transition will never be observed in a human lifetime. [1]
This leads to the idea that we can trap a system in a specific structure by changing thermodynamic quantities like temperature and pressure. We can utilize this feature to control the structure of a system. The main goal is to find the optimal temperature and pressure curves that transform a material into the desired structure.
To actually find those curves we need to understand how the energy of a system changes with temperature and pressure and how the transition rates from one structure to another can be calculated.

1.2. Interface Polymorphism

Polymorphism is also present for interface structures where two different materials are in contact with each other. In this thesis, we investigate interfaces between metals and organic materials. Those systems are relevant for technical applications in the field of organic semiconductors for example. Interfaces between metallic contacts and the active organic material usually determine the efficiency of these organic semiconductor devices [2, 3].
The properties of organic-inorganic interfaces are usually mainly determined by the first

few molecular layers, where the first layer is the most important one. Usually the first molecular monolayer of a system already reflects the main properties of an interface. For preliminary studies we can simplify the interface system to a model of a monolayer of organic molecules adsorbed on top of a metal surface. For real technical applications one still need to consider the transition to a molecular bulk phase.
The molecules in this monolayer can arrange in a huge number of different ways [4]. Each of those possible polymorphs gives the interface different properties and some of them have better properties for technical applications than others. In the example of tetracyanoethylene (TCNE) molecules adsorbed on a Copper (111) surface the work function of this interface can change up to 3 eV between different polymorphs [5]. In Figure 1.1 two different polymorphs of the TCNE - Cu(111) system are shown where the molecules are adsorbed in a lying and standing configuration.

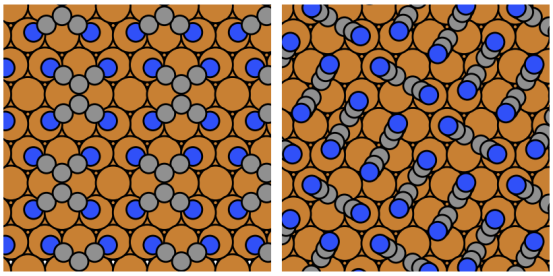

Figure 1.1.: Two different polymorphs of TCNE on a Copper (111) surface [6].

To actually find which polymorphs can be formed by the system we need to evaluate its potential energy surface. We need to vary the positions $\vec{R}_i$ of the atoms in the system and calculate for each geometry its energy. This will give us a function $E(\vec{R}_i)$ for the potential energy surface (PES). A local minimum of the PES represents a possible stable surface structure of the molecules. The evaluation of the PES is computationally very expensive and is usually done by density functional theory (DFT).

1.3. Ab-initio thermodynamics

In a thermodynamic picture, the structure with the lowest Gibbs free energy is formed. The question is now, how we can use the zero temperature energies of the density functional theory calculation and extend it to conditions at finite temperatures and pressures.
First, we need to find an expression for the total Gibbs free energy G of a metal in contact with a molecular gas. We can find that the total Gibbs free energy G consists of

a contribution from the metal bulk G_{solid}, the molecular gas G_{gas} and the contribution of the interface between the two phases ΔG_{surf} [7].

$$G = G_{solid} + G_{gas} + \Delta G_{surf} \tag{1.1}$$

If we divide this expression by the total surface area A and transform Equation 1.1 to express ΔG_{surf} we find

$$\gamma = \frac{\Delta G_{surf}}{A} = \frac{1}{A}(G - G_{solid} - G_{gas}) \tag{1.2}$$

where γ is the surface free energy per unit area.

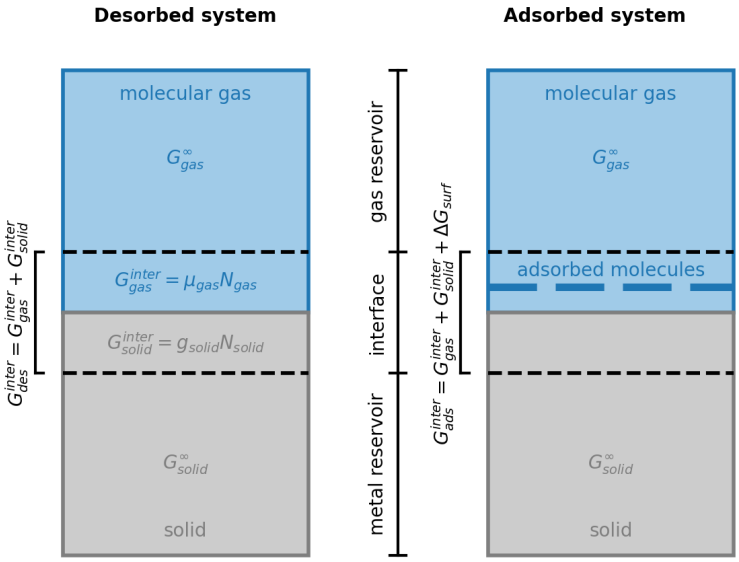

Figure 1.2.: Comparison of the desorbed and adsorbed system. Here we can see that the Gibbs free energies of the reservoirs cancels out and only the Gibbs free energies close to the interface are relevant. The difference of the Gibbs free energies of the interface regions G^{inter}_{des} and G^{inter}_{ads} gives the surface contribution ΔG_{surf}.

At large distances from the interface the system becomes homogeneous and is not influenced by the surface anymore which means that regions far away from the surface cancels out in Equation 1.2 and the only relevant region for the Gibbs free energy contribution of the surface ΔG_{surf} is the one close to the interface. In Figure 1.2 the region close to the interface is indicated by a dashed line. The total Gibbs free energy of this smaller interface region is then

$$G^{inter}_{ads}(T, p, N_{gas}, N_{solid}) = \underbrace{G^{inter}_{gas}(T, p, N_{gas})}_{\mu_{gas}(T,p)N_{gas}} + \underbrace{G^{inter}_{solid}(T, p, N_{solid})}_{g_{solid}(T,p)N_{solid}} + \Delta G_{surf} \tag{1.3}$$

where G_{gas}^{inter} and G_{solid}^{inter} are the Gibbs free energy contributions of the gas molecules and the substrate atoms in the interface region, N_{gas} are the number of molecules and N_{solid} the number of substrate atoms in the surface region.
In Equation 1.3 we introduced the Gibbs free energy of a metal atom g_{solid} in the homogeneous bulk and the chemical potential μ_{gas} of a molecule in an homogeneous gas which are dependent on temperature T and pressure p. We can rewrite Equation 1.3 and divide by the total area A and find the surface free energy

$$\gamma = \frac{1}{A}\left[G_{ads}^{inter}(T,p,N_{gas},N_{solid}) - g_{solid}(T,p)N_{solid} - \mu_{gas}(T,p)N_{gas}\right] \tag{1.4}$$

We can compare the surface free energy γ with the surface free energy of the clean surface γ_{clean} where we do not have a molecular gas in the system.

$$\gamma_{clean} = \frac{1}{A}\left[G_{ads}^{inter}(T,p,N_{gas}=0,N_{solid}) - g_{solid}(T,p)N_{solid}\right] \tag{1.5}$$

The difference of the two we call the surface Gibbs free energy of adsorption γ_{ads}

$$\begin{aligned}\gamma_{ads}(T,p) &= \gamma(T,p,N_{gas},N_{solid}) - \gamma_{clean}(T,p,N_{gas}=0,N_{solid}) \\ &= \frac{1}{A}[\underbrace{G_{ads}^{inter}(T,p,N_{gas},N_{solid}) - G_{ads}^{inter}(T,p,N_{gas}=0,N_{solid})}_{\Delta G_{ads}} - \mu_{gas}(T,p)N_{gas}]\end{aligned} \tag{1.6}$$

In general the Gibbs free energy can be calculated with

$$G = E_{tot} + F_{vib} + F_{conf} + pV \tag{1.7}$$

where E_{tot} is the total internal energy, F_{vib} the vibrational free energy, F_{conf} the configurational free energy, p the pressure and V the volume of the system [7]. If we look at differences of Gibbs free energies like in the case of the Gibbs free energy of adsorption ΔG_{ads} it can be often approximated only by the total internal energy evaluated with a density functional theory calculation and neglect all other terms. The argumentation why this approximation is often valid can be looked up in [7, 8].
This means the surface free energy of adsorption can be approximated with the expression

$$\gamma_{ads}(T,p) = \frac{1}{A}[E_{ads} - \mu_{gas}(T,p)N_{gas}] \tag{1.8}$$

where E_{ads} is the difference between the internal energy of the surface with the adsorbed molecules and the clean surface. We only consider the adsorbed molecules on the surface and do not include any gas phase molecules in our calcualtions which means that N_{gas} is the number of adsorbed molecules.
With this findings we are now able to predict which polymorph is predominantly formed on a metal surface in contact with a molecular gas. We can evaluate with density functional theory the adsorption energies E_{ads} of possible polymorphs and the coverage

$\theta = \frac{N_{gas}}{A}$. The chemical potential μ_{gas} is determined with an ideal gas approximation. The polymorph with the lowest surface free energy γ_{ads} is the most likely formed polymorph in a thermodynamic picture.

1.3.1. Chemical potential

The chemical potential of a molecular gas can be described with an ideal gas model at temperature T and pressure p and turns out to be [7, 9]

$$\mu_{gas}(T,p) = -\frac{1}{N}\left(k_B T \ln\left(Q_{gas}^{tot}\right) - pV\right) \tag{1.9}$$

where N is the number of indistinguishable molecules in the volume V. To evaluate this expression we need to calculate the partition function Q_{gas}^{tot}.

$$Q_{gas}^{tot} = \frac{1}{N!}(q^{trans}q^{rot}q^{vib}q^{electr}q^{nucl})^N \tag{1.10}$$

It consists of a translational, rotational, vibrational, electronic and a nuclei contribution. If we insert the expression for the partition function into Equation 1.9 we get a sum of contributions instead of a product and we can write

$$\mu_{gas} = \mu^{trans} + \mu^{rot} + \mu^{vib} + \mu^{electr} + \mu^{nucl} \tag{1.11}$$

where we put $\frac{1}{N!}$ and pV into the translational contribution μ^{trans}. The detailed derivation of these chemical potential contributions can be looked up in [7]. In summary we find

$$\mu^{trans} = -k_B T \ln\left(\left(\frac{2\pi m}{h^2}\right)^{\frac{3}{2}} \frac{(k_B T)^{\frac{5}{2}}}{p}\right) \tag{1.12}$$

$$\mu_{rot} = -k_B T \ln\left(\frac{\sqrt{\pi \prod_{i=1}^{3} I_i}}{\sigma}\left(\frac{8\pi^2 k_B T}{h^2}\right)^{\frac{3}{2}}\right) \tag{1.13}$$

$$\mu_{vib} = k_B T \sum_i \left(\ln\left(1 - e^{-\frac{\hbar\omega_i^{vib}}{k_B T}}\right) + \frac{1}{2}\hbar\omega_i^{vib}\right) \tag{1.14}$$

$$\mu_{electr} = E_{gas}^{tot} - k_B T \ln(J) \tag{1.15}$$

$$\mu_{nucl} = 0 \quad \text{(neglected)} \tag{1.16}$$

m ... total mass of molecule

h ... Planck constant

$\hbar$ ... reduced Planck constant

k_B ... Boltzmann constant

I_i ... moments of inertia of the molecule

σ ... symmetry number of the molecule (number of indistinguishable orientations)

ω_i ... harmonic vibrational modes of the molecule

E_{gas}^{tot} ... total internal energy of one molecule in gas phase

J ... spin degeneracy of the molecule in its ground state

Since we neglected the vibrational contribution to the Gibbs free energy we also neglect it for the chemical potential, otherwise we would introduce a systematic error in calculating the surface free energy γ_{ads}. We can also neglect the nuclei contribution since in chemical processes the state of the nucleus changes almost never. We find then for the chemical potential of an ideal molecular gas

$$\mu_{gas} \approx E_{gas}^{tot} - k_B T \ln \left(\left(\frac{2\pi m}{h^2} \right)^{\frac{3}{2}} \frac{(k_B T)^{\frac{5}{2}}}{p} \frac{\sqrt{\pi \prod_{i=1}^{3} I_i}}{\sigma} \left(\frac{8\pi^2 k_B T}{h^2} \right)^{\frac{3}{2}} J \right) \tag{1.17}$$

In the appendix A.1 this approximation is evaluated for the tetracyanoethylene (TCNE) molecule. This molecule will be used later in an example in Chapter 5 for evaluating the chemical potential.

1.4. Transition rates

To understand kinetic processes of polymorphs we need to find a way how to calculate or approximate transition rates. They should describe how fast a polymorph at given thermodynamic conditions would transform into another polymorph.

One way to do this is using Transition State theory [10, 11]. A naive approach would be to find a polymorph transition state (saddle point of the potential energy surface) which would introduce a Gibbs free energy barrier $\Delta G^{\ddagger}$ between two distinct polymorphs. With this energy barrier we can approximate the transition rate k with the Arrhenius rate equation of the form

$$k = f_a e^{-\frac{\Delta G^{\ddagger}}{k_B T}}. \tag{1.18}$$

Here f_a is an exponential prefactor which is also known as attempt frequency [11, 12], k_B is the Boltzmann constant an T is the temperature.

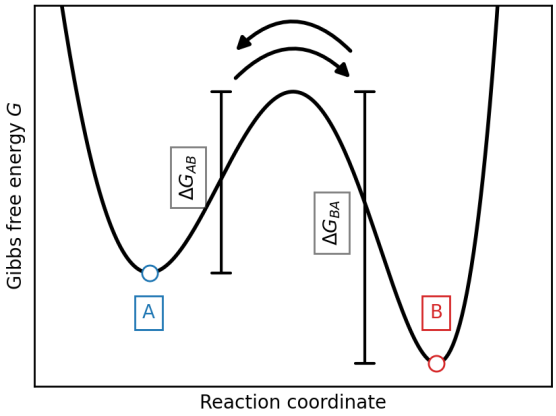

Figure 1.3.: Transition rate between two polymorphs are determined by the energy barriers ΔG_{AB} and ΔG_{BA} separating the two phases

The problem with this approach is that we can not assume that there is only one dominant transition state between two polymorphs. In reality this transition process is a multistage process where individual molecules start to change positions and orientations and start a global phase transition in the system.
To simulate the system more realistically we would need to look at these individual transition processes of the molecules on the surface. One technique to efficiently simulate such kinetic systems are Kinetic Monte Carlo (KMC) methods [13–15]. To apply this technique one need to know the transition rates for the different processes of the molecules on the surface. They can be effectively determined with Transition State theory [10–12]. In the case of TCNE on Copper (111), single molecule transitions are calculated for example in [16]. By randomly choosing those individual processes weighted by their probability one can simulate the dynamics of the formation process of a new phase and extract the transition rate out of the simulation.
However, these simulations are computationally still very expensive. We would need to repeat them for different temperatures and pressures to get a temperature and pressure dependence of the transition rates. Therefore we will stick to the assumption that we can express the transition rate via the Arrhenius equation. With that we require that there exists one single global transition state between two polymorph phases. As already mentioned above this is not the case since we have to deal with multiple single molecule transitions and not a single global transition. But if we assume that the real transition rates have the same exponential behaviour with temperature as the Arrhenius equation 1.18 then this assumption is justified. We just need to find an energy barrier $\Delta G^{\ddagger}$ which represents this complicated molecular multi stage process.
We assume that this artificial energy barrier $\Delta G^{\ddagger}$ behaves like a difference between two Gibbs free energies of a finite interface system with area A.

$$\begin{aligned} \Delta G^{\ddagger} &= A(\gamma^{\ddagger}_{ads} - \gamma_{ads}) = [E^{\ddagger}_{ads} - \mu_{gas} N^{\ddagger}_{gas}] - [E_{ads} - \mu_{gas} N_{gas}] = \\ &= (E^{\ddagger}_{ads} - E_{ads}) - \mu_{gas}(N_{gas} - N^{\ddagger}_{gas}) = \Delta E_{ads} - \mu_{gas} \Delta N_{gas} \end{aligned} \tag{1.19}$$

Here $\gamma_{ads}^{\ddagger}$ is the surface free energy of the transition polymorph.
With this energy barrier we can formulate the temperature and pressure dependent transition rates with

$$k(T,p) = f_a e^{-\frac{\Delta G^{\ddagger}}{k_B T}} = f_a e^{-\frac{\Delta E_{ads}^{\ddagger} - \mu_{gas}(T,p)\Delta N_{gas}^{\ddagger}}{k_B T}} \tag{1.20}$$

You can see here that we need to approximate the barrier of the adsorption energy of the transition polymorph and the starting polymorph $\Delta E_{ads}^{\ddagger}$ and the difference between the molecule numbers $\Delta N_{gas}^{\ddagger}$.
These transition rates $k(T,p)$ can be now used to describe the time evolution of polymorph concentrations in a system dependent on temperature T and pressure p.

2. Kinetics of a polymorph system

2.1. Polymorph transition system

In order to describe the transition dynamics of our polymorph system we need to find an underlying physical model. This model should describe the change of the polymorph concentrations over time. For this we first need some basic transition rates between two distinct polymorphs. How to calculate those transition rates is described in Chapter 1.4. Independent of the theory for calculating transition rates, in the end you get an expression $k(\vec{u})$ for the rates which depends on some external system parameters combined in the vector $\vec{u}$. Some examples for such system parameters are the temperature T and the pressure p of the system. Usually the transition rates have the form of an exponential $e^{-\frac{\Delta G^{\ddagger}(T,p)}{k_B T}}$ where $\Delta G^{\ddagger}$ is some kind of energy barrier which the system has to overcome to do a transition. Here we can clearly see that with increasing temperature also the transition rate increases exponentially, which means the dynamics of the system is highly dependent on temperature T. The dependence on other external parameters, like the pressure p, is incorporated in the energy barrier $\Delta G^{\ddagger}(T,p)$ itself.

2.1.1. State equation

Assuming we are able to calculate individual transition rates between two polymorphs we can begin to build up a transition network between multiple polymorphs. For this we think of the system as a graph network where each node represents a polymorph in the system and all polymorphs are connected via edges which represent the transition between two polymorphs (see Figure 2.1).
Mathematically this graph network can be described by a two dimensional matrix $K \in \mathbb{R}^{N\times N}$. The component k_{ij} of the matrix K is the transition rate from polymorph i to polymorph j and the diagonal elements k_{ii} of K are zero.

$$K = \begin{pmatrix} 0 & k_{12} & k_{13} & \dots \\ k_{21} & 0 & k_{23} & \\ k_{31} & k_{32} & 0 & \\ \vdots & & & \ddots \end{pmatrix} \tag{2.1}$$

The Arrhenius equation 1.18 is used to calculate transition rates. This means a component in the matrix K is defined as

$$k_{ij} = \begin{cases} i \neq j : f_a e^{-\frac{\Delta G_{ij}}{k_B T}} \\ i = j : 0 \end{cases} \tag{2.2}$$

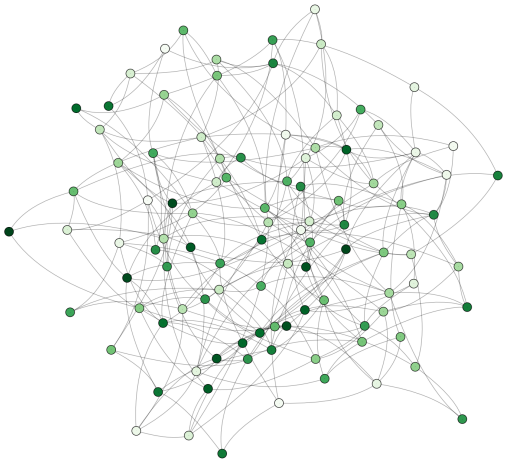

Figure 2.1.: Graph representation of a polymorph transition system. Each node represents a possible polymorph of the system. Each edge represents an allowed transition.

where f_a is the constant attempt frequency, ΔG_{ij} is the energy barrier between polymorph i to polymorph j. Notice that the energy barrier matrix G_{ij} is not symmetric. The energy barrier in direction $i \to j$ is not the same as $j \to i$. Through out this thesis we assume that the attempt frequency is the same for every transition even though in real systems it can slightly differ. The transition rate matrix K depends on the system parameters $\vec{u}$ as explained before.

$$K = K(\vec{u}) \tag{2.3}$$

The current concentrations of the polymorphs in the system can be described by a state vector $\vec{y}$ where each component y_i represents the relative concentration of a polymorph in the system.

$$\vec{y} = \begin{pmatrix} y_1 \\ y_2 \\ \vdots \end{pmatrix} \tag{2.4}$$

A component y_i of the concentration vector is the ratio between the occupied area A_i of this polymorph and the total area A_{total}.

$$y_i = \frac{A_i}{A_{total}} \tag{2.5}$$

Since the total concentration in the system needs to be one, the sum of the vector components of $\vec{y}$ needs to sum up to one.

$$\sum_i y_i = 1 \tag{2.6}$$

With these definitions we can start to construct an equation which describes the time evolution of the polymorph concentrations in the system. For this we construct a simple balance equation where we calculate the change in concentration of a polymorph after a time step Δt. Also note that the system parameter $\vec{u}(t)$ is now dependent on time t which corresponds to a change in temperature and pressure with passing time.

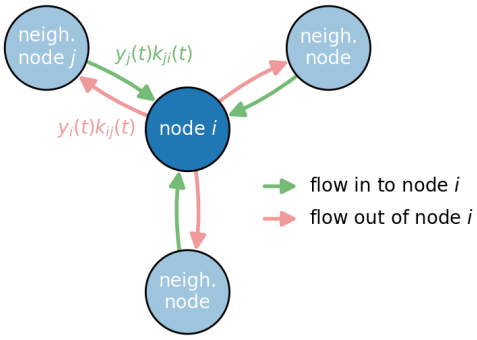

Figure 2.2.: Concentration flow of the i^{th} polymorph in the system.

$$y_i(t+\Delta t) = y_i(t) + \Bigg[\underbrace{-\sum_{j=1}^{N} y_i(t)\ k_{ij}(\vec{u}(t))}_{\text{flow out of node } i} + \underbrace{\sum_{j=1}^{N} k_{ji}(\vec{u}(t))\ y_j(t)}_{\text{flow in to node } i}\Bigg]\Delta t \tag{2.7}$$

The term in squared brackets is the net change of the concentration of polymorph i after time step Δt. This term consists of the flow in and out of the representative node in the graph for polymorph i. In Figure 2.2 the flow in and out of the i^{th} polymorph node is illustrated. The absolute flow rate at time t is the product of the transition rate k and the current concentration of the polymorph in the system at time t. Now we can transform the equation to a difference equation.

$$\frac{y_i(t+\Delta t) - y_i(t)}{\Delta t} = \left[-\sum_{j=1}^{N} y_i(t)\ k_{ij}(\vec{u}(t)) + \sum_{j=1}^{N} k_{ji}(\vec{u}(t))\ y_j(t)\right] \tag{2.8}$$

If we do the limit $\Delta t \to 0$ we find our underlying state equation of our polymorph system.

$$\frac{d}{dt}y_i = \left[-\sum_{j=1}^{N} y_i(t)\ k_{ij}(\vec{u}(t)) + \sum_{j=1}^{N} k_{ji}(\vec{u}(t))\ y_j(t)\right] \tag{2.9}$$

To get rid of the clumsy component notation we can write the equation in matrix notation. We can see that the first term in the squared bracket with the minus sign in front is simply a diagonal matrix K_D and the second term is the transition rate matrix K times the transposed state vector $\vec{y}$

$$\dot{\vec{y}}^T = \vec{y}^T(t) \underbrace{\begin{pmatrix} -\sum_j k_{1j}(\vec{u}(t)) & 0 & 0 & \dots \\ 0 & -\sum_j k_{2j}(\vec{u}(t)) & 0 & \\ 0 & 0 & -\sum_j k_{3j}(\vec{u}(t)) & \\ \vdots & & & \ddots \end{pmatrix}}_{K_D(\vec{u}(t))} + \vec{y}^T(t) K(\vec{u}(t)) \tag{2.10}$$

The state equation has now the form

$$\dot{\vec{y}}^T = \vec{y}^T(t)\ A(\vec{u}(t)) \tag{2.11}$$

with

$$\begin{aligned} A(\vec{u}(t)) &= K_D(\vec{u}(t)) + K(\vec{u}(t)) = \\ &= \begin{pmatrix} -\sum_j k_{1j}(\vec{u}(t)) & k_{12}(\vec{u}(t)) & k_{13}(\vec{u}(t)) & \dots \\ k_{21}(\vec{u}(t)) & -\sum_j k_{2j}(\vec{u}(t)) & k_{23}(\vec{u}(t)) & \\ k_{31}(\vec{u}(t)) & k_{32}(\vec{u}(t)) & -\sum_j k_{3j}(\vec{u}(t)) & \\ \vdots & & & \ddots \end{pmatrix} \end{aligned} \tag{2.12}$$

We can now solve the state equation for a given system parameter protocol $\vec{u}(t)$ for $t \in (0, t_f)$. Usually this differential equation can not be solved in a closed form and only numerical techniques provide solutions for the state trajectory $\vec{y}(t)$.

2.1.2. Accuracy of the state equation

The state equation derived in the previous chapter is a very rough approximation for a polymorph transition system. It assumes that the state can be fully described only by knowing the concentrations of the different polymorphs currently existing on the surface. To be more precise one would also need to account for the spatial distribution of the polymorphs currently existing in the system. It is a difference if there is for example only one single area on the surface where a new polymorph emerges or if there are many small islands growing to form a new polymorph. In the latter case the length of the phase front between the two polymorphs is much longer than in the first case. The growth of a polymorph happens at this phase front and if there are many phase boundaries in the system then there are also bigger absolute growth rates. But in the derivation of the state equation in the previous chapter we weighted the transition rate by the concentration of the starting polymorph and not by the length of the phase front. This results in treating the many small polymorph islands case and the one big single island case exactly the same way, despite they would not behave in the same way kinetically.

But including the spatial distribution in the state equation would complicate the calculation of the time evolution of the concentrations tremendously. There does not exist any easy model which describes such solid state processes with an easy first order differential equation. Therefore we will stick to the simple model where we weight the transition rate by the concentration and not the phase front length and accept this systematic error in the system.

2.1.3. Example system

Consider a two state system where the two states are separated by an energy barrier ΔE_{AB} and ΔE_{BA} (see Figure 2.3).

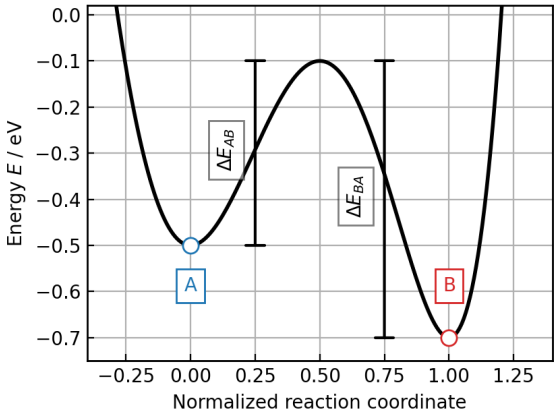

Figure 2.3.: Two polymorph system example with two barriers $\Delta E_{AB} = 0.4\,\mathrm{eV}$ and $\Delta E_{BA} = 0.6\,\mathrm{eV}$

We can calculate the transition rate from one state to another by using the Arrhenius equation.

$$k(T) = f_a e^{-\frac{\Delta E}{k_B T}} \tag{2.13}$$

Here f_a is the attempt frequency, k_B is the Boltzmann constant, T is the temperature and ΔE is the corresponding energy barrier for this transition.
With the help of this equation we can construct the transition matrix of this system and the matrix A for the state equation.

$$K(T) = \begin{pmatrix} 0 & k_{AB}(T) \\ k_{BA}(T) & 0 \end{pmatrix} \tag{2.14}$$

$$A(T) = \begin{pmatrix} -k_{AB}(T) & k_{AB}(T) \\ k_{BA}(T) & -k_{BA}(T) \end{pmatrix} \tag{2.15}$$

The state equation of this example is then

$$\dot{\vec{y}}^T = \vec{y}^T(t)\ A(T(t)) \tag{2.16}$$

The state equation can be simply solved by transforming it to its corresponding integral equation. This can be done by integrating both sides by t.

$$\begin{aligned} \int_0^t \dot{\vec{y}}^T \mathrm{d}t' &= \int_0^t \vec{y}^T(t') A(T(t')) \mathrm{d}t' \\ \vec{y}^T(t) - \vec{y}^T(0) &= \int_0^t \vec{y}^T(t') A(T(t')) \mathrm{d}t' \\ \vec{y}^T(t) &= \vec{y}^T(0) + \int_0^t \vec{y}^T(t') A(T(t')) \mathrm{d}t' \end{aligned} \tag{2.17}$$

To solve the state equation we need to know the initial state $\vec{y}^T(0) = \vec{y}^T_{init}$. Here in this example we use $\vec{y}^T_{init} = (0.95, 0.05)$ meaning that polymorph A has an initial concentration of 95 % and polymorph B 5 %. With some iterative integration scheme we can solve the state equation. In the equation below only the simple Forward Euler integration scheme is used. For more accurate solutions one need to use higher order numerical techniques, like Runge Kutta integration methods [17]. To actually solve the state equation we need to discretize the time domain in N points where the time point at position $n \in \mathbb{N}$ is labeled by t_n and adjacent time points are separated by Δt. We also define $\vec{y}_n = \vec{y}(t_n)$. With this we can find the recursive equation

$$\vec{y}^T_{n+1} = \vec{y}^T_n + \vec{y}^T_n A(T(t_n)) \Delta t \tag{2.18}$$

with the initial condition

$$\vec{y}^T_0 = \vec{y}^T_{init}$$

In Figure 2.4 one can see how the state $\vec{y}(t)$ evolves in time for a specific temperature protocol $T(t)$.

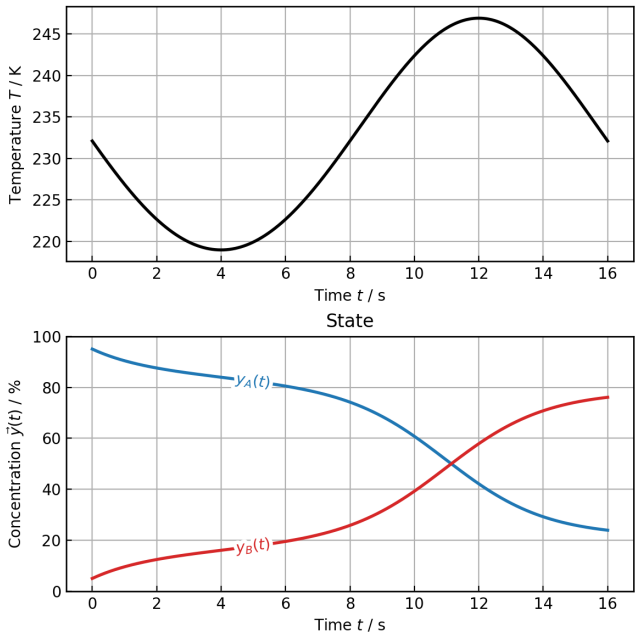

Figure 2.4.: Time evolution of the concentrations y_A and y_B for a sine shaped temperature protocol. The energy barriers are chosen to be $\Delta E_{AB} = 0.4\,\mathrm{eV}$ and $\Delta E_{BA} = 0.6\,\mathrm{eV}$, the pre-exponential factor $f_a = 3 \times 10^7\,\mathrm{s}^{-1}$

2.2. Accessibility of polymorphs

Before we actually start trying to optimize the concentration of a specific polymorph in a polymorph transition network we should think about how accessible a polymorph in such a network is. A naive approach would be to look at the graph representation of the polymorph transition system, like the one in Figure 2.1, and check if the graph is fully connected and can not be reduced into two separated graphs. This means there exists for each polymorph pair a transition path through the graph and every polymorph is accessible. In theory this is true but if we assume for example that one polymorph in this graph has the highest Gibbs free energy for the whole temperature-pressure phase space, then the energy barriers which we need to overcome to reach this unfavorable polymorph are very high and the barriers for leaving it are always lower. This means that the concentration flow out of the unfavorable polymorph is always bigger than in to it. Such a polymorph can only be increased in concentration if we go to very high temperatures. At very high temperatures the difference between forward and backward transition becomes smaller and at infinite temperature they are as close as possible. We can see this very easily with the Arrhenius equation introduced in Chapter 1.4. If the temperature reaches infinity the exponent vanishes and the rate equals the attempt frequency f_a.

$$k = f_a e^{-\frac{\Delta G^{\ddagger}}{k_B T}} \overset{T\to\infty}{=} f_a \tag{2.19}$$

Usually the attempt frequency for a transition is very similar compared to other transitions and through out this thesis we assume that they are equal for every transition in a system. Then in the infinite temperature limit all transition rates are the same and if we wait long enough all concentrations of the polymorphs in the system are the same. For the unfavorable polymorph in the system this is the maximum concentration it can potentially reach. This maximum concentration $y_{T\to\infty} = 1/N$ becomes smaller with increasing system size N, where N is the number of polymorphs.
This example showed us that not all polymorphs can be accessed from another polymorph. There exists polymorphs which can only be maximized by distributing the concentrations uniformly over the system via a very high temperature.
This leads us to a different definition of accessibility of a polymorph in a polymorph transition network.
We look at all edges of the polymorph graph and check if one transition rate is always bigger than the reverse rate for our temperature-pressure phase space. If this is the case only the transition direction with the bigger rate is considered to be relevant for accessibility. If we do this for the whole polymorph graph we find an accessibility graph where edges exist which only have one transition direction. In Figure 2.5 this accessibility check is done for an example network consisting of six polymorphs

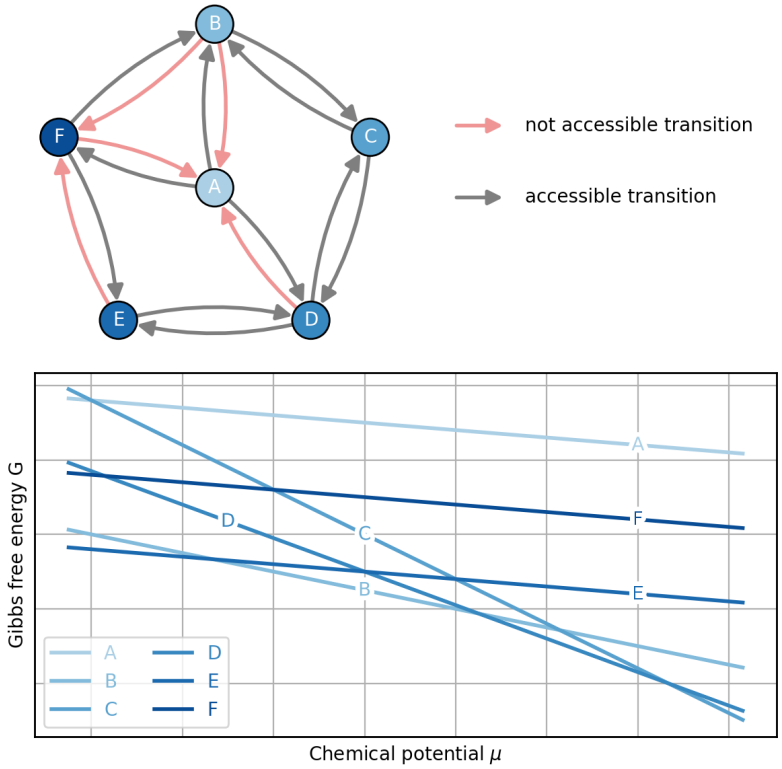

Figure 2.5.: Example graph containing six polymorphs. If we do an accessibility check all the red transition directions are inaccessible, which means they are smaller than their back transition at every point in the considered temperature-pressure phase space. One can see in the Gibbs free energy of two connected polymorphs if they can transform in both directions. If the lines intersect in a point within the considered phase space (chemical potential $\mu(T, p)$) both directions are allowed.

3. Optimal control theory

In this section we follow closely the book of D. Kirk [18] for deriving the mathematical framework of optimal control theory. In the previous chapter we derived a differential equation to describe the system dynamics of a polymorph system. The question now is how we need to change external parameters of the system like temperature and pressure to maximize the concentration of a specific polymorph B in the system. A change in temperature or pressure usually influences the transition rates in the system and therefore you can control the system up to a certain degree.

3.1. Mathematical framework

3.1.1. Performance measure

The dynamics of the system is incorporated in the state equation. This differential equation describes the time evolution of the state vector $\vec{y}(t)$ and has the form

$$\dot{\vec{y}}(t) = \vec{a}(\vec{y}(t), \vec{u}(t), t) \tag{3.1}$$

It consists of the first time derivative of the state vector and the vector valued function $\vec{a}(\vec{y}(t), \vec{u}(t), t)$ which depends on the state vector $\vec{y}(t)$, the control vector $\vec{u}(t)$ and time t. If you compare the general state equation 3.1 with the one we derived in Chapter 2 one can identify $\vec{a}(\vec{y}(t), \vec{u}(t), t) = A^T(\vec{u}(t))\ \vec{y}(t)$.
Further to find the optimal control we need a performance measure J which maps the control function $\vec{u}$ to a real number. The performance measure $J[\vec{u}]$ is a functional which has its minimum at the optimal control $\vec{u}^*$. The performance measure has the general form

$$J[\vec{u}] = h(\vec{y}(t_f), t_f) + \int_0^{t_f} g(\vec{y}(t), \vec{u}(t), t)\ \mathrm{d}t \tag{3.2}$$

where $h(\vec{y}(t_f), t_f)$ is the terminal cost and $g(\vec{y}(t), \vec{u}(t), t)$ are the running costs. We will define these terms for our special problem of polymorphs in the subsequent chapter. However it will be easier to express the terminal cost in integral form assuming h is a differentiable function.

$$h(\vec{y}(t_f), t_f) = \int_0^{t_f} \frac{\mathrm{d}}{\mathrm{d}t} h(\vec{y}(t), t)\ \mathrm{d}t + h(\vec{y}(0), 0) \tag{3.3}$$

With this the performance measure J will look like

$$J[\vec{u}] = \int_0^{t_f} \left\{ g(\vec{y}(t), \vec{u}(t), t) + \frac{\mathrm{d}}{\mathrm{d}t} h(\vec{y}(t), t) \right\} \, \mathrm{d}t \tag{3.4}$$

Here we removed the constant term $h(\vec{y}(0), 0)$ because it will only shift the performance measure by a constant value and does not change the minimum. With using the chain rule for differentiation we will arrive at an expression for the performance measure

$$J[\vec{u}] = \int_0^{t_f} \left\{ g(\vec{y}(t), \vec{u}(t), t) + \left[\frac{\partial h}{\partial \vec{y}} (\vec{y}(t), t) \right]^T \cdot \dot{\vec{y}}(t) + \frac{\partial h}{\partial t} (\vec{y}(t), t) \right\} \, \mathrm{d}t \tag{3.5}$$

The expression $\frac{\partial h}{\partial \vec{y}}$ is the gradient of h where we differentiate with respect to every component of $\vec{y}$.

$$\frac{\partial h}{\partial \vec{y}} = \nabla_{\vec{y}} h(\vec{y}, t) = \begin{pmatrix} \frac{\partial}{\partial y_1} h(\vec{y}, t) \\ \frac{\partial}{\partial y_2} h(\vec{y}, t) \\ \vdots \end{pmatrix}$$

3.1.2. Augmented functional

Until now the derived performance measure J is dependent on the state vector $\vec{y}$ and the control vector $\vec{u}$. We can find pairs of solutions for $\vec{y}$ and $\vec{u}$ which minimizes the performance measure J but completely ignores the fact that the state vector $\vec{y}(t)$ also needs to fulfill the state equation. To incorporate this constraint in the performance measure we can use the technique of Lagrange multipliers. We can simply put the state equation constraint into the integral of the performance measure multiplied by the Lagrange multiplier $\vec{\lambda}(t)$.

$$\begin{aligned} J_a[\vec{u}] = \int_0^{t_f} \Bigg\{ & g(\vec{y}(t), \vec{u}(t), t) + \left[\frac{\partial h}{\partial \vec{y}} (\vec{y}(t), t) \right]^T \cdot \dot{\vec{y}}(t) + \frac{\partial h}{\partial t} (\vec{y}(t), t) + \\ & + \vec{\lambda}^T(t) \left[\vec{a}(\vec{y}(t), \vec{u}(t), t) - \dot{\vec{y}}(t) \right] \Bigg\} \, \mathrm{d}t \end{aligned} \tag{3.6}$$

We define the augmented running cost g_a as

$$\begin{aligned} & g_a(\vec{y}(t), \dot{\vec{y}}(t), \vec{u}(t), \vec{\lambda}(t), t) = \\ & \quad = g(\vec{y}(t), \vec{u}(t), t) + \left[\frac{\partial h}{\partial \vec{y}} (\vec{y}(t), t) \right]^T \cdot \dot{\vec{y}}(t) + \frac{\partial h}{\partial t} (\vec{y}(t), t) + \vec{\lambda}^T(t) \left[\vec{a}(\vec{y}(t), \vec{u}(t), t) - \dot{\vec{y}}(t) \right] \end{aligned} \tag{3.7}$$

so that

$$J_a[\vec{u}] = \int_0^{t_f} g_a(\vec{y}(t), \dot{\vec{y}}(t), \vec{u}(t), \vec{\lambda}(t), t) \, \mathrm{d}t \tag{3.8}$$

By minimizing this new augmented functional J_a we automatically fulfill the constraint of the state equation for the state vector $\vec{y}$. This means since $\vec{y}$ is completely determined by the state equation the only independent variable left is the control function $\vec{u}(t)$.

3.1.3. Necessary conditions for optimality

To derive the necessary conditions for optimal control of the system we need to dive into the theory of calculus of variations. The goal is to find the conditions where the augmented functional J_a is minimal. If we have a maximization problem we can transform it to a minimization problem by using the negative performance measure, which means no new formalism is needed for this kind of problem. This will be important for our special use case of maximizing a specific polymorph.
However finding an extremum of an functional is similar to finding the extremum of a function. For functions we look for the case where the first derivative vanishes. In the case of functionals we will look for extremal curves where the first variation of the functional vanishes. But let us start from the beginning.
We assume that the function $\vec{u}^*(t)$ [1] minimizes the functional J_a. Then we can define the increment ΔJ_a of the functional in the vicinity of the extremal curve by

$$\Delta J_a = J_a[\vec{u}^*(t) + \delta\vec{u}(t)] - J_a[\vec{u}^*(t)] \tag{3.9}$$

The function $\delta\vec{u}(t)$ is called the variation of function $\vec{u}(t)$. If we now insert the expression for the augmented functional from 3.8 in 3.9 we get

$$\begin{aligned}\Delta J_a = &\int_0^{t_f} g_a(\vec{y}^*(t) + \delta\vec{y}(t),\ \dot{\vec{y}}^*(t) + \delta\dot{\vec{y}}(t),\ \vec{u}^*(t) + \delta\vec{u}(t),\ \vec{\lambda}^*(t) + \delta\vec{\lambda}(t),\ t)\ \mathrm{d}t \\ &- \int_0^{t_f} g_a(\vec{y}^*(t),\ \dot{\vec{y}}^*(t),\ \vec{u}^*(t),\ \vec{\lambda}^*(t),\ t)\ \mathrm{d}t\end{aligned}$$

Expanding the integrand expression in a Taylor series around the fixed $(*)$-arguments with using the symbol $(*) = (\vec{y}^*(t),\ \dot{\vec{y}}^*(t),\ \vec{u}^*(t),\ \vec{\lambda}^*(t),\ t)$ will give us

$$\begin{aligned}\Delta J_a = \int_0^{t_f} \Bigg\{ & g_a(*) + \left[\frac{\partial g_a}{\partial \vec{y}}(*)\right]^T \delta\vec{y}(t) + \left[\frac{\partial g_a}{\partial \dot{\vec{y}}}(*)\right]^T \delta\dot{\vec{y}}(t) + \left[\frac{\partial g_a}{\partial \vec{u}}(*)\right]^T \delta\vec{u}(t) \\ & + \left[\frac{\partial g_a}{\partial \vec{\lambda}}(*)\right]^T \delta\vec{\lambda}(t) + [\text{higher order terms}] - g_a(*) \Bigg\} \mathrm{d}t\end{aligned} \tag{3.10}$$

Notice that $\delta\dot{\vec{y}} = \frac{d}{dt}\delta\vec{y}$ which means they are not independent from each other. Using this relation and integration by parts we find for the term with variation $\delta\dot{\vec{y}}$ an expression which only has the variation $\delta\vec{y}$ in it.

[1] All quantites marked with a * are optimal, they minimize or maximize the performance measure.

$$\int_0^{t_f} \left[\frac{\partial g_a}{\partial \dot{\vec{y}}}(*)\right]^T \delta\dot{\vec{y}}(t)\ \mathrm{d}t = \left[\frac{\partial g_a}{\partial \dot{\vec{y}}}(*)\right]^T \delta\vec{y}(t)\Bigg|_0^{t_f} - \int_0^{t_f} \left[\frac{d}{dt}\frac{\partial g_a}{\partial \dot{\vec{y}}}(*)\right]^T \delta\vec{y}(t)\ \mathrm{d}t$$

Since we know the initial state vector at time $t = 0$, the variation of the state vector $\delta\vec{y}$ at $t = 0$ vanishes.

$$\delta\vec{y}(0) = 0$$

This leads to the expression for the increment of the augmented functional

$$\begin{aligned}\Delta J_a = &\left[\frac{\partial g_a}{\partial \dot{\vec{y}}}(*))\right]_{t=t_f}^T \delta\vec{y}(t_f) + \int_0^{t_f}\Bigg\{\left[\frac{\partial g_a}{\partial \vec{y}}(*) - \frac{d}{dt}\frac{\partial g_a}{\partial \dot{\vec{y}}}(*)\right]^T \delta\vec{y}(t)\\ &+ \left[\frac{\partial g_a}{\partial \vec{u}}(*)\right]^T \delta\vec{u}(t) + \left[\frac{\partial g_a}{\partial \vec{\lambda}}(*)\right]^T \delta\vec{\lambda}(t)\Bigg\}\mathrm{d}t + \text{higher order terms}\end{aligned} \tag{3.11}$$

The first variation δJ_a is determined by extracting only the terms of 3.11 which are linear in their variation.

$$\begin{aligned}\delta J_a = &\left[\frac{\partial g_a}{\partial \dot{\vec{y}}}(*))\right]_{t=t_f}^T \delta\vec{y}(t_f) + \int_0^{t_f}\Bigg\{\left[\frac{\partial g_a}{\partial \vec{y}}(*) - \frac{\mathrm{d}}{\mathrm{d}t}\frac{\partial g_a}{\partial \dot{\vec{y}}}(*)\right]^T \delta\vec{y}(t)\\ &+ \left[\frac{\partial g_a}{\partial \vec{u}}(*)\right]^T \delta\vec{u}(t) + \left[\frac{\partial g_a}{\partial \vec{\lambda}}(*)\right]^T \delta\vec{\lambda}(t)\Bigg\}\mathrm{d}t\end{aligned} \tag{3.12}$$

The fundamental theorem of calculus of variations states that δJ_a needs to vanish at the minimum of J_a. For a proof see [18].

$$\delta J_a = 0 \tag{3.13}$$

To make use of the relation 3.12 for the first variation of the augmented functional we will use the fundamental lemma of calculus [19] which states that

$$\int_a^b h(t)\delta x(t)\mathrm{d}t = 0$$

for arbitrary continuous $\delta x(t)$ only if $h(t) = 0$.
All the first variations in Equation 3.12 are independent from each other. The consequence of this is that each term needs to vanish individually. This leads us to the necessary conditions of optimality.

$$
\begin{aligned}
&(i) \quad \frac{\partial g_a}{\partial \dot{\vec{y}}}(*)\bigg|_{t=t_f} = 0 \\
&(ii) \quad \frac{\partial g_a}{\partial \vec{y}}(*) - \frac{d}{dt}\frac{\partial g_a}{\partial \dot{\vec{y}}}(*) = 0 \\
&(iii) \quad \frac{\partial g_a}{\partial \vec{u}}(*) = 0 \\
&(iv) \quad \frac{\partial g_a}{\partial \vec{\lambda}}(*) = 0
\end{aligned}
\tag{3.14}
$$

If we insert the actual expression for g_a from Equation 3.7

$$
\begin{aligned}
g_a(*) = g(\vec{y}^*(t), \vec{u}^*(t), t) + \left[\frac{\partial h}{\partial \vec{y}}(\vec{y}^*(t), t)\right]^T \cdot \dot{\vec{y}}^*(t) + \frac{\partial h}{\partial t}(\vec{y}^*(t), t) \\
+ \vec{\lambda}^{*T}(t) \cdot \left[\vec{a}(\vec{y}^*(t), \vec{u}^*(t), t) - \dot{\vec{y}}^*(t)\right]
\end{aligned}
$$

we find for the necessary conditions:

(i) For $\frac{\partial g_a}{\partial \dot{\vec{y}}}(*)\Big|_{t=t_f} = 0$:

$$
\frac{\partial g_a}{\partial \dot{\vec{y}}}(*)\bigg|_{t=t_f} = \frac{\partial h}{\partial \vec{y}}(\vec{y}^*(t_f), t_f) - \vec{\lambda}^*(t_f) = 0 \quad \Rightarrow \quad \vec{\lambda}^*(t_f) = \frac{\partial h}{\partial \vec{y}}(\vec{y}^*(t_f), t_f) \tag{3.15}
$$

This equation can be seen as the final value of the costate equation which will be derived in the next point.

(ii) For $\frac{\partial g_a}{\partial \vec{y}}(*) - \frac{d}{dt}\frac{\partial g_a}{\partial \dot{\vec{y}}}(*) = 0$:

$$
\begin{aligned}
&\frac{\partial g_a}{\partial \vec{y}}(*) - \frac{d}{dt}\frac{\partial g_a}{\partial \dot{\vec{y}}}(*) = \\
&\quad = \frac{\partial g}{\partial \vec{y}}(\vec{y}^*(t), \vec{u}^*(t), t) + \cancel{\frac{\partial}{\partial \vec{y}}\left[\frac{\partial h}{\partial \vec{y}}\right]^T (\vec{y}^*(t), t) \cdot \dot{\vec{y}}^*(t)} + \cancel{\frac{\partial}{\partial \vec{y}}\frac{\partial h}{\partial t}(\vec{y}^*(t), t)} \\
&\quad + \left[\frac{\partial \vec{a}}{\partial \vec{y}}(\vec{y}^*(t), \vec{u}^*(t), t)\right]^T \cdot \vec{\lambda}^*(t) - \cancel{\frac{\partial}{\partial t}\frac{\partial h}{\partial \vec{y}}(\vec{y}^*(t), t)} \\
&\quad - \cancel{\frac{\partial}{\partial \vec{y}}\left[\frac{\partial h}{\partial \vec{y}}\right]^T (\vec{y}^*(t), t) \cdot \dot{\vec{y}}^*(t)} + \dot{\vec{\lambda}}^*(t) = 0
\end{aligned}
$$

$$
\dot{\vec{\lambda}}^*(t) = -\frac{\partial g}{\partial \vec{y}}(\vec{y}^*(t), \vec{u}^*(t), t) - \left[\frac{\partial \vec{a}}{\partial \vec{y}}(\vec{y}^*(t), \vec{u}^*(t), t)\right]^T \cdot \vec{\lambda}^*(t) \tag{3.16}
$$

This equation is the so called costate equation where we define the Lagrange multiplier $\lambda(t)$ as the costate. The final value for this differential equation is defined in the first necessary condition.

(iii) For $\frac{\partial g_a}{\partial \vec{u}}(*) = 0$:

$$\frac{\partial g_a}{\partial \vec{u}}(*) = \frac{\partial g}{\partial \vec{u}}(\vec{y}^*(t), \vec{u}^*(t), t) + \left[\frac{\partial \vec{a}}{\partial \vec{u}}(\vec{y}^*(t), \vec{u}^*(t), t)\right]^T \cdot \vec{\lambda}^*(t) = 0$$

This equation we will reference to as the control equation. This equation will be used later to numerically find the optimal control function $u^*(t)$

(iv) For $\frac{\partial g_a}{\partial \vec{\lambda}}(*) = 0$:

$$\frac{\partial g_a}{\partial \vec{\lambda}}(*) = \vec{a}(\vec{y}^*(t), \vec{u}^*(t), t) - \dot{\vec{y}}^*(t) = 0 \quad \Rightarrow \quad \dot{\vec{y}}^*(t) = \vec{a}(\vec{y}^*(t), \vec{u}^*(t), t)$$

This equation is the already familiar state equation which needs to be fulfilled by design.

The gradient of the vector function $\frac{\partial \vec{a}}{\partial \vec{y}}$ has to be seen as an outer product of the form

$$\frac{\partial \vec{a}}{\partial \vec{y}} = \begin{pmatrix} \frac{\partial a_1}{\partial y_1} & \frac{\partial a_1}{\partial y_2} & \frac{\partial a_1}{\partial y_3} & \cdots \\ \frac{\partial a_2}{\partial y_1} & \frac{\partial a_2}{\partial y_2} & \frac{\partial a_2}{\partial y_3} & \\ \frac{\partial a_3}{\partial y_1} & \frac{\partial a_3}{\partial y_2} & \frac{\partial a_3}{\partial y_3} & \\ \vdots & & & \ddots \end{pmatrix}$$

same applies for the gradient $\frac{\partial \vec{a}}{\partial \vec{u}}$.
To summarize, the general necessary conditions for optimal control are

(i) Final condition costate equation

$$\vec{\lambda}^*(t_f) = \frac{\partial h}{\partial \vec{y}}(\vec{y}^*(t_f), t_f) \tag{3.17}$$

(ii) Costate equation

$$\dot{\vec{\lambda}}^*(t) = -\frac{\partial g}{\partial \vec{y}}(\vec{y}^*(t), \vec{u}^*(t), t) - \left[\frac{\partial \vec{a}}{\partial \vec{y}}(\vec{y}^*(t), \vec{u}^*(t), t)\right]^T \cdot \vec{\lambda}^*(t) \tag{3.18}$$

(iii) Control equation

$$0 = \frac{\partial g}{\partial \vec{u}}(\vec{y}^*(t), \vec{u}^*(t), t) + \left[\frac{\partial \vec{a}}{\partial \vec{u}}(\vec{y}^*(t), \vec{u}^*(t), t)\right]^T \cdot \vec{\lambda}^*(t) \tag{3.19}$$

(iv) State equation

$$\dot{\vec{y}}^*(t) = \vec{a}(\vec{y}^*(t), \vec{u}^*(t), t) \tag{3.20}$$

In some cases it is convenient to define a function $\mathcal{H}$ called Hamiltonian to simplify the necessary conditions.

$$\mathcal{H}(\vec{y}(t), \vec{u}(t), \vec{\lambda}(t), t) = g(\vec{y}(t), \vec{u}(t), t) + \vec{\lambda}^T(t) \cdot \vec{a}(\vec{y}(t), \vec{u}(t), t) \tag{3.21}$$

With the Hamiltonian $\mathcal{H}$ we can write the necessary conditions in the form

(i) Final condition costate equation

$$\vec{\lambda}^*(t_f) = \frac{\partial h}{\partial \vec{y}}(\vec{y}^*(t_f), t_f) \tag{3.22}$$

(ii) Costate equation

$$\dot{\vec{\lambda}}^*(t) = -\frac{\partial \mathcal{H}}{\partial \vec{y}}(\vec{y}^*(t), \vec{u}^*(t), t) \tag{3.23}$$

(iii) Control equation

$$0 = \frac{\partial \mathcal{H}}{\partial \vec{u}}(\vec{y}^*(t), \vec{u}^*(t), t) \tag{3.24}$$

(iv) State equation

$$\dot{\vec{y}}^*(t) = \frac{\partial \mathcal{H}}{\partial \vec{\lambda}}(\vec{y}^*(t), \vec{u}^*(t), t) \tag{3.25}$$

3.1.4. Performance measure with a control derivative

In some cases the performance measure J is dependent on the first derivative $\dot{\vec{u}}$ of the control vector. For example if we want to penalize optimal controls which vary a lot in time we can add a term of the form $\frac{\gamma}{2}\dot{\vec{u}}^2(t)$ to the performance measure J [20]. This term becomes big for control functions which changes a lot and will shift the minimum of the performance measure to optimal controls which do not vary too much. The parameter γ regularizes this term and can be adjusted to a suitable value for the problem. Generally we find for the performance measure something like

$$J[\vec{u}] = h(\vec{y}(t_f), t_f) + \int_0^{t_f} g(\vec{y}(t), \vec{u}(t), \dot{\vec{u}}(t), t)\mathrm{d}t \tag{3.26}$$

The problem here now is that the integrand g depends on the first time derivative of the control $\dot{\vec{u}}$. This would change the derived necessary conditions in the previous Section 3.1.3. To avoid deriving new necessary conditions we can transform the problem in to the familiar version where no derivative of the control appears [21]. This can be done by introducing a new variable

$$\vec{v}(t) = \dot{\vec{u}}(t) \tag{3.27}$$

which will be the new control variable of the system. The old control variable $\vec{u}$ will be treated now as a state variable and will be merged to a new state vector

$$\hat{\vec{y}} = \begin{pmatrix} \vec{y} \\ \vec{u} \end{pmatrix} \tag{3.28}$$

The modified state equation for this artificial state looks like

$$\dot{\hat{\vec{y}}}(t) = \begin{pmatrix} \vec{a}(\hat{\vec{y}}(t), t) \\ \vec{v}(t) \end{pmatrix} \tag{3.29}$$

With this new quantities we can use the same necessary conditions as derived before with the difference that the control vector is now $\vec{v}$ and not $\vec{u}$ and the state vector is $\hat{\vec{y}}$ not $\vec{y}$.

3.2. Numerical solution technique

In order to solve an optimal control problem the state equation, costate equation and control equation with the corresponding initial conditions needs to be satisfied. If all of those three equations are fulfilled simultaneously we found a stationary point of the performance measure functional. Solving these three coupled equations usually needs numerical techniques. Only in special cases it can be solved analytically.
The usual procedure to solve an optimal control problem are the following steps:

1. Guess the optimal control function $\vec{u}^*(t)$

2. Solve the initial value problem of the state equation using the initial condition for the state vector $\vec{y}(0) = \vec{y}_0$.

3. Solve the final value problem of the costate equation backward in time using the final condition $\vec{\lambda}^*(t_f) = \vec{\lambda}_f$ at final time t_f.

4. Calculate the improvement of the control function by using the control equation and the solutions to the state and costate equations.

5. Calculate the new control function by adding the improvement determined in the previous step. If the change in the control function is still big we start again at step 2 and stop if the calculated improvement is smaller than the defined threshold.

To calculate the improvement for the control function as it is imposed in step 4 we need to have a look at the performance measure functional J_a again. In the derivation of the necessary conditions for optimality we derived an expression for the first variation δJ_a (Equation 3.12) of the performance measure.

$$\delta J_a = \underbrace{\left[\frac{\partial g_a}{\partial \dot{\vec{y}}}\right]^T_{t=t_f}}_{\substack{\text{final condition}\\ \text{of costate}}} \delta\vec{y}(t_f) + \int_0^{t_f} \Bigg\{ \underbrace{\left[\frac{\partial g_a}{\partial \vec{y}} - \frac{\mathrm{d}}{\mathrm{d}t}\frac{\partial g_a}{\partial \dot{\vec{y}}}\right]^T}_{\text{costate equation}} \delta\vec{y}(t) + \underbrace{\left[\frac{\partial g_a}{\partial \vec{u}}\right]^T}_{\text{control equation}} \delta\vec{u}(t) + \underbrace{\left[\frac{\partial g_a}{\partial \vec{\lambda}}\right]^T}_{\text{state equation}} \delta\vec{\lambda}(t) \Bigg\} \mathrm{d}t \tag{3.30}$$

Since we calculated the solution of the state and costate equation for the current control equation $\vec{u}$ in step 2 and 3 the corresponding terms in Equation 3.30 will vanish and the remaining term is only the term of the control equation

$$\delta J_a = \int_0^{t_f} \left[\frac{\partial g_a}{\partial \vec{u}}\right]^T \delta\vec{u}(t)\ \mathrm{d}t \tag{3.31}$$

This expression for the first variation is the linear part of the change of the performance measure functional $\Delta J_a = J_a[\vec{u}(t) + \delta\vec{u}] - J_a[\vec{u}(t)]$. If the change $\delta\vec{u}(t)$ of the control function is small enough, the sign of δJ_a is the same as in ΔJ_a. Since our goal is to maximally reduce the performance measure functional J_a we want to make ΔJ_a negative. If the change $\delta\vec{u}(t)$ is small we can use the first variation δJ_a as approximation for the change ΔJ_a.
We can choose for the change in the control function $\delta\vec{u}(t)$

$$\delta\vec{u}(t) = -\epsilon\frac{\partial g_a}{\partial \vec{u}} \quad \text{with} \quad \epsilon > 0 \tag{3.32}$$

where ϵ is a small step factor which makes sure that $\delta\vec{u}(t)$ is small. We insert it into Equation 3.31 and find for the first variation

$$\delta J_a = -\epsilon \int_0^{t_f} \left[\frac{\partial g_a}{\partial \vec{u}}\right]^T \frac{\partial g_a}{\partial \vec{u}}\ \mathrm{d}t < 0 \tag{3.33}$$

This expression for δJ_a is always negative because the integrand is positive. This shows us that if we change our control function $\vec{u}(t)$ with $\delta\vec{u}(t) = -\epsilon\frac{\partial g_a}{\partial \vec{u}}$ the performance measure functional will always decrease in value or at least stays the same. This means we can find a better control function by adding the variation $\delta\vec{u}(t)$ to it.

$$\vec{u}_{new}(t) = \vec{u}(t) + \delta\vec{u}(t) = \vec{u}(t) - \epsilon\frac{\partial g_a}{\partial \vec{u}} \tag{3.34}$$

If the performance measure functional J_a is bounded from below we will find after some iterations an extremal function $\vec{u}^*(t)$ where the first variation vanishes.

3.3. Optimization algorithms

3.3.1. Gradient descent

The algorithm described in Chapter 3.2 is basically a gradient descent algorithm for functionals.
In the case of a regular function $f : \mathbb{R}^n \to \mathbb{R};\ \vec{x} \mapsto f(\vec{x})$ the gradient descent algorithm goes into the direction of the negative gradient of f because f decreases the most in this direction. The iterative scheme is

$$\vec{x}_{n+1} = \vec{x}_n - \epsilon \nabla f(\vec{x}_n) \Rightarrow f(\vec{x}_{n+1}) \leq f(\vec{x}_n) \tag{3.35}$$

where the step factor ϵ scales the gradient to an appropriate size to make sure, that not too much or enough progress is made during each iteration. If we start at some position $\vec{x}_0$ in the domain of f and do enough iterations the sequence $\{\vec{x}_i\}_{i\in\mathbb{N}}$ is then a descending path to a minimum of f.
To actually apply these technique to our optimal control problem we need to discretize our control function $\vec{u}(t)$ to a time grid. In that way we no longer need to deal with continuous functions but with discrete vectors.

$$\vec{u}(t) \to \vec{u} = \begin{pmatrix} \vec{u}(t_0) \\ \vec{u}(t_1) \\ \vec{u}(t_2) \\ \vdots \\ \vec{u}(t_N) \end{pmatrix} \tag{3.36}$$

We introduced here an equidistant time grid $\{t_i\}_{i\in[1,\dots,N]}$ of size N. Now we can evaluate the discretized correction $\delta\vec{u}$ on this time grid.

$$\delta\vec{u}(t) = -\epsilon \frac{\partial g_a}{\partial \vec{u}}(t) \to \delta\vec{u} = -\epsilon \begin{pmatrix} \frac{\partial g_a}{\partial \vec{u}}(t_0) \\ \frac{\partial g_a}{\partial \vec{u}}(t_1) \\ \frac{\partial g_a}{\partial \vec{u}}(t_2) \\ \vdots \\ \frac{\partial g_a}{\partial \vec{u}}(t_N) \end{pmatrix} = -\epsilon \nabla_{\vec{u}} J_a \tag{3.37}$$

The column vector in this expression can be identified as the gradient of the performance measure $\nabla_{\vec{u}} J_a$. Notice that this identification is only valid because of the discretization performed on the system.
Now we can use the same procedure (Equation 3.35) as in the case of a regular function to iteratively find the minimum of the functional J_a.

$$\vec{u}_{n+1} = \vec{u} - \epsilon \nabla_{\vec{u}} J_a \tag{3.38}$$

The algorithm for solving the optimal control problem numerically described in Chapter 3.2 can be used now on the discretized version of the optimal control problem. This

means we also need to discretize the solution of the state and costate equation to the same time grid $\{t_i\}_{i\in[1,\dots,N]}$.

3.3.2. BFGS optimization

Besides the negative gradient direction, the Newton direction is a very efficient search direction [22]. It can be derived from a second order Taylor expansion for the objective function f at a point $\vec{x}_k$.

$$f(\vec{x}_k + \vec{p}_k) = f_k + \vec{p}_k^T \nabla f_k + \frac{1}{2}\vec{p}_k^T \nabla^2 f_k \vec{p}_k + \text{higher order terms} \tag{3.39}$$

The Newton search direction is the vector $\vec{p}_k$ which minimizes this second order Taylor series. We assume that the hessian $\nabla^2 f_k$ is a positive definite matrix which means $\vec{x}_k$ is in a convex region of f. If it would be negative definite we would start moving towards a maximum instead. To find the Newton direction $\vec{p}_k$ we need to set the gradient with respect to $\vec{p}_k$ of the Taylor expansion to zero.

$$\nabla_{p_k} f(\vec{x}_k + \vec{p}_k) = \nabla f_k + \nabla^2 f_k \ \vec{p}_k \stackrel{!}{=} 0 \tag{3.40}$$

If we rearrange this equation we find for the Newton direction

$$\vec{p}_k = -(\nabla^2 f_k)^{-1} \nabla f_k \tag{3.41}$$

where $(\nabla^2 f_k)^{-1}$ is the inverse of the positive definite hessian matrix. To summarize, we approximate the objective function f with a convex paraboloid at $\vec{x}_k$ by building the second order Taylor expansion. Then we find the minimum of this paraboloid and the direction from our building point $\vec{x}_k$ to the found minimum. This direction $\vec{p}_k$ is a good search direction to find the minimum of f. We can show that $\vec{p}_k$ is a descent direction if the hessian matrix is positive definite. From Equation 3.39 we need to show that $f(\vec{x}_k + \vec{p}_k) - f_k < 0$:

$$f(\vec{x}_k + \vec{p}_k) - f_k = \vec{p}_k^T \nabla f_k + \frac{1}{2}\vec{p}_k^T \nabla^2 f_k \vec{p}_k \tag{3.42}$$

We can insert from Equation 3.40 that $\nabla f_k = -\nabla^2 f_k \vec{p}_k$ and this leads to

$$f(\vec{x}_k + \vec{p}_k) - f_k = -\vec{p}_k^T \nabla^2 f_k \vec{p}_k + \frac{1}{2}\vec{p}_k^T \nabla^2 f_k \vec{p}_k = -\frac{1}{2}\underbrace{\vec{p}_k^T \nabla^2 f_k \vec{p}_k}_{>0} < 0 \tag{3.43}$$

The quadratic term in this expression is positive because of the positive definiteness of $\nabla^2 f_k$. This shows that the Newton direction is indeed a descent direction. If we move along this direction and repeatedly calculate the Newton direction we will end up very quickly in a local minimum of the objective function f.
One problem with this simple approach is that the computation of the inverse hessian matrix is very expensive. To speed up this algorithm we can use a quasi-Newton method like the Broyden-Fletcher-Goldfarb-Shanno (BFGS) algorithm [23–26]. In this method

we approximate the Hessian by a matrix B_k and improve it along the way with the gradient information.
We can compute a new point x_{k+1} with the search direction $\vec{p_k}$ with

$$x_{k+1} = \vec{x} + \alpha_k \vec{p_k} \tag{3.44}$$

where α_k is an appropriate step length determined by the Wolfe conditions [27, 28].
We do again a second order Taylor expansion of the form

$$m_{k+1}(\vec{p}) = f_{k+1} + \vec{p}^T \nabla f_{k+1} + \frac{1}{2}\vec{p}^T B_{k+1}\vec{p} \tag{3.45}$$

where we do not use the exact Hessian but the approximation B_{k+1}.
We should try to approximate B_{k+1} in a way that the gradient of $m_{k+1}(\vec{p})$ at the point $\vec{p} = \vec{x}_k - \vec{x}_{k+1} = -\alpha_k \vec{p_k}$ matches the previous gradient of the objective function ∇f_k.
We obtain

$$\nabla m_{k+1}(-\alpha_k \vec{p_k}) = \nabla f_{k+1} - \alpha_k B_{k+1}\vec{p_k} = \nabla f_k \tag{3.46}$$

after rearranging we find

$$\nabla f_{k+1} - \nabla f_k = \alpha_k B_{k+1}\vec{p_k} \tag{3.47}$$

To simplify notation we define

$$\begin{aligned} \vec{s_k} &= \vec{x}_{k+1} - \vec{x}_k = \alpha_k \vec{p_k} \\ \vec{y_k} &= \nabla f_{k+1} - \nabla f_k \end{aligned} \tag{3.48}$$

Then Equation 3.47 simplifies to the secant equation

$$B_{k+1}\vec{s_k} = \vec{y_k} \tag{3.49}$$

Since for calculating the Newton direction we need the inverse Hessian we can multiply the secant equation 3.49 with the inverse Hessian approximation B_{k+1}^{-1} and find

$$B_{k+1}^{-1}\vec{y_k} = \vec{s_k} \tag{3.50}$$

The goal now is to find a matrix B_{k+1}^{-1} which solves the secant equation 3.50 and is symmetric $B_{k+1}^{-1} = (B_{k+1}^{-1})^T$. There exist infinite solutions because there are only n equations in 3.50 but a symmetric positive matrix has $\frac{1}{2}n(n+1)$ degrees of freedom. The BFGS algorithm tries to find the unique solution which changes the matrix B_{k+1}^{-1} the least compared to the previous matrix B_k^{-1} by employing a weighted Frobenius matrix norm $\|\cdot\|_F$ to measure the change. The Frobenius norm is just the sum of all squared matrix components $\|A\|_F^2 = \sum_i \sum_j a_{ij}^2$.
We try to solve

$$\min_{B_{k+1}^{-1}} \|B_{k+1}^{-1} - B_k^{-1}\|_F \tag{3.51}$$

$$B_{k+1}^{-1}\vec{y_k} = \vec{s_k} \tag{3.52}$$

$$B_{k+1}^{-1} = (B_{k+1}^{-1})^T \tag{3.53}$$

The solution to this set of equations is

$$B_{k+1}^{-1} = \frac{\vec{s}_k \vec{s}_k^T}{\vec{y}_k^T \vec{s}_k} + \left(I - \frac{\vec{s}_k \vec{y}_k^T}{\vec{y}_k^T \vec{s}_k} \right) B_k^{-1} \left(I - \frac{\vec{y}_k \vec{s}_k^T}{\vec{y}_k^T \vec{s}_k} \right) \tag{3.54}$$

where I is the unity matrix. A derivation of this expression can be found in the appendix A.2. To apply the BFGS algorithm to the optimal control problem we use the performance measure J_a as our objective function and the discretized control function $\vec{u}$ as position variable. With this update formula for the inverse Hessian we can summarize the steps of the BFGS algorithm:

1. Compute the search direction

   $$\vec{p}_k = -B_k^{-1}(\nabla_{\vec{u}} J_a)_k$$

   using the gradient of the performance measure $\nabla_{\vec{u}} J_a$ as defined in 3.37. At the first step we need to make a guess for the inverse Hessian B_0^{-1}. In this thesis we use the identity matrix as initial guess.

2. Perform an inexact Wolfe line search to determine the step length α_k

3. Calculate new position

   $$\vec{u}_{k+1} = \vec{u}_k + \alpha_k \vec{p}_k$$

4. Compute updated inverse Hessian B_{k+1}^{-1} with Equation 3.54

If you repeat those steps you will go towards a minimum. It turns out that generally the BFGS algorithm is one of the most efficient optimization techniques which exists so far.

4. Optimal control of a polymorph transition system

In this section we try to apply the derived mathematical framework in Section 3 on the specific problem of maximizing the concentration of a specific polymorph B in a polymorph transition system.

4.1. Unconstrained optimal control

First we need to find the performance measure which describes the optimum of the system. Intuitively we would think of something like

$$J[\vec{u}] = -y_B(t_f) \tag{4.1}$$

where y_B is the component of the state vector which represents the concentration of the target polymorph. Notice the minus sign which transforms the maximization problem to a minimization problem. Now we can apply the mathematical theory for optimal control derived in the previous section.
To formulate the Hamiltonian we will use the state equation which we derived in Chapter 2 and the following terms which results from comparing to the general theory

$$\vec{a}(\vec{y}(t), \vec{u}(t), t) = A^T(\vec{u}(t))\ \vec{y}(t)$$

$$h(\vec{y}(t), t) = -y_B(t)$$

$$g(\vec{y}(t), \vec{u}(t), t) = 0$$

The Hamiltonian of the system reads then

$$\mathcal{H}(\vec{y}(t), \vec{u}(t), \vec{\lambda}(t), t) = \vec{\lambda}^T(t) A^T(\vec{u}(t))\ \vec{y}(t) \tag{4.2}$$

With this we can formulate the necessary conditions for the special problem of maximizing the yield of a specific polymorph after time t_f.

(i) Final condition costate

$$\vec{\lambda}^*(t_f) = -\left[\frac{\partial}{\partial \vec{y}} y_B(t)\right]_{t=t_f} = -\begin{pmatrix} 0 \\ \vdots \\ 1 \\ \vdots \\ 0 \end{pmatrix} = -\mathbb{I}_B \tag{4.3}$$

The symbol $\mathbb{I}_B$ can be seen as an indicator vector where all components are zero except the B^{th} component which is one. One can think of it as the B^{th} column of the identity matrix.

(ii) Costate equation

$$\dot{\vec{\lambda}}^*(t) = -A(\vec{u}^*(t))\ \vec{\lambda}^*(t) \tag{4.4}$$

(iii) Control equation

$$0 = \vec{\lambda}^{*T}(t)\frac{\partial A}{\partial \vec{u}}^T(\vec{u}^*(t))\ \vec{y}^*(t) \tag{4.5}$$

(iv) State equation

$$\dot{\vec{y}}^*(t) = A^T(\vec{u}^*(t))\ \vec{y}^*(t) \tag{4.6}$$

One interesting property of this special system is that the time derivative of the scalar product between the state and the costate vector vanishes.

$$\begin{aligned} \frac{d}{dt}\left(\vec{\lambda}^T(t)\cdot\vec{y}(t)\right) &= \left(\frac{d}{dt}\vec{\lambda}^T(t)\right)\vec{y}(t) + \vec{\lambda}^T(t)\left(\frac{d}{dt}\vec{y}(t)\right) \\ &= -\vec{\lambda}^T(t)\ A^T(\vec{u}(t))\ \vec{y}(t) + \vec{\lambda}^T(t)\ A^T(\vec{u}(t))\ \vec{y}(t) = 0 \end{aligned} \tag{4.7}$$

This can be used to check the numerical implementation of calculating the state and the costate equations in a computer.

4.1.1. Analytical discussion

Before trying to solve the optimal control problem for a polymorph transition system numerically we should discuss the found necessary conditions in an analytical way. If we take a closer look at the control equation for the unconstrained case 4.5 where we only consider one control variable being the inverse temperature $\beta = \frac{1}{k_B T}$ we can find that it takes the form of an exponential sum or an exponential polynomial. To ease notation we skip the function arguments and keep in mind that all terms depend on time t and we identify the gradient with respect to β of the time evolution matrix as

$$D = \frac{\partial A^T}{\partial \beta} = f_a \begin{pmatrix} \sum_j e^{-\beta \Delta G_{1j}} \Delta G_{1j} & -e^{-\beta \Delta G_{21}} \Delta G_{21} & -e^{-\beta \Delta G_{31}} \Delta G_{31} & \dots \\ -e^{-\beta \Delta G_{12}} \Delta G_{12} & \sum_j e^{-\beta \Delta G_{2j}} \Delta G_{2j} & -e^{-\beta \Delta G_{32}} \Delta G_{32} & \\ -e^{-\beta \Delta G_{13}} \Delta G_{13} & -e^{-\beta \Delta G_{23}} \Delta G_{23} & \sum_j e^{-\beta \Delta G_{3j}} \Delta G_{3j} & \\ \vdots & & & \ddots \end{pmatrix} \tag{4.8}$$

Here we define the diagonal elements of the barrier matrix to vanish $\Delta G_{ii} = 0$. Additionally we only look at the case where the Gibbs free energy barriers are constant an do not vary with temperature and pressure. This means the only control variable is the inverse temperature β. The control equation with the notation introduced above is then

$$\begin{aligned} \vec{\lambda}^T D\ \vec{y} &= \sum_{i=1}^{M} \sum_{j=1}^{M} \lambda_i D_{ij} y_j = \underbrace{\sum_{i=1}^{M} \lambda_i D_{ii} y_i}_{\text{diagonal part}} + \underbrace{\sum_{\substack{l=1 \\ l \neq m}}^{M} \sum_{m=1}^{M} \lambda_l D_{lm} y_m}_{\text{non diagonal part}} = \\ &= \sum_{i=1}^{M} \lambda_i \sum_{j=1}^{M} (e^{-\beta \Delta G_{ij}} \Delta G_{ij}) y_i - \sum_{l=1}^{M} \sum_{m=1}^{M} \lambda_l e^{-\beta \Delta G_{ml}} \Delta G_{ml} y_m = \\ &= \sum_{i=1}^{M} \sum_{j=1}^{M} \lambda_i (e^{-\beta \Delta G_{ij}} \Delta G_{ij}) y_i - \sum_{j=1}^{M} \sum_{i=1}^{M} \lambda_j e^{-\beta \Delta G_{ij}} \Delta G_{ij} y_i = \\ &= \sum_{i=1}^{M} \sum_{j=1}^{M} \Delta G_{ij} y_i (\lambda_i - \lambda_j) e^{-\beta \Delta G_{ij}} \end{aligned} \tag{4.9}$$

In the second step we renamed the summation indices to be able to combine the two sums. The summation limit M is the number of polymorphs in the system. The result is an exponential polynomial which has in general the form

$$\phi(\beta) = \sum_{k=1}^{n} a_k e^{\alpha_k \beta} \tag{4.10}$$

where we can identify $\alpha_k = \Delta G_{ij}$ and $a_k = \Delta G_{ij} y_i (\lambda_i - \lambda_j)$ with flattended indices $ij \to k$. The summation limit n is the number of all possible combinations of the indices i and j which is $n = N^2$. To have a solution for the optimal control problem all necessary conditions of optimality needs to be fulfilled. The control equation should be zero at the optimum. This means we would need to find the roots of this exponential polynomial. Unfortunately there exists no closed form for the zeros of an exponential polynomial but we can estimate an upper bound for the number of zeros and lower and upper bounds for the position of the roots.

Number of solutions

For regular polynomials there exists Decartes' rule of signs [29] to estimate an upper bound for the number of positive real roots. This rule can be extended to exponential

polynomials as shown in [30]. Decartes' rule of signs for exponential polynomials states that an upper bound for the roots is given by the number of sign changes in the sequence of the coefficients of the polynomial.
Assume we have the exponential polynomial

$$\phi(\beta) = \sum_{i=1}^{n} a_i e^{\alpha_i \beta} \tag{4.11}$$

where the terms in the sum are ordered by the exponent α_i ($\alpha_1 < \alpha_2 < ... < \alpha_n$). Then the number of sign changes $S(\{a_i\})$ in the sequence of the coefficients a_i determines an upper bound for the number of zeros.

$$\{\overbrace{a_1, \underbrace{a_2}_{s_2}}^{s_1}, \overbrace{a_3, \underbrace{a_4}_{s_4}}^{s_3}, a_5 ..., \overbrace{a_i, a_{i+1}}^{s_i}, ..., \overbrace{a_{n-1}, a_n}^{s_{n-1}}\} \quad \text{with} \quad s_i = \begin{cases} 1 & \text{if} \quad \text{sgn}(a_i) \neq \text{sgn}(a_{i+1}) \\ 0 & \text{if} \quad \text{sgn}(a_i) = \text{sgn}(a_{i+1}) \end{cases} \tag{4.12}$$

$$S(\{a_i\}) = \sum_{i=1}^{n-1} s_i \tag{4.13}$$

In the case of the control equation for a polymorph transition system the exponential polynomial has at most $M(M-1)$ terms which means according to Decartes' rule of signs there are at most $M(M-1)-1$ zeros if the signs of the coefficients are alternating.

Upper and lower bound for solutions

Upper bound We can also estimate an upper bound for the position of the real roots of the exponential polynomial. For a regular polynomial Lagrange formulated a rule to determine an upper bound for the position of the real roots [31]. This rule can be extended to an exponential polynomial like it is defined in 4.11.
If a root of 4.11 is located at $\beta^+ \geq 0$ then

$$\begin{aligned} 0 = \sum_{i=1}^{n} a_i e^{\alpha_i \beta^+} \Rightarrow |a_n| e^{\alpha_n \beta^+} &= \left| \sum_{i=1}^{n-1} a_i e^{\alpha_i \beta^+} \right| \\ |a_n| e^{\alpha_n \beta^+} \leq \sum_{i=1}^{n-1} |a_i| \, e^{\alpha_i \beta^+} &\leq \sum_{i=1}^{n-1} |a_i| \, e^{\alpha_{n-1} \beta^+} \qquad (4.14) \\ \frac{e^{\alpha_n \beta^+}}{e^{\alpha_{n-1} \beta^+}} &\leq \sum_{i=1}^{n-1} \frac{|a_i|}{|a_n|} \\ \beta^+ &\leq \frac{\ln\left(\sum_{i=1}^{n-1} \frac{|a_i|}{|a_n|}\right)}{\alpha_n - \alpha_{n-1}} \qquad (4.15) \end{aligned}$$

This is true for all positive roots of 4.11 therefore 4.15 is an upper bound for all positive real roots.

Lower bound For the lower bound we do a similar estimation. If a root is located at $\beta^- \leq 0$ then

$$\begin{aligned} |a_1|e^{\alpha_1\beta^-} &= \left|\sum_{i=2}^{n} a_i e^{\alpha_i\beta^-}\right| \\ |a_1|e^{\alpha_1\beta^-} &\leq \sum_{i=2}^{n} |a_i|e^{\alpha_i\beta^-} \leq \sum_{i=2}^{n} |a_i|e^{\alpha_2\beta^-} \\ \frac{e^{\alpha_1\beta^-}}{e^{\alpha_2\beta^-}} &\leq \sum_{i=2}^{n} \frac{|a_i|}{|a_1|} \\ \beta^- &\geq \frac{\ln\left(\sum_{i=2}^{n} \frac{|a_i|}{|a_1|}\right)}{\alpha_1 - \alpha_2} \end{aligned} \tag{4.16}$$

We can conclude here that if there exists a root β_0 of the exponential polynomial it lies between the boundaries

$$\beta^- \leq \beta_0 \leq \beta^+. \tag{4.17}$$

Self consistent cycle

Usually optimal control problems can not be solved analytically only in very rare cases. An example for an optimal control problem with an analytical solution is the two-polymorph system. The solution is shown in the next chapter. In general one need to rely on numerical algorithms to solve such problems. We already showed some techniques in Chapter 3.2. In this Chapter we will use a different approach solving the problem with a self consistent cycle. This algorithm starts very similar to the already described numerical techniques but updating the control function is different.

1. Guess the optimal control function $\beta^*(t)$
2. Solve the initial value problem of the state equation using the initial condition for the state vector $\vec{y}(0) = \vec{y}_0$.
3. Solve the final value problem of the costate equation backward in time using the final condition $\vec{\lambda}^*(t_f) = \vec{\lambda}_f$ at final time t_f.
4. Find the root $\beta_0(t)$ of the control equation closest to the current control $\beta(t)$ for every time t using the upper and lower bounds described in Chapter 4.1.1
5. Update the control function $\beta(t)$ to the root function $\beta_0(t)$ and start over at step 2

This algorithm converges quite fast if you have a good initial guess for the control function. If you are not very close to a solution it can happen that it does not converge at all. To improve the performance it is helpful updating the control function for the

next iterations with a mix of the new solution and the previous solution. This prevents from oscillating around the optimal control function and accelerates convergence.

It turns out that a good solution strategy is to use the numerical technique described in Chapter 3.2 with very loose convergence settings and use the obtained control function as initial guess for the self consistent cycle to find the final solution.

We will apply the self consistent cycle algorithm to the three state system in Chapter 5.3.

4.1.2. Analytical discussion: Two control variables

In the previous discussion we only considered the inverse temperature β as our only control variable of the system. Here we want to see what happens if we consider a second control namely the pressure p. The main change here is that the barriers ΔG are now also dependent on inverse temperature β and pressure p.

$$\Delta G(\beta, p) = \Delta E - \mu(\beta, p)\Delta N \tag{4.18}$$

where $\mu(\beta, p)$ is the chemical potential of a molecule in gas phase, ΔE is the adsorption energy barrier and ΔN is the change of the number of adsorbed molecules (see Chapter 1.3). Two independent control parameters means that the control equation has two components which need to be zero simultaneously. It is convenient to do a variable transformation where we introduce a new variable η

$$\eta = \beta\mu(\beta, p) \tag{4.19}$$

If we insert this in our exponential function for the rates $e^{-\beta\Delta G_{ij}(\beta,p)}$ we find the decoupled function

$$e^{-\beta\Delta G_{ij}(\beta,p)} = e^{-\beta(\Delta E_{ij} - \mu(\beta,p)\Delta N_{ij})} = e^{-\beta\Delta E_{ij} + \eta\Delta N_{ij}} \tag{4.20}$$

which is nicer to work with.

Now we have two control variables β and η with which we can formulate the two control equations.

$$
\begin{aligned}
0 = \vec{\lambda}^T D_\beta \vec{y} = \vec{\lambda}^T \frac{\partial A^T}{\partial \beta} \vec{y} = \\
= f_a \vec{\lambda}^T \begin{pmatrix} \sum_j e^{-\beta\Delta E_{1j}+\eta\Delta N_{1j}} \Delta E_{1j} & -e^{-\beta\Delta E_{21}+\eta\Delta N_{21}} \Delta E_{21} & \dots \\ -e^{-\beta\Delta E_{12}+\eta\Delta N_{12}} \Delta E_{12} & \sum_j e^{-\beta\Delta E_{2j}+\eta\Delta N_{2j}} \Delta E_{2j} & \\ \vdots & & \ddots \end{pmatrix} \vec{y} \\
0 = \vec{\lambda}^T D_\eta \vec{y} = \vec{\lambda}^T \frac{\partial A^T}{\partial \eta} \vec{y} = \\
= f_a \vec{\lambda}^T \begin{pmatrix} -\sum_j e^{-\beta\Delta E_{1j}+\eta\Delta N_{1j}} \Delta N_{1j} & e^{-\beta\Delta E_{21}+\eta\Delta N_{21}} \Delta N_{21} & \dots \\ e^{-\beta\Delta E_{12}+\eta\Delta N_{12}} \Delta N_{12} & -\sum_j e^{-\beta\Delta E_{2j}+\eta\Delta N_{2j}} \Delta N_{2j} & \\ \vdots & & \ddots \end{pmatrix} \vec{y}
\end{aligned}
\tag{4.21}
$$

We can represent those two equations in the form of two exponential sums.

$$
\begin{aligned}
0 = \vec{\lambda}^T D_\beta \vec{y} = \sum_{ij} \Delta E_{ij} (\lambda_i - \lambda_j) y_i e^{-\beta\Delta E_{ij}+\eta\Delta N_{ij}} \\
0 = \vec{\lambda}^T D_\eta \vec{y} = \sum_{ij} \Delta N_{ij} (\lambda_j - \lambda_i) y_i e^{-\beta\Delta E_{ij}+\eta\Delta N_{ij}}
\end{aligned}
\tag{4.22}
$$

In a more general form we can identify those two equations as

$$
\phi_\beta(\beta, \eta) = \sum_{k=1}^{n} a_k e^{\beta\alpha_k} e^{\eta\gamma_k} = 0 \tag{4.23}
$$

$$
\phi_\eta(\beta, \eta) = \sum_{i=1}^{n} b_k e^{\beta\alpha_k} e^{\eta\gamma_k} = 0 \tag{4.24}
$$

where $a_k = \Delta E_{ij}(\lambda_i - \lambda_j) y_i$, $b_k = \Delta N_{ij}(\lambda_j - \lambda_i) y_i$, $\alpha_k = -\Delta E_{ij}$ and $\gamma_k = \Delta N_{ij}$ with a flattended index $k \leftrightarrow ij$.
For a root to exist in those two equations there need to be at least one sign change in the coefficients a_i and b_i. In the case of the exponential polynomial ϕ_β this is actually the case because all the terms building the coefficient a_i are positive except the difference of the costates $(\lambda_i - \lambda_j)$ which can potentially be negative. This difference occurs in the coefficients two times with opposite sign, which means we have at least one sign change. In the case of the ϕ_η polynomial we have the special case that the change in particle number ΔN_{ij} can be positive and negative. Usually we assume that the fictional transition polymorph has a particle number which lies between the initial and final polymorph particle number, which means $N_{init} < N^\ddagger < N_{final}$ or $N_{init} > N^\ddagger > N_{final}$. With that the forward and backward reaction direction have opposite sign in the particle number change ΔN, so that ΔN_{ij} has opposite sign compared to ΔN_{ji}. Because of this alternating sign change in ΔN in the case of a two state system only positive or only negative

coefficients b_1 and b_2 exists in ϕ_η. The consequence is that in the two polymorph system case ϕ_η has only positive or only negative values. Therefore ϕ_η has no root and no optimal $\eta(t)$ can exist. It only make sense to start optimizing at least a three state system in this case.

Upper and lower bounds for solutions

We can now estimate a region, in a similar way as we did in the one dimensional case, where the roots of those two equations are located. For each of the control equations we get a bounded area in the $\beta\eta$-plane. These two root areas need to overlap to be able to find a common root for both control equations. For finding these root containing areas we keep one of the control variables fixed and apply the same estimation for the remaining free variable as we did in the one dimensional case. In the case of the ϕ_β polynomial we need to find four curves in the $\beta\eta$ plane which are the upper and lower boundaries of the root containing area.

$$\begin{aligned}\phi_\beta(\beta,\eta) &= \sum_{i=1}^{n} \bar{a}_i(\eta) e^{\beta\alpha_i} = 0 \quad \text{with} \quad \alpha_1 < \alpha_2 < ... < \alpha_n \text{ and } \bar{a}_i(\eta) = a_i e^{\eta\gamma_i} \\ \phi_\beta(\beta,\eta) &= \sum_{i=1}^{n} \bar{a}_i(\beta) e^{\eta\gamma_i} = 0 \quad \text{with} \quad \gamma_1 < \gamma_2 < ... < \gamma_n \text{ and } \bar{a}_i(\beta) = a_i e^{\beta\alpha_i}\end{aligned} \tag{4.25}$$

$$\begin{aligned}\beta^+_{\phi_\beta}(\eta) &\leq \frac{\ln\left(\sum_{i=1}^{n-1} \frac{|\bar{a}_i(\eta)|}{|\bar{a}_n(\eta)|}\right)}{\alpha_n - \alpha_{n-1}} \\ \beta^-_{\phi_\beta}(\eta) &\geq \frac{\ln\left(\sum_{i=2}^{n} \frac{|\bar{a}_i(\eta)|}{|\bar{a}_1(\eta)|}\right)}{\alpha_1 - \alpha_2}\end{aligned} \tag{4.26}$$

$$\begin{aligned}\eta^+_{\phi_\beta}(\beta) &\leq \frac{\ln\left(\sum_{i=1}^{n-1} \frac{|\bar{a}_i(\beta)|}{|\bar{a}_n(\beta)|}\right)}{\gamma_n - \gamma_{n-1}} \\ \eta^-_{\phi_\beta}(\beta) &\geq \frac{\ln\left(\sum_{i=2}^{n} \frac{|\bar{a}_i(\beta)|}{|\bar{a}_1(\beta)|}\right)}{\gamma_1 - \gamma_2}\end{aligned} \tag{4.27}$$

We do the exact thing again for the ϕ_η polynomial and find for the bounds

$$\begin{aligned}\phi_\eta(\beta,\eta) &= \sum_{i=1}^{n} \bar{b}_i(\eta) e^{\beta\alpha_i} = 0 \quad \text{with} \quad \bar{b}_i(\eta) = b_i e^{\eta\gamma_i} \\ \phi_\eta(\beta,\eta) &= \sum_{i=1}^{n} \bar{b}_i(\beta) e^{\eta\gamma_i} = 0 \quad \text{with} \quad \bar{b}_i(\beta) = b_i e^{\beta\alpha_i}\end{aligned} \tag{4.28}$$

$$\begin{aligned}\beta^{+}_{\phi_\eta}(\eta) &\leq \frac{\ln\left(\sum_{i=1}^{n-1}\frac{|\bar{b}_i(\eta)|}{|\bar{b}_n(\eta)|}\right)}{\alpha_n-\alpha_{n-1}}\\ \beta^{-}_{\phi_\eta}(\eta) &\geq \frac{\ln\left(\sum_{i=2}^{n}\frac{|\bar{b}_i(\eta)|}{|\bar{b}_1(\eta)|}\right)}{\alpha_1-\alpha_2}\end{aligned} \tag{4.29}$$

$$\begin{aligned}\eta^{+}_{\phi_\eta}(\beta) &\leq \frac{\ln\left(\sum_{i=1}^{n-1}\frac{|\bar{b}_i(\beta)|}{|\bar{b}_n(\beta)|}\right)}{\gamma_n-\gamma_{n-1}}\\ \eta^{-}_{\phi_\eta}(\beta) &\geq \frac{\ln\left(\sum_{i=2}^{n}\frac{|\bar{b}_i(\beta)|}{|\bar{b}_1(\beta)|}\right)}{\gamma_1-\gamma_2}\end{aligned} \tag{4.30}$$

If these two root containing areas overlap we can do a zero search only in this overlapping area to find a root.
Anyhow, we are not focusing on finding optimal pressure curves in this thesis and only stick to the more important optimal temperature curve. This section should only show how theoretically a second control parameter could be optimized via the self consistent algorithm. Also finding roots of a two dimensional exponential polynomial is much more difficult than in the one dimensional case.

4.2. Constrained optimal control

If the performance measure J depends also on the control derivative we need to introduce a new control variable $\vec{v}$ as shown in Section 3.1.4. We can add to the performance measure J a penalty term $\frac{\gamma}{2}\dot{\vec{u}}^2(t)$ [20] which shifts the minima to optimal controls which do not vary too much. The penalized performance measure for our polymorph system then looks like

$$J_p[\vec{u}] = -y_B(t_f) + \int_0^{t_f}\frac{\gamma}{2}\dot{\vec{u}}^2(t)\mathrm{d}t = -y_B(t_f) + \int_0^{t_f}\frac{\gamma}{2}\vec{v}^2(t)\mathrm{d}t \tag{4.31}$$

by using the new control variable $\vec{v} = \dot{\vec{u}}$.
Further we need to define the modified state vector which is the original state vector merged with the former control vector $\vec{u}$

$$\hat{\vec{y}} = \begin{pmatrix}\vec{y}\\ \vec{u}\end{pmatrix}$$

The state equation has now the modified form

$$\dot{\hat{\vec{y}}}(t) = \begin{pmatrix}A^T(\hat{\vec{y}}(t))\cdot\vec{y}(t)\\ \vec{v}(t)\end{pmatrix} \tag{4.32}$$

Notice that the argument in the matrix A is now the new state vector $\hat{\vec{y}}$ and not the original control vector $\vec{u}$. The matrix A is still exactly the same as previously, the change

in the argument is just to not forget that the differential of A with respect to $\hat{\vec{y}}$ does not vanish anymore, since $\vec{u}$ is part of the state vector $\hat{\vec{y}}$ now.
With this modified quantities we find by comparing the equations to the general theory

$$\vec{a}(\hat{\vec{y}}(t), \vec{v}(t), t) = \begin{pmatrix} A^T(\hat{\vec{y}}(t)) \cdot \vec{y}(t) \\ \vec{v}(t) \end{pmatrix}$$

$$h(\hat{\vec{y}}(t), t) = -y_B(t)$$

$$g(\hat{\vec{y}}(t), \vec{v}(t), t) = \frac{\gamma}{2}\vec{v}^2(t)$$

this leads us again to the Hamiltonian

$$\mathcal{H}_p(\hat{\vec{y}}(t), \vec{v}(t), \hat{\vec{\lambda}}(t), t) = \frac{\gamma}{2}\vec{v}^2(t) + \begin{pmatrix} \vec{\lambda}(t) \\ \vec{\lambda}_v(t) \end{pmatrix}^T \cdot \begin{pmatrix} A^T(\hat{\vec{y}}(t)) \cdot \vec{y}(t) \\ \vec{v}(t) \end{pmatrix} \tag{4.33}$$

with an additional costate vector $\vec{\lambda}_v$ for the new variable $\vec{v}$.
The necessary conditions for the penalized system then look like

(i) Final condition of costate

$$\hat{\vec{\lambda}}^*(t_f) = -\left[\frac{\partial}{\partial \hat{\vec{y}}} y_B(t)\right]_{t=t_f} = -\begin{pmatrix} 0 \\ \vdots \\ 1 \\ \vdots \\ 0 \end{pmatrix} = -\hat{\mathbb{I}}_B \tag{4.34}$$

(ii) Costate equation

$$\dot{\vec{\lambda}}_k^*(t) = -\begin{pmatrix} \vec{\lambda}^*(t) \\ \vec{\lambda}_v^*(t) \end{pmatrix}^T \frac{\partial}{\partial \hat{y}_k} \begin{pmatrix} A^T(\hat{\vec{y}}^*(t)) \cdot \vec{y}^*(t) \\ \vec{v}^*(t) \end{pmatrix}$$
$$= -\vec{\lambda}^{*T}(t)\frac{\partial A^T}{\partial \hat{y}_k}(\hat{\vec{y}}^*(t))\ \vec{y}^*(t) - \vec{\lambda}^{*T}(t)A^T(\hat{\vec{y}}^*(t))\frac{\partial \vec{y}}{\partial \hat{y}_k}$$

In vector notation we find

$$\dot{\vec{\lambda}}^*(t) = \begin{pmatrix} 0 \\ \vdots \\ 0 \\ -\vec{\lambda}^{*T}(t)\frac{\partial A^T}{\partial u_1}(\hat{\vec{y}}^*(t))\ \vec{y}^*(t) \\ -\vec{\lambda}^{*T}(t)\frac{\partial A^T}{\partial u_2}(\hat{\vec{y}}^*(t))\ \vec{y}^*(t) \\ \vdots \end{pmatrix} - \begin{pmatrix} \\ A(\hat{\vec{y}}^*(t))\ \vec{\lambda}^*(t) \\ \\ 0 \\ 0 \\ \vdots \end{pmatrix} =$$

$$= - \begin{pmatrix} A(\hat{\vec{y}}^*(t))\ \vec{\lambda}^*(t) \\ \vec{\lambda}^{*T}(t)\frac{\partial A^T}{\partial \vec{u}}(\hat{\vec{y}}^*(t))\ \vec{y}^*(t) \end{pmatrix}$$

(iii) Control equation

$$0 = \gamma \vec{v}^*(t) + \vec{\lambda}_v^*(t) \tag{4.35}$$

(iv) State equation

$$\dot{\vec{y}}^*(t) = \begin{pmatrix} A^T(\hat{\vec{y}}^*(t)) \cdot \vec{y}^*(t) \\ \vec{v}^*(t) \end{pmatrix} \tag{4.36}$$

5. Results

Now we derived all necessary methods to optimize the concentration of a specific interface polymorph. In this chapter we are solving multiple polymorph transition systems. The first system we investigate is a two polymorph system, where we do not put any constraints on the optimal temperature curve we try to find 5.1. Because of its simplicity this example is ideal for demonstrating how Optimal Control theory works and how it can be used to obtain optimal temperature curves. Another convenient property of the unconstrained two state system is that it can be solved analytically. We use the analytic solution here to compare it to a solution obtained numerically.
In the second example we demonstrate how to put a constraint on the optimal temperature curve such that the curve is not varying too much over time.
In the last two examples we start to go towards more realistic systems where we extend the system by a third polymorph. In the first three state example we keep the Gibbs free energy barriers constant for different temperatures and apply an alternative very efficient solution technique to the optimal control problem (self consistent cycle approach described in Section 4.1.1).
The last example deals with the interesting problem of an "elevator polymorph" system. The rough idea is that if two polymorphs are intrinsically not connected in the transition network graph they can be connected via a third polymorph which we call "elevator polymorph". The goal is to find the optimal temperature curve which first occupies the elevator polymorph ("loading the elevator"), then change the temperature quickly ("elevate") and finally start to occupy the target polymorph ("unloading the elevator"). In this example we use Gibbs free energy barriers which vary with temperature, making the problem even more complex.

5.1. Two polymorph system unconstrained

We try to solve the optimal control problem for a simple two-state system with one constant barrier between the two polymorphs (see Figure 5.1). This example is the simplest possible polymorph network and also the easiest one to solve with Optimal Control theory. The most interesting aspect of this system is that it can be solved analytically. This is the perfect starting situation to test and compare the numerical algorithms, developed in previous chapters, to the exact solution.
In this example we use fictional barrier heights which are convenient to calculate with. They are chosen in such a way that we can set the attempt frequency f_a (pre-exponential factor of the Arrhenius equation 1.18) to one and the resulting optimal inverse temperature curve will have values which are in a reasonable range.
In a later example we will use more realistic transition barrier heights which we assume will be similar to the barrier heights of a single molecular process on a metal surface. Typical values for the transition barriers of this single molecular processes are in the range of tens to hundreds of meV [16].

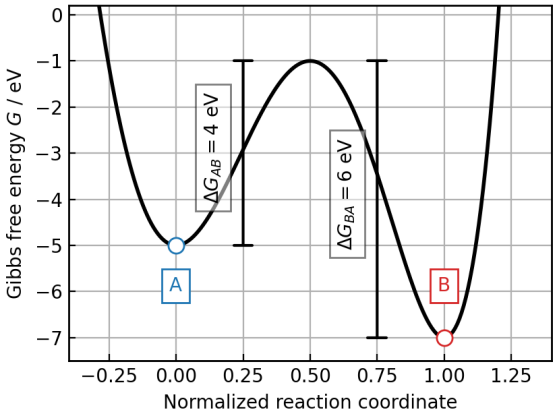

Figure 5.1.: Two state system: polymorph A and B are separated by a common barrier on the Gibbs free potential energy surface with the forward barrier $\Delta G_{AB} = 4\,\mathrm{eV}$ and the backward barrier $\Delta G_{BA} = 6\,\mathrm{eV}$

In this example the goal is to maximize the concentration y_B of polymorph B within the time frame $t \in [0, t_f]$. The performance measure $J_{2-state}$ of this problem is

$$\begin{aligned} J_{2-state} &= -(y_B(t_f) - y_B(0)) = -\int_0^{t_f} \dot{y}_B(t)\mathrm{d}t = \\ &= -\int_0^{t_f} f_a \left(e^{-\beta(t)\Delta G_{AB}} y_A(t) - e^{-\beta(t)\Delta G_{BA}} y_B(t) \right) \mathrm{d}t \end{aligned} \tag{5.1}$$

which means we want to maximize the concentration yield of the second polymorph B.

The necessary conditions for this kind of problem are

- State equation:

$$\begin{pmatrix}\dot{y}_A\\ \dot{y}_B\end{pmatrix} = \underbrace{f_a \begin{pmatrix}-e^{-\beta\Delta G_{AB}} & e^{-\beta\Delta G_{BA}}\\ e^{-\beta\Delta G_{AB}} & -e^{-\beta\Delta G_{BA}}\end{pmatrix}}_{A(\beta)} \begin{pmatrix}y_A\\ y_B\end{pmatrix} \quad \text{with} \quad \begin{pmatrix}y_A(0)\\ y_B(0)\end{pmatrix} = \begin{pmatrix}y_{A0}\\ 1-y_{A0}\end{pmatrix} \tag{5.2}$$

- Costate equation:

$$\begin{pmatrix}\dot{\lambda}_A\\ \dot{\lambda}_B\end{pmatrix} = -f_a \begin{pmatrix}-e^{-\beta\Delta G_{AB}} & e^{-\beta\Delta G_{AB}}\\ e^{-\beta\Delta G_{BA}} & -e^{-\beta\Delta G_{BA}}\end{pmatrix} \begin{pmatrix}\lambda_A\\ \lambda_B\end{pmatrix} \quad \text{with} \quad \begin{pmatrix}\lambda_A(t_f)\\ \lambda_B(t_f)\end{pmatrix} = \begin{pmatrix}0\\ -1\end{pmatrix} \tag{5.3}$$

- Control equation:

$$\begin{pmatrix}\lambda_A & \lambda_B\end{pmatrix} \begin{pmatrix}\Delta G_{AB}e^{-\beta\Delta G_{AB}} & -\Delta G_{BA}e^{-\beta\Delta G_{BA}}\\ -\Delta G_{AB}e^{-\beta\Delta G_{AB}} & \Delta G_{BA}e^{-\beta\Delta G_{BA}}\end{pmatrix} \begin{pmatrix}y_A\\ y_B\end{pmatrix} = 0 \tag{5.4}$$

If the temperature is infinite, which corresponds to an inverse temperature β of zero, the concentrations approach an uniform distribution. This is because all the entries in the time evolution matrix $A(\beta = 0)$ are equal to the attempt frequency f_a. The other extreme is a temperature of zero, which corresponds to an infinite inverse temperature β. In that case all entries in $A(\beta \to \infty)$ are zero and the concentrations do not change at all. As you can see in Figure 5.2 for different constant inverse temperatures β we get different yields for our target polymorph B. Usually there exists an optimal constant β^* between ultra cold condition $\beta = \infty$ and ultra hot conditions $\beta = 0$. Dependent on the initial value of the concentrations the maximum yield can be achieved at different constant inverse temperatures β. If we apply optimal control theory and determine the optimal time dependent inverse temperature function $\beta^*(t)$ we can increase the concentration yield of polymorph B even more, this is indicated by the dashed line in Figure 5.2.

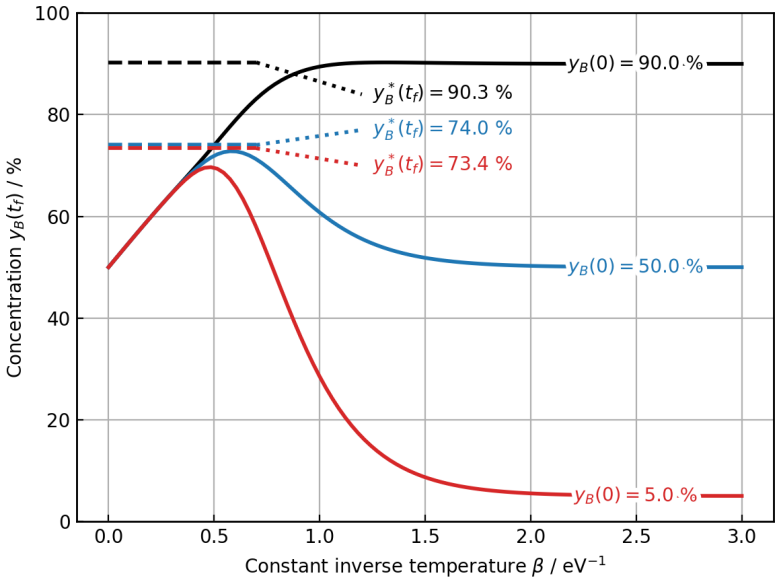

Figure 5.2.: Final concentration $y_B(t_f)$ of the target polymorph B at different constant inverse temperatures β and different initial concentrations $y_B(0)$. The dashed lines are the concentrations resulting of the optimized inverse temperature curves $\beta^*(t)$. Here we used the barriers $\Delta G_{AB} = 4\,\text{eV}$, $\Delta G_{BA} = 6\,\text{eV}$. For the attempt frequency we used $f_a = 1\,\text{s}^{-1}$ and the final time is $t_f = 16\,\text{s}$. At zero inverse temperature (hot temperature) we get an uniform distribution in the concentrations where $y_A = y_B = 50\,\%$. At high inverse temperatures (cold temperature) the initial distribution of the concentrations do not change and we find the same concentrations at the end of the time frame. We can also observe that the improvement of the optimal inverse temperature curve compared to the optimal constant inverse temperature is getting smaller with higher initial concentrations in the target state.

5.1.1. Analytical solution

In the simple case of a two-state system we can rearrange the control equation 5.4 to have an explicit expression for the control β. If we do the matrix multiplications in 5.4 we find

$$0 = f_a y_A \Delta G_{AB} e^{-\beta \Delta G_{AB}} (\lambda_A - \lambda_B) + f_a y_B \Delta G_{BA} e^{-\beta \Delta G_{BA}} (\lambda_B - \lambda_A) \tag{5.5}$$

Here, we can see that there exists at most one solution if we apply Decartes' rule of signs for exponential polynomials [30], since there can only be one sign change in the coefficients.
We can now divide by $e^{-\beta \Delta G_{AB}} > 0$ and get

$$0 = f_a y_A \Delta G_{AB}(\lambda_A - \lambda_B) + f_a y_B \Delta G_{BA} e^{\beta(\Delta G_{AB} - \Delta G_{BA})}(\lambda_B - \lambda_A) \tag{5.6}$$

Then one can find for the control β if $\lambda_A \neq \lambda_B$

$$\beta(t) = \frac{\ln\left(\frac{y_A(t)\Delta G_{AB}}{y_B(t)\Delta G_{BA}}\right)}{\Delta G_{AB} - \Delta G_{BA}} \tag{5.7}$$

Notice that if one of the concentrations $y_A(t)$ or $y_B(t)$ is zero the inverse temperature diverges to infinity or negative infinity. To only deal with finite values the initial concentrations at $t = 0$ needs to be different to zero. This finding is very interesting because this means we can not reach the perfect situation where the target concentration is 100 % because β would need to diverge.
Now we insert the closed form of β into the state equation 5.2 and costate equation 5.3 and find

$$\begin{aligned}\begin{pmatrix}\dot{y}_A\\ \dot{y}_B\end{pmatrix} &= f_a \begin{pmatrix} -\left(\frac{y_A\Delta G_{AB}}{y_B\Delta G_{BA}}\right)^{-\frac{\Delta G_{AB}}{\Delta G_{AB}-\Delta G_{BA}}} & \left(\frac{y_A\Delta G_{AB}}{y_B\Delta G_{BA}}\right)^{-\frac{\Delta G_{BA}}{\Delta G_{AB}-\Delta G_{BA}}} \\ \left(\frac{y_A\Delta G_{AB}}{y_B\Delta G_{BA}}\right)^{-\frac{\Delta G_{AB}}{\Delta G_{AB}-\Delta G_{BA}}} & -\left(\frac{y_A\Delta G_{AB}}{y_B\Delta G_{BA}}\right)^{-\frac{\Delta G_{BA}}{\Delta G_{AB}-\Delta G_{BA}}} \end{pmatrix}\begin{pmatrix}y_A\\ y_B\end{pmatrix} = \\ &= f_a \begin{pmatrix} -r^{\Delta G_{AB}} & r^{\Delta G_{BA}} \\ r^{\Delta G_{AB}} & -r^{\Delta G_{BA}} \end{pmatrix}\begin{pmatrix}y_A\\ y_B\end{pmatrix}\end{aligned} \tag{5.8}$$

$$\begin{aligned}\begin{pmatrix}\dot{\lambda}_A\\ \dot{\lambda}_B\end{pmatrix} &= -f_a \begin{pmatrix} -\left(\frac{y_A\Delta G_{AB}}{y_B\Delta G_{BA}}\right)^{-\frac{\Delta G_{AB}}{\Delta G_{AB}-\Delta G_{BA}}} & \left(\frac{y_A\Delta G_{AB}}{y_B\Delta G_{BA}}\right)^{-\frac{\Delta G_{AB}}{\Delta G_{AB}-\Delta G_{BA}}} \\ \left(\frac{y_A\Delta G_{AB}}{y_B\Delta G_{BA}}\right)^{-\frac{\Delta G_{BA}}{\Delta G_{AB}-\Delta G_{BA}}} & -\left(\frac{y_A\Delta G_{AB}}{y_B\Delta G_{BA}}\right)^{-\frac{\Delta G_{BA}}{\Delta G_{AB}-\Delta G_{BA}}} \end{pmatrix}\begin{pmatrix}\lambda_A\\ \lambda_B\end{pmatrix} = \\ &= -f_a \begin{pmatrix} -r^{\Delta G_{AB}} & r^{\Delta G_{AB}} \\ r^{\Delta G_{BA}} & -r^{\Delta G_{BA}} \end{pmatrix}\begin{pmatrix}\lambda_A\\ \lambda_B\end{pmatrix}\end{aligned} \tag{5.9}$$

where $r = \left(\frac{y_A\Delta G_{AB}}{y_B\Delta G_{BA}}\right)^{-\frac{1}{\Delta G_{AB}-\Delta G_{BA}}}$.
If we solve the state equation 5.8 with the initial condition $\vec{y}(0) = \vec{y}_0$ we find an extremum of the performance measure. In Figure 5.3 the solutions to these differential equations are plotted for some example values. The found solution only satisfies the necessary conditions of optimality, which means we do not know if we found a minimum, maximum or saddle point. In the Appendix A.3 we can show that the found solution is indeed a minimum.
In Figure 5.3 one can see that the optimal inverse temperature curve is negative in one region. This is unphysical because the inverse temperature can only be positive.
Nevertheless, we continue to discuss the method of optimal control theory on this example. To avoid non positive inverse temperatures in later examples (see Sections 5.2, 5.3, 5.4) further constraints are introduced then. But in this example we will stick to the unphysical negative inverse temperature values because this example is to demonstrate

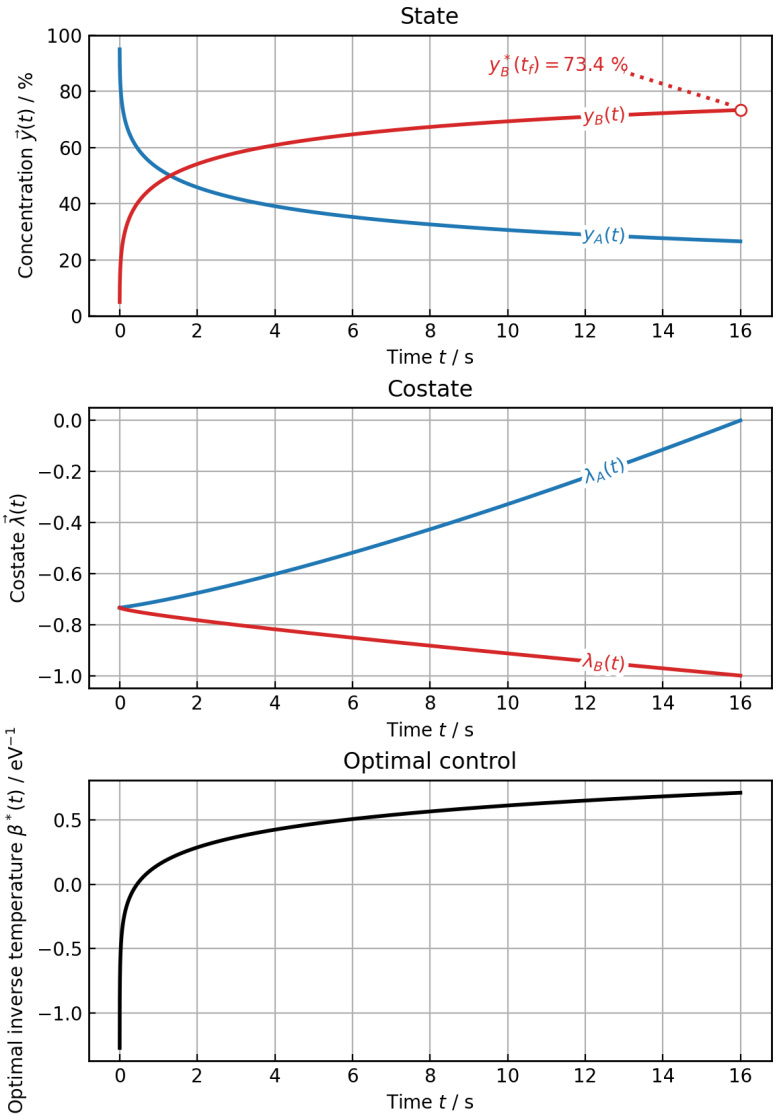

Figure 5.3.: Solutions to the state and costate equations and the optimal control β defined in 5.7 to 5.9. The values used are $y_A(0) = 95\,\%$, $y_B(0) = 5\,\%$, $\Delta G_{AB} = 4\,\mathrm{eV}$, $\Delta G_{BA} = 6\,\mathrm{eV}$, $f_a = 1\,\mathrm{s}^{-1}$, $t_f = 16\,\mathrm{s}$.

how an optimal control problem can be solved. For physical results we need to constrain the admissible inverse temperature to positive values which means we would need to set all negative values to zero or a small number.

5.1.2. Numerical solution with gradient descent

Now we try to solve the two polymorph system with the numerical technique described in Chapter 3.2. This should ideally compute the same optimal inverse temperature curve as in the analytical solution. We will use the gradient descent method to find the optimal control.

We tested different fixed step factors ϵ, introduced in Section 3.3.1, with which we scale the gradient of the performance measure $\nabla_{\vec{u}} J_a$. In Figure 5.4 the number of iterations for convergence for different step factors is plotted. There is an optimum around $\epsilon = 7.5$. At higher step lengths the number of iterations increases very sharply. This means the step length is too big and we overshoot the minimum at every iteration quite a lot. At some point it will not converge at all. The other extreme are very small step factors. The problem here is that we do not make much progress during one iteration but if we wait long enough it will converge at some point.

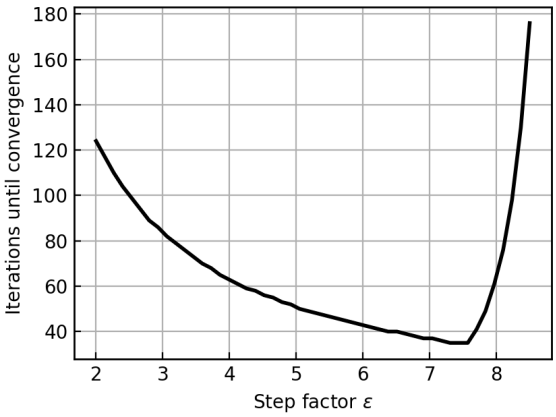

Figure 5.4.: Number of iterations in dependence of the step factor ϵ to satisfy the convergence criteria that the absolute value of the control equation is smaller than $f_{max} = 10^{-5}$.

As expected the result of the numerical gradient descent method in Figure 5.6 is exactly the same as in the analytical solution. In Figure 5.5 one can see the change of the performance measure and the control equation for different iterations i.

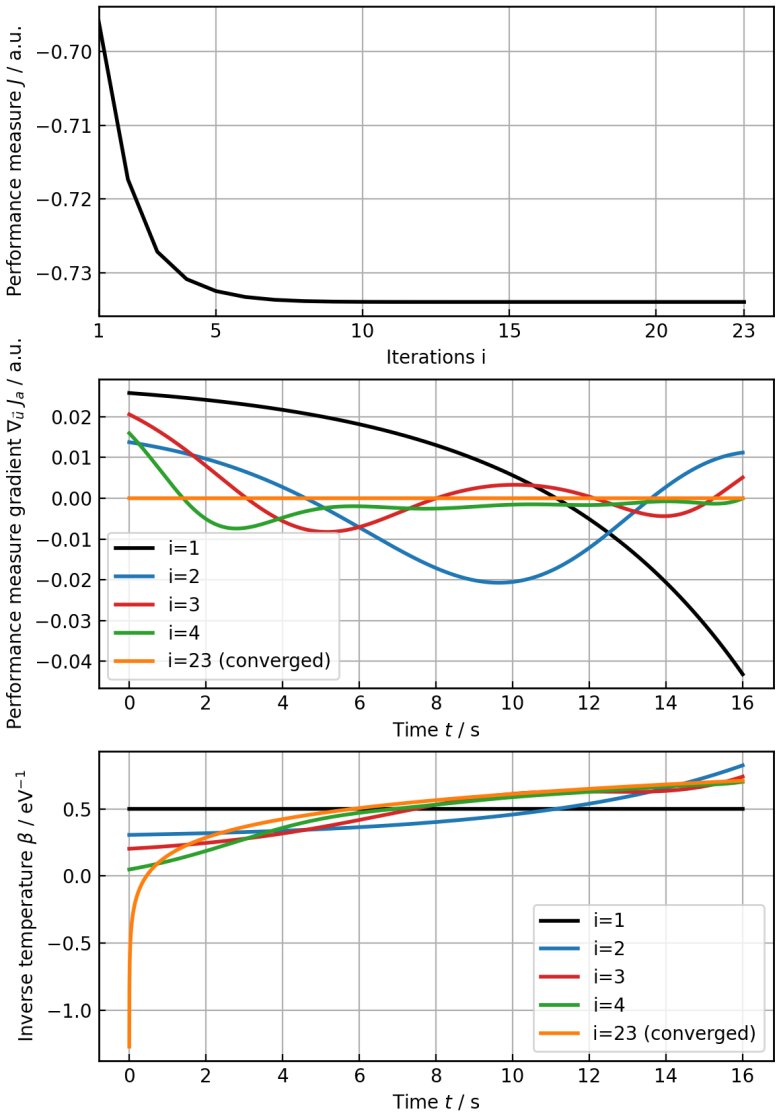

Figure 5.5.: Performance measure J improves (decreases) at every iteration i. The gradient of the performance measure with respect to the inverse temperature converges towards zero. Plotted are the first four and the last iteration. Convergence setting is $|\nabla_{\vec{u}} J_a| < 10^{-5}$.

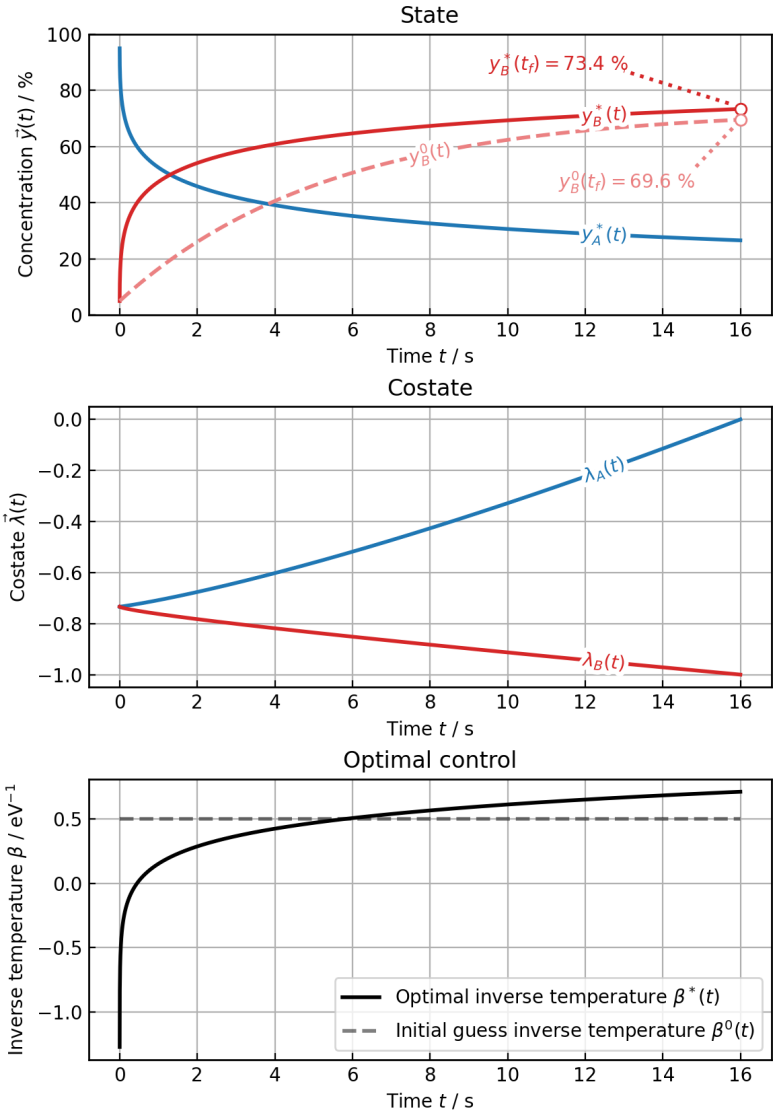

Figure 5.6.: Result to the state and costate equations and the optimal control β with the gradient descent method. The dashed line in the first plot is the concentration time evolution of the target polymorph B for the initial inverse temperature guess $\beta^0(t)$. The values used are $y_A(0) = 95.0\,\%$, $y_B(0) = 5.0\,\%$, $\Delta G_{AB} = 4\,\mathrm{eV}$, $\Delta G_{BA} = 6\,\mathrm{eV}$, $f_a = 1\,\mathrm{s}^{-1}$, $t_f = 16\,\mathrm{s}$. For the step factor in the gradient descent algorithm we used $\epsilon = 7.5$ and convergence is reached if $|\nabla_{\vec{u}} J_a| < 10^{-5}$ which was the case after 23 iterations.

5.2. Two polymorph system constrained

To illustrate how the constrained version of an optimal control problem described in Chapter 4.2 works we will apply it to the same two state system as before (see Figure 5.1). The goal is to get optimal inverse temperature curves which do not vary too much in time. If we would have a temperature curve which oscillates rapidly in time it is maybe not realizable in an experiment. What we do is we penalize optimal control solutions for fast changes of β by adding the term $\gamma\frac{\dot{\beta}^2}{2}$ to the performance measure. This will give temperature curves with very steep or highly oscillating regions a worse performance measure. Meaning that smoother or flatter temperature curves are preferred .
As already derived in Section 4.2 the main difference to before is that we now have a modified state vector $\hat{\vec{y}}$ where the inverse temperature β is contained. The new control variable v is the time derivative of the inverse temperature β.
The performance measure of this problem is

$$J_{2-state-constr} = -(\vec{y}_B(t_f) - \vec{y}_B(0)) + \int_0^{t_f} \gamma\frac{\dot{\beta}^2}{2}\ \mathrm{d}t \tag{5.10}$$

where we included the penalty term. The parameter γ determines how strong the penalty should be. Larger γ gives flatter or less oscillating inverse temperature curves. If γ is zero we would have the unconstrained case again. If γ is very large we worsen the yield of our target polymorph.
The necessary conditions are

- State equation

$$\begin{pmatrix}\dot{y}_A\\ \dot{y}_B\\ \dot{\beta}\end{pmatrix} = \begin{pmatrix}-f_a e^{-\beta\Delta G_{AB}} y_A + f_a e^{-\beta\Delta G_{BA}} y_B\\ f_a e^{-\beta\Delta G_{AB}} y_A - f_a e^{-\beta\Delta G_{BA}} y_B\\ v\end{pmatrix} \tag{5.11}$$

- Costate equation

$$\begin{pmatrix}\dot{\lambda}_A\\ \dot{\lambda}_B\\ \dot{\lambda}_v\end{pmatrix} = -\begin{pmatrix}-f_a e^{-\beta\Delta G_{AB}}\lambda_A + f_a e^{-\beta\Delta G_{AB}}\lambda_B\\ f_a e^{-\beta\Delta G_{BA}}\lambda_A - f_a e^{-\beta\Delta G_{BA}}\lambda_B\\ (\Delta G_{AB} e^{-\beta\Delta G_{AB}} y_A - \Delta G_{BA} e^{-\beta\Delta G_{BA}} y_B)(\lambda_A - \lambda_B)\end{pmatrix} \tag{5.12}$$

- Control equation

$$0 = \gamma v + \lambda_v \tag{5.13}$$

For this example we choose $\gamma = 0.1$. This value is chosen because it gives a reasonable flat inverse temperature curve without decreasing the target polmorph yield too much. For solving the optimal control problem we use the BFGS algorithm from Chapter 3.3.2. Now the time derivative of the inverse temperature is our control function and we need to give an initial guess for it. Here, we use the zero function as initial guess. To solve the state equation we also need to set an initial value for the inverse temperature curve at

time $t = 0$, we set it to $\beta(0) = 0.7$. In Figure 5.7 the result for the constrained optimal control is plotted. Because of the penalty term in the performance measure we do not have very steep regions in the optimal inverse temperature curve $\beta^*(t)$ compared to the unconstrained case. The achieved optimized concentration y_B of our target polymorph B is slightly less but almost similar to the unconstrained case. Here we achieved for the final concentration $y_B(t_f)$ =72.2 %. Compared to the previous unconstrained case it is only 1.2 % less.

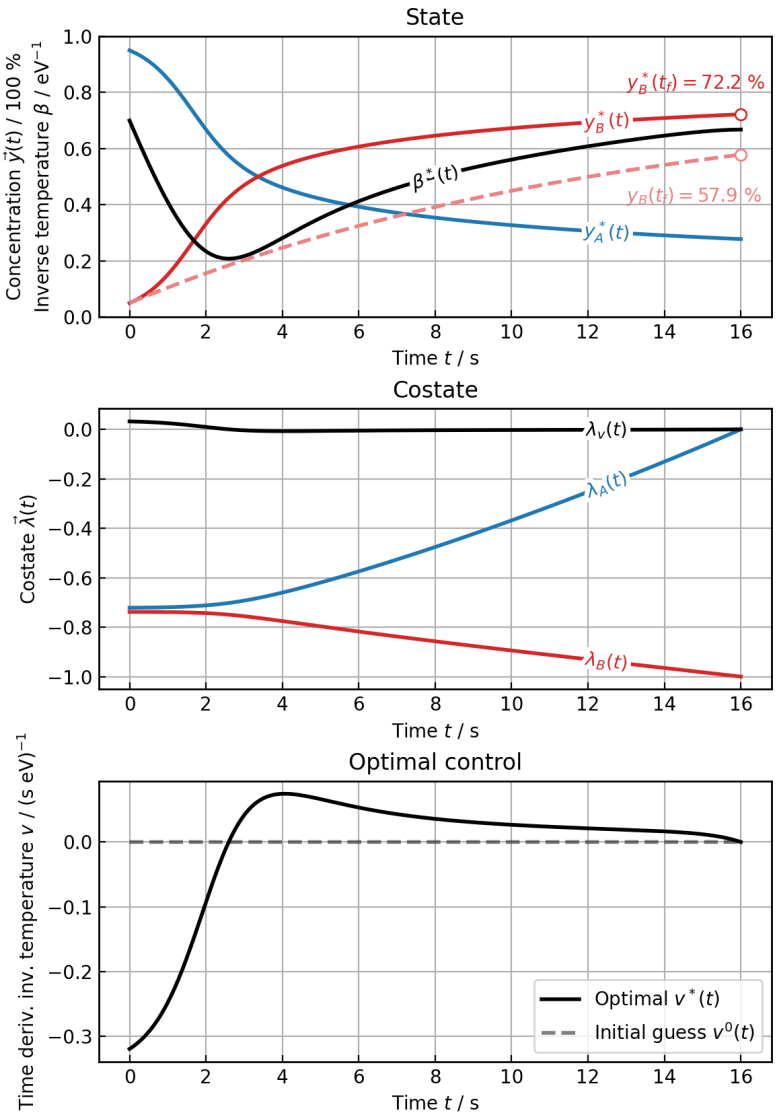

Figure 5.7.: Optimal curves for the constrained two state system. The optimal control v is the time derivative of the inverse temperature β. The dashed line in the first plot is the time evolution of the target polymorph concentration y_B for the initial control guess $v^0(t)$.

5.3. Three polymorph system

A more complex system is a three-state system where three polymorphs are involved. The corresponding Gibbs free energies and barriers are drawn in Figure 5.8. Our goal is again to maximize the concentration for polymorph B.

In contrast to the two-polymorph system our target polymorph B is not the energetic most favorable structure anymore. As you can see in Figure 5.8 polymorph C is lower in Gibbs free energy. It can happen that concentration escapes from our target polymorph B to the low energy polymorph C and can never gained back because the backward transition rate from C to B is always lower than the forward transition rate. We need to find an optimal temperature curve which traps the system in polymorph B and tries to prevent the transition further to polymorph C. In the second part of this example we also try to vary the barrier heights and see how the optimized target polymorph concentrations change for different barrier combinations.

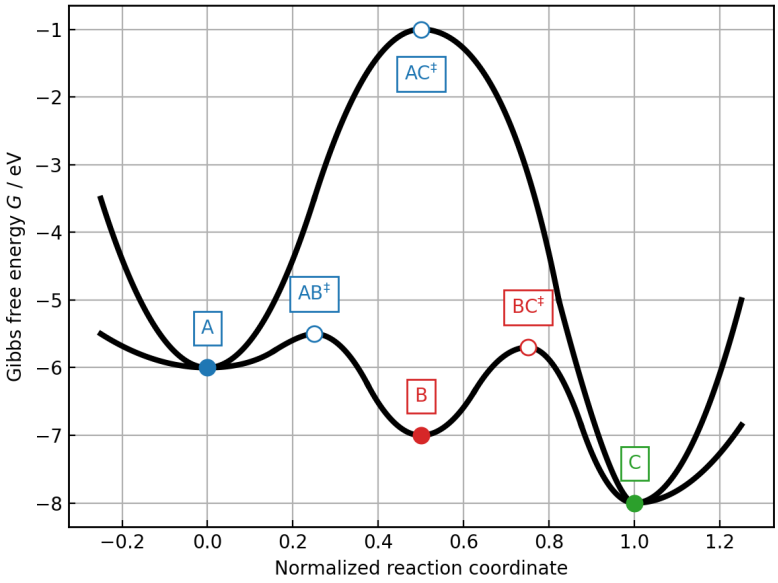

Figure 5.8.: Schematic Gibbs free energy landscape chosen for the three-state system.

The Gibbs free energy barriers used in this example are:

$$\begin{aligned} \Delta G_{AB} &= 0.5\,\mathrm{eV} \quad \Delta G_{BA} = 1.5\,\mathrm{eV} \\ \Delta G_{AC} &= 5.0\,\mathrm{eV} \quad \Delta G_{CA} = 7.0\,\mathrm{eV} \\ \Delta G_{BC} &= 1.3\,\mathrm{eV} \quad \Delta G_{CB} = 2.3\,\mathrm{eV} \end{aligned}$$

and we set the attempt frequency, like in the previous example, to $f_a = 1\,\mathrm{s}^{-1}$. The initial

concentration distribution in the system is set to

$$\vec{y}(0) = \begin{pmatrix} y_{A0} \\ y_{B0} \\ y_{C0} \end{pmatrix} = \begin{pmatrix} 90.0\,\% \\ 5.0\,\% \\ 5.0\,\% \end{pmatrix} \tag{5.14}$$

Meaning we start with a majority in polymorph A. The barrier between our starting polymorph A and polymorph C is set very high compared to the other barriers, so it does not contribute very much to the process. Our focus in this example is the transition path $A \to B \to C$. If we would decrease the barrier height between polymorph A and C we would loose concentration to polymorph C and the maximally gained concentration in the target polymorph B would be lower because of this "leak". We will see later in this example how varying barriers effect which optimal concentration is reachable in polymorph B.
We start by determining the state equation for the concentrations $\vec{y} = \left(y_A, y_B, y_C\right)^T$ and find

$$\begin{pmatrix} \dot{y}_A \\ \dot{y}_B \\ \dot{y}_C \end{pmatrix} = f_a \begin{pmatrix} -e^{-\beta\Delta G_{AB}} - e^{-\beta\Delta G_{AC}} & e^{-\beta\Delta G_{BA}} & e^{-\beta\Delta G_{CA}} \\ e^{-\beta\Delta G_{AB}} & -e^{-\beta\Delta G_{BA}} - e^{-\beta\Delta G_{BC}} & e^{-\beta\Delta G_{CB}} \\ e^{-\beta\Delta G_{AC}} & e^{-\beta\Delta G_{BC}} & -e^{-\beta\Delta G_{CA}} - e^{-\beta\Delta G_{CB}} \end{pmatrix} \begin{pmatrix} y_A \\ y_B \\ y_C \end{pmatrix} \tag{5.15}$$

with the initial condition $\vec{y}(0) = \left(y_{A0}, y_{B0}, y_{C0}\right)^T = \left(90.0\,\%, 5.0\,\%, 5.0\,\%\right)^T$.
In Figure 5.9 we solved the state equation for a constant inverse temperature $\beta = 1.5\,\mathrm{eV}^{-1}$. Here we can see nicely how the concentration first increases in polymorph B, reaches a maximum and then decreases again. This decreasing is because we loose the concentration in B again due to the transition $B \to C$. We suppose that the optimal inverse temperature curve needs to increase (cool down) around the concentration maximum of polymorph B. Then the transition rate from B to C is low and we can trap the system in our target polymorph B.

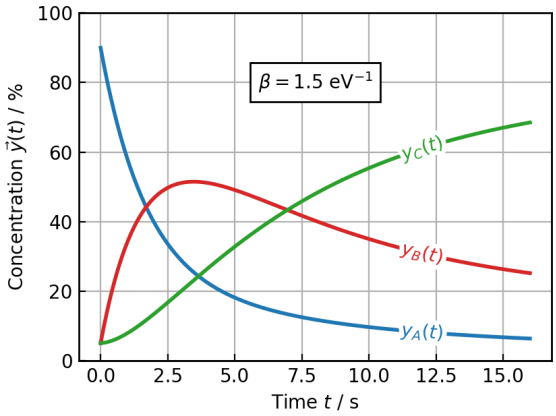

Figure 5.9.: Concentration time evolution for a constant inverse temperature $\beta = 1.5\,\mathrm{eV}^{-1}$. Here we can see that at first polymorph B gets populated and then transform further to polymorph C.

Now we can apply Optimal Control theory to actually find the optimal inverse temperature curve. The performance measure for this Optimal Control problem is given by

$$\begin{aligned} J_{3-state} &= -\int_0^{t_f} \dot{y}_B(t)\mathrm{d}t = \\ &= -\int_0^{t_f} \left[e^{-\beta\Delta G_{AB}} y_A - (e^{-\beta\Delta G_{BA}} + e^{-\beta\Delta G_{BC}}) y_B + e^{-\beta\Delta G_{CB}} y_C\right] \mathrm{d}t \end{aligned} \tag{5.16}$$

The costate equation has the form

$$\begin{pmatrix} \dot{\lambda}_A \\ \dot{\lambda}_B \\ \dot{\lambda}_C \end{pmatrix} = -f_a \begin{pmatrix} -e^{-\beta\Delta G_{AB}} - e^{-\beta\Delta G_{AC}} & e^{-\beta\Delta G_{AB}} & e^{-\beta\Delta G_{AC}} \\ e^{-\beta\Delta G_{BA}} & -e^{-\beta\Delta G_{BA}} - e^{-\beta\Delta G_{BC}} & e^{-\beta\Delta G_{BC}} \\ e^{-\beta\Delta G_{CA}} & e^{-\beta\Delta G_{CB}} & -e^{-\beta\Delta G_{CA}} - e^{-\beta\Delta G_{CB}} \end{pmatrix} \begin{pmatrix} \lambda_A \\ \lambda_B \\ \lambda_C \end{pmatrix} \tag{5.17}$$

with the final condition $\vec{\lambda}(t_f) = \big(0, -1, 0\big)^T$ and the control equation is

$$\begin{aligned} 0 = {} & e^{-\beta\Delta G_{AB}} \Delta G_{AB} y_A (\lambda_A - \lambda_B) + e^{-\beta\Delta G_{AC}} \Delta G_{AC} y_A (\lambda_A - \lambda_C) + \\ & + e^{-\beta\Delta G_{BA}} \Delta G_{BA} y_B (\lambda_B - \lambda_A) + e^{-\beta\Delta G_{BC}} \Delta G_{BC} y_B (\lambda_B - \lambda_C) + \\ & + e^{-\beta\Delta G_{CA}} \Delta G_{CA} y_C (\lambda_C - \lambda_A) + e^{-\beta\Delta G_{CB}} \Delta G_{CB} y_C (\lambda_C - \lambda_B) \end{aligned} \tag{5.18}$$

Solution with self consistent cycle

In the case of a three state system no analytical solution exists, as the control equation cannot be transformed into a explicit form where the control β depends only on the state $\vec{y}$ and costate $\vec{\lambda}$. The only way to solve it is numerically. We can use the numerical techniques we already used in the previous two examples, which are described in Chapter 3.2. Here we will try to solve it with the self consistent cycle approach from Chapter 4.1.1.

In Figure 5.10 the first step of this self consistent cycle algorithm is illustrated. One can see that there are two root trajectories $\beta_0(t)$ for the three state system for an constant initial inverse temperature guess $\beta_{init}(t) = 6.0\,\mathrm{eV}^{-1}$. We use the positive root trajectory and update the inverse temperature curve via equally weighted linear mixing

$$\beta^{i+1}(t) = (1 - w)\ \beta^{i-1}(t) + w\ \beta^{i}(t) \tag{5.19}$$

For the first step $i = 1$ we set $\beta^0 = \beta_{init}(t)$ to the initial guess and $\beta^1 = \beta_0(t)$ to the first found positive root trajectory. In this example the weight w for the linear mixture is set to $w = \frac{1}{2}$. To converge faster one can increase the weight w on the newly found root trajectory β^i. If the weight is too big the updated curves β^{i+1} start to alternate around the real optimal solution with every iteration i.

One also need to be very careful with the initial guess for the inverse temperature $\beta_{init}(t)$. It can happen that a root trajectory is only defined in a part of the time frame $t \in [0, t_f]$,

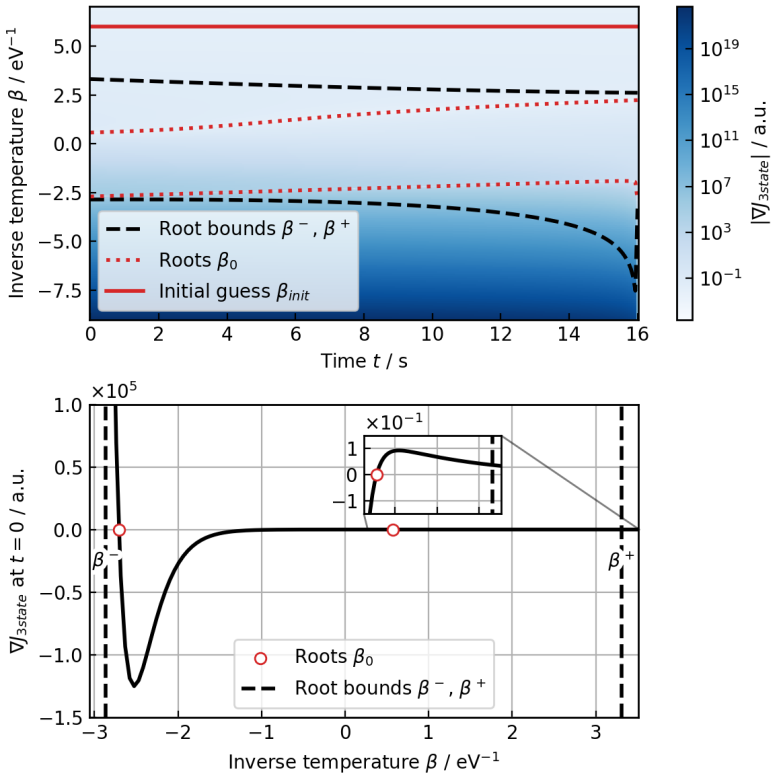

Figure 5.10.: First step of the self consistent cycle algorithm. Between the black dashed lines two root trajectories $\beta_0(t)$ are found (red dotted lines). We choose one of them to update our guess. The second figure is a cross section of the upper plot at time zero.

like in Figure 5.11. Finding a good initial guess is kind of a trial and error task. In the case illustrated in Figure 5.11 we can adjust our initial guess to be closer to the region of the incomplete root trajectory and restart the self consistent algorithm and hope that the upper root trajectory is now complete over the whole time frame.

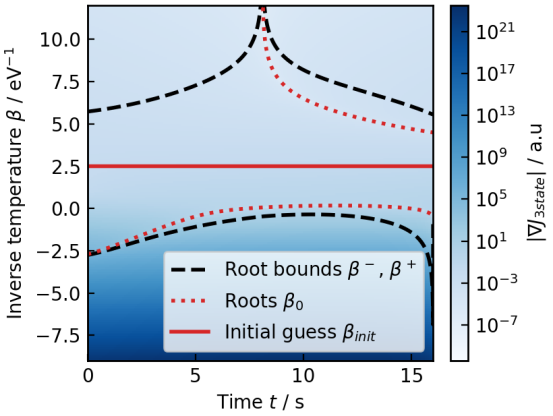

Figure 5.11.: First step of the self consistent cycle algorithm with a suboptimal initial guess, $\beta_{init}(t) = 2.0\,\mathrm{eV}^{-1}$. The upper root trajectory starts in the middle of the time range and cannot be used for updating the inital inverse temperature β_{init}.

If we found a proper initial guess for the inverse temperature the self consistent cycle algorithm converges quite fast (see Figure 5.12) and it gives us the optimal state $\vec{y}^*(t)$, optimal costate $\vec{\lambda}^*(t)$ and the optimal inverse temperature $\beta^*(t)$, all plotted in Figure 5.13.

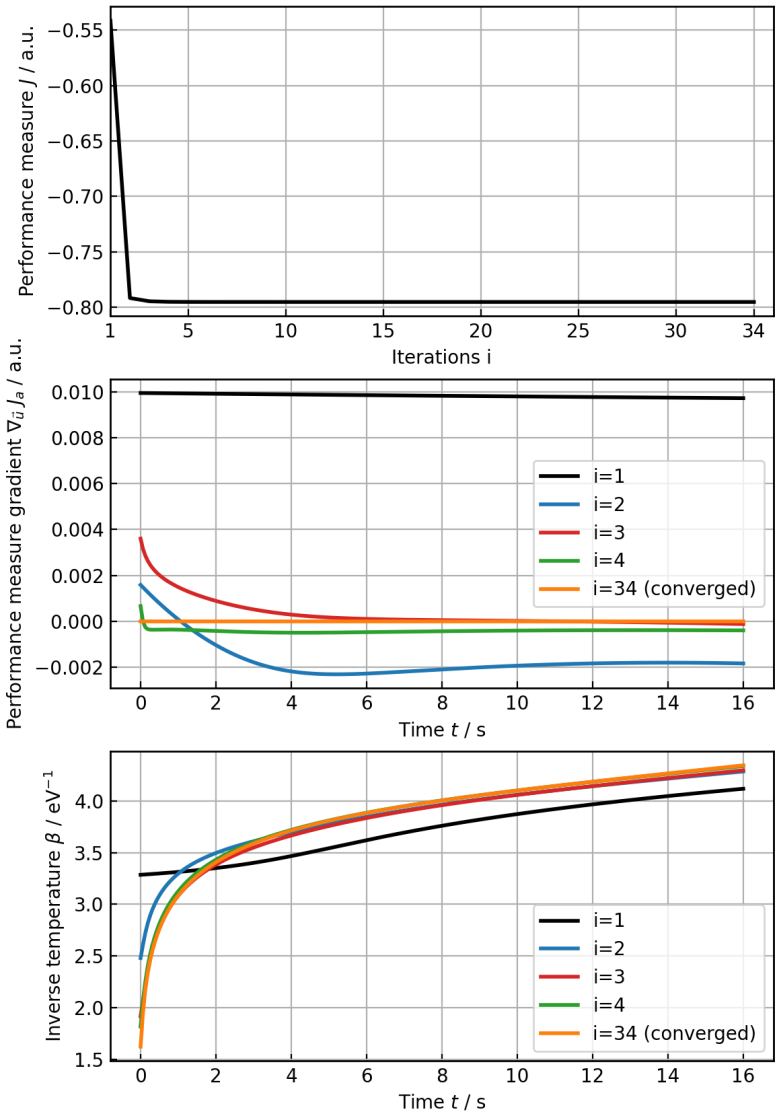

Figure 5.12.: Convergence of the self consistent cycle algorithm. The performance measure in the first plot improves in the first step already quite a lot. It took the algorithm 34 iterations to reach the convergence criteria that $|\nabla_{\vec{u}} J_a| < 10^{-9}$. In the second plot one can see how the performance measure gradient gets closer and closer to zero. In the third plot the inverse temperature curves for a few iterations i are shown.

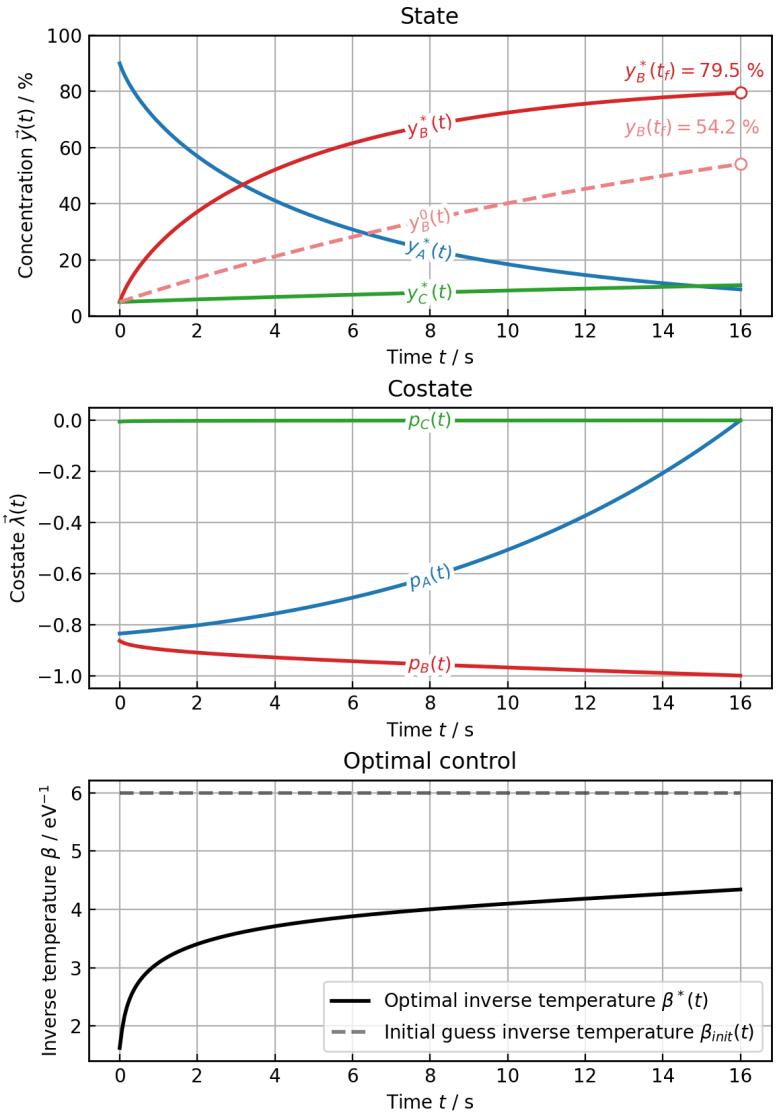

Figure 5.13.: Optimal curves for the three state system. In the fist plot the dashed line shows the target polymorph concentration over time for the initial inverse temperature guess. Compared to the initial guess the concentration of the target polymorph $y_B(t_f)$ increased from $y_B(t_f) = 54.2\,\%$ to $79.5\,\%$. The second plot shows the costates $\vec{\lambda}$. In the last plot the optimal inverse temperature curve $\beta^*(t)$ and the initial guess $\beta_{init}(t)$ is shown.

Varying the barrier heights $A \rightarrow B$ and $B \rightarrow C$

Now we want to investigate how varying barrier heights of the system influence the maximal possible concentration of our target polymorph B. For that, we first vary the barrier height ΔG_{AB} between 0.3 eV and 1.8 eV. The barrier ΔG_{BC} is varied between 1.2 eV and 3.3 eV (see Figure 5.14).

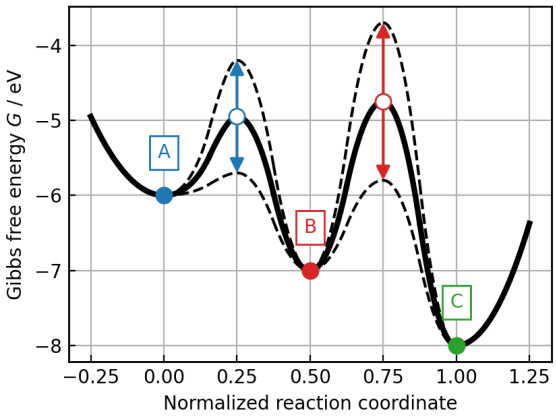

Figure 5.14.: Gibbs free energy landscape of the model system with barrier variation. ΔG_{AB} is varied between (0.3 to 1.8) eV and ΔG_{BC} between (1.2 to 3.3) eV. The barrier between polymorph A and C is not drawn, as it remains unchanged with $\Delta G_{AC} = 5.0$ eV

In Figure 5.15 one can see the influence of different barrier height combinations on the optimized target polymorph concentration. One interesting aspect is, the closer we get to the region where the two barriers are equally high the lower is the optimized concentration. In the region where the barrier ΔG_{BC} is lower than the barrier ΔG_{AB} we were not able to converge the self consistent cycle. It is not surprising that this region is difficult to control since we first need to overcome the higher barrier $A \rightarrow B$ and then stabilize polymorph B which is quite unstable because of the low $B \rightarrow C$ barrier. The highest concentration yield is found for a low $A \rightarrow B$ barrier and a high $B \rightarrow C$ barrier. Here we can reach polymorph B concentrations of 90 % and beyond.

In Figure 5.16 we show how the average of the optimal inverse temperature curve changes for different barrier combinations. We can clearly see that for higher barriers we need higher temperatures (lower inverse temperature) to find an optimal result.

Varying the barrier height $A \rightarrow C$

To also see the effect of different barrier heights for the transition $A \rightarrow C$ we vary it between 0.7 eV - 5.0 eV and keep all the other barriers constant at $\Delta G_{AB} = 0.7$ eV and $\Delta G_{BC} = 2.5$ eV. In Figure 5.17 all the used barriers are shown.

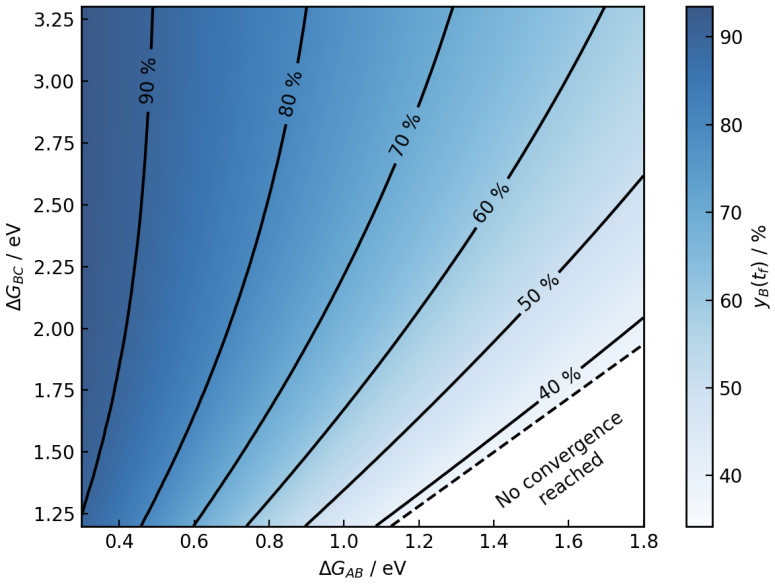

Figure 5.15.: Optimized target polymorph concentration $y_B(t_f)$ for different Gibbs free energy barriers. Here we used a 40×40 equidistant grid for the different barrier combinations and linearly interpolated on it. The convergence criteria was $|\nabla_{\vec{u}} J_a| < 10^{-9}$.

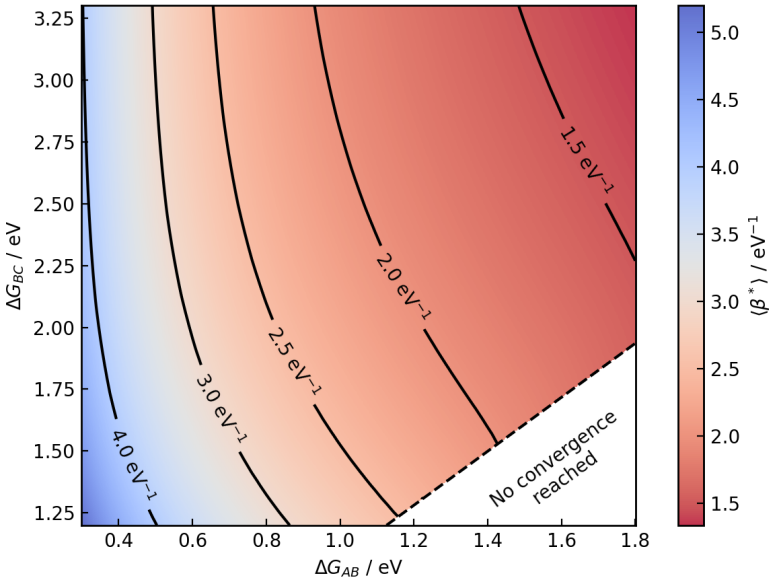

Figure 5.16.: Average of optimal inverse temperature curve $\langle \beta^* \rangle$ for different barrier height combinations. Increasing barrier heights decreases the optimal inverse temperature, meaning higher temperatures are required to find optimal results for higher barriers.

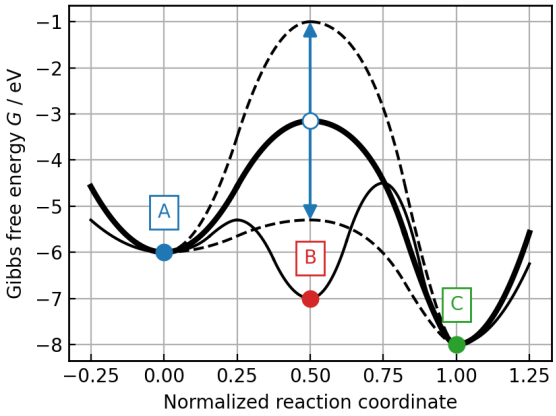

Figure 5.17.: Gibbs free energy landscape of the model system for variation of the barrier between polymorph A and C. The other barriers are held constant at $\Delta G_{AB} = 0.7\,\mathrm{eV}$ and $\Delta G_{BC} = 2.5\,\mathrm{eV}$.

In Figure 5.18 the effect of different barrier heights on the maximized concentration on the target polymorph B is plotted. As expected, the lower the barrier between polymorph A and C the lower the achieved optimal concentration is. With decreasing barrier height we loose more and more concentration via the $A \to C$ transition and we get less concentration into our target polymorph B. As soon as the barrier height ΔG_{AC} gets close to ΔG_{AB} we were not able to converge the optimization algorithm anymore. If the barrier $A \to C$ is lower than $A \to B$ almost all concentration flows from polymorph A directly to C and convergence for our target polymorph B can not be reached within the applied convergence criteria.

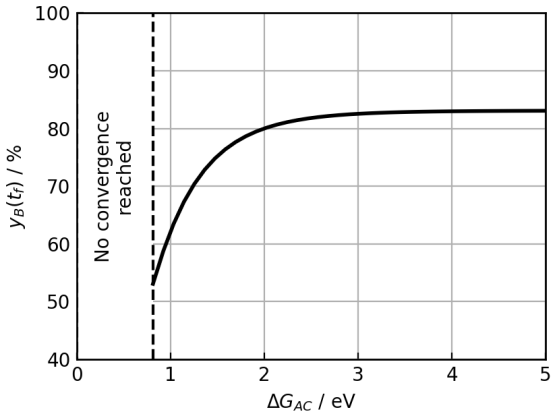

Figure 5.18.: Optimized target polymorph concentration $y_B(t_f)$ for different barriers ΔG_{AC} between 0.7 eV and 5.0 eV. The convergence criteria was again $|\nabla_{\vec{u}} J_a| < 10^{-9}$.

5.4. Three-polymorph system - "Elevator polymorph" problem

Another interesting example for a three polymorph transition system is what we call an "elevator polymorph" system. Think of the situation where we have a polymorph A which is always lower in Gibbs free energy through out the whole accessible temperature range than another polymorph B (see Figure 5.20). If our goal would be to maximize the concentration in polymorph B we will have difficulties to do so because in this situation the transition rate from A to B will always be lower than the backward transition B to A. Meaning we will never observe a higher concentration in B than in A. The only possibility to maximize the concentration in B would be to increase the temperature towards infinity because then we would occupy all the polymorphs uniformly which would be for two polymorphs 50 %(see Section 2.2).
To actually maximize the concentration in polymorph B without any diverging temperatures we need a third polymorph E (*elevator polymorph*) in the system. The idea is to use this elevator polymorph E to connect polymorph A and B and use it as a bridge to let the concentration flow through the elevator polymorph E to the target polymorph B. In Figure 5.19 the graph representation of the system is shown.

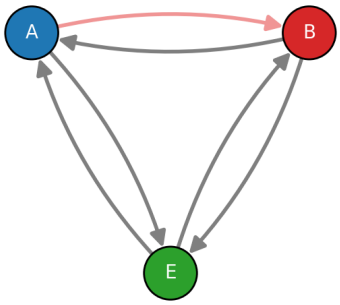

Figure 5.19.: Graph representation of the elevator system. The red arrow is a non accessible transition. That means that the transition rate in this direction is never larger than the rate of the reverse direction. Polymorph A can not reach polymorph B directly but has to go via the elevator polymorph E to the target polymorph B.

To use the elevator polymorph E as a mediator for transforming the system from polymorph A to B, we need a temperature region where we can populate E starting from A ("loading the elevator") and a region where we unpopulate E to B ("unloading the elevator"). In Figure 5.20 an example which fulfills this requirements is drawn. The corresponding Gibbs free energy curves are plotted for the three polymorphs A, B and E and additionally the corresponding transition states as well. In the high temperature region the elevator polymorph E is the lowest in Gibbs free energy. This region can be used for "loading" the elevator polymorph. At low temperature polymorph E is highest

in Gibbs free energy and it can transform to polymorph B and A, this is the region where we can "unload" the elevator.
In Section 1.3 we derived how to calculate these Gibbs free energy curves. They are linear equations of the form

$$G_{ads}(T,p) = E_{ads} - \mu_{gas}(T,p)N = E_{ads} - \mu_{gas}(T,p)\theta A_{unit} \tag{5.20}$$

where we have the adsorption energy E_{ads}, the number of adsorbed molecules N in the unit cell area A_{unit} and the coverage θ. Notice that the coverage θ determines the slope of the Gibbs free energy with changing chemical potential μ. This leads to the important fact that more densely packed structures are preferred at higher chemical potentials (low temperatures, high pressures).
To get to the situation that polymorph A has always a lower Gibbs free energy than polymorph B they need to have the same coverage θ. Then the Gibbs free energy curves for A and B are parallel, like in Figure 5.20. For the elevator polymorph E we need the possibility that the net concentration flow can change its direction. This means we need to be able to populate the elevator polymorph at some temperature and unpopulate it at an different temperature. This can be achieved if the Gibbs free energy curve of the elevator polymorph E intersect the Gibbs free energy curves of A and B. Meaning the coverage θ (slope of the Gibbs free energy curve) of the elevator polymorph needs to be different compared to the coverages of A and B.
Here the elevator polymorph is chosen to be lower in coverage than the other two polymorphs because then the system is easier to control. The reason for that is the phase space range where we try to populate our target polymorph B is located at low temperatures which means all rates are generally low and easier to control compared to the high temperature range. Occupying the elevator polymorphs happens at a high temperature but here we do not really need to control a lot since the elevator polymorph is anyway the lowest in Gibbs free energy in this region and will be populated very easily since it is the thermodynamically most favorable.
We now try to find the optimal temperature curve to maximize the concentration of polymorph B. We use the BFGS algorithm from Chapter 3.3.2 to solve the optimal control problem. The numerical values used for calculating the Gibbs free energy curves for the polymorphs and the transition states (‡) in Figure 5.20 are listed Table 5.1
With these values we can calculate the effective Gibbs free energy barriers and therefore also the transition rates at a certain temperature. The transition rates are also plotted in Figure 5.20.
The optimal result is plotted in Figure 5.21. You can see that we started with an sinusoidal initial guess for the temperature curve. Since we expected we need to go to higher temperatures first and then change to lower temperatures at a later time a sine function is a good rough guess how the curve will look like in the optimal case. We could have also started with a constant temperature curve guess as we did in the previous examples but it turns out that it takes quite a long time in this case to converge.
It is nicely illustrated in Figure 5.21 how the temperature needs to change in a time frame of one hour (3600 s) for an optimal result. The temperature first increases to

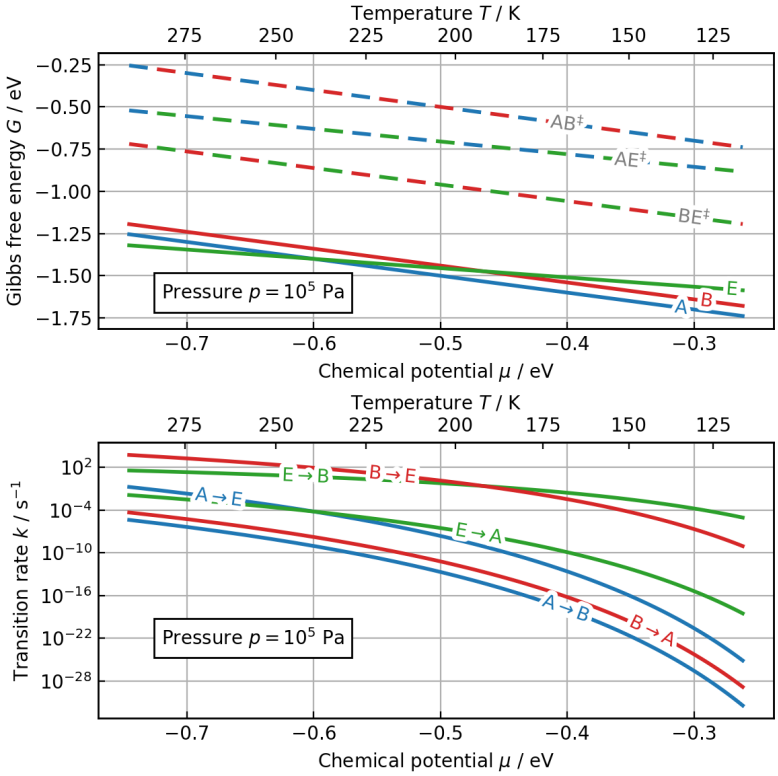

Figure 5.20.: Gibbs energies and transition rates of the elevator polymorph system. The two polymorphs A and B have the same coverage and the so called elevator polymorph E is slightly less densely packed. The Gibbs free energy of the elevator polymorph E intersects the Gibbs curves of A and B. We keep the pressure of the system constant at around atmospheric pressure 1×10^5 Pa and for the chemical potential we use the one of tetracyanoethylene (TCNE), the attempt frequency is fixed for all transitions at $f_a = 1 \times 10^{12}\,\mathrm{s}^{-1}$.

Table 5.1.: Numerical values for the Gibbs free energy and coverages

	Adsorption energies / eV		Coverage / molecules nm^{-2}
E_{ads}^{A}	-2.00	θ^{A}	1.00
E_{ads}^{B}	-1.94	θ^{B}	1.00
E_{ads}^{E}	-1.73	θ^{E}	0.55
$E_{ads}^{AB^{\ddagger}}$	-1.00	$\theta^{AB^{\ddagger}}$	1.00
$E_{ads}^{AE^{\ddagger}}$	-1.08	$\theta^{AE^{\ddagger}}$	0.75
$E_{ads}^{BE^{\ddagger}}$	-1.45	$\theta^{BE^{\ddagger}}$	0.98

populate the elevator polymorph (load the elevator). At around $t = 1200\,\mathrm{s}$ (20 min) we can identify the "elevating" phase, meaning the temperature changes quickly to the region where we are going to "unload" the elevator polymorph. This elevating phase needs to be very short, as otherwise we would loose the concentration in E to the thermodynamically more favorable polymorph A again. In the third plot of Figure 5.21 the rate of temperature change is plotted. There is a peak at the elevating phase ($t = 1200\,\mathrm{s}$) with a change rate of $v_{max} = -1.3\,\mathrm{K\,s^{-1}}$. After the elevating phase we stay at low temperatures to populate our target polymorph B. In this example we achieved a concentration for our target polymorph B of almost 90 %.

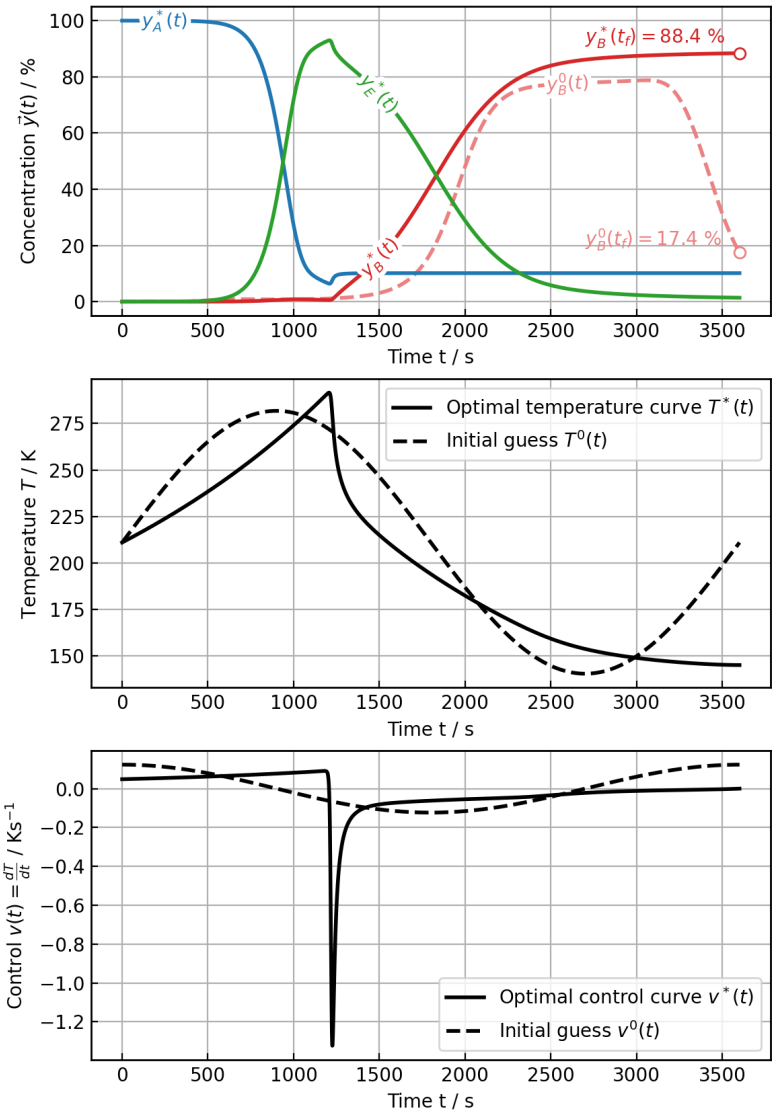

Figure 5.21.: Optimal curves for the elevator polymorph system. Here we can see very nicely how the temperature needs to increase to populate the elevator polymorph and then decrease again to unload to the target polymorph B. For this system we can get close to 90 % for the concentration of polymorph B. Compared to the initial sinusoidal temperature guess (dashed lines) this is an increase of 71 % in concentration. The BFGS algorithm needed 27 iterations to converge. The smoothing factor for the first derivative of the temperature curve is set to $\gamma = 0.05$.

6. Conclusions and Outlook

This thesis deals with the investigation of the possibility to control the interface polymorphism of organic-inorganic interfaces with temperature. This is realized by finding optimal time-dependent growth conditions, here specifically temperature protocols, which maximize the concentration of a target polymorph.

Kinetics of a polymorph transition system

The kinetics of a polymorph system is described as graph network, where each node represents a relevant polymorph of the system and each edge of the graph corresponds to a transition rate from one polymorph to another (see Chapter 2). The transition rates between two polymorphs are approximated using the Arrhenius equation. By applying a simple balance equation on this graph network using these transition rates a first order differential equation (state equation) is obtained, which describes the concentration dynamics of the polymorph system.

Optimizing the concentration of a specific polymorph

To optimize one specific polymorph in concentration, the temperature can be used to modify the transition rates between polymorphs in such a way that one specific polymorph is maximized in concentration. This optimal temperature curve is determined within the framework of Optimal Control theory (see Chapter 3). A main focus is laid on diverse technical pitfalls that occur in Optimal Control theory for this specific application and their solutions. One problem are fast changing optimal temperature curves which tends to not converge very easily. For these problems a constrained version of Optimal Control theory is used, a detailed description can be found in Section 4.2.

Results

Finally, to demonstrate how the developed framework can be utilized to obtain optimal temperature curves, four different problem scenarios are presented in Chapter 5. The first two examples (Section 5.1 and 5.2) are the simplest possible ones, namely a two polymorph system. They are used to demonstrate how an Optimal Control problem in principle works and how a solution would look like. In the third example (Section 5.3) a three polymorph system with temperature independent energy barriers is investigated. In this example the influence of different barrier heights on the optimized target polymorph concentration is shown.
The last example (Section 5.4) offers a strategy for growing and stabilizing metastable polymorphs. In this scenario two polymorphs are intrinsically not accessible from one

to another but can be connected via a third polymorph ("elevator polymorph"). In this example temperature dependent barriers are used which makes the system even more complex.

Outlook

In the present work only one possible control parameter, the time dependent growth temperature, is optimized. As next step it would be sensible to include the pressure p as a second control parameter. The current mathematical framework is already ready to tackle such a two-parameter problem. Anyhow, it seems like that reaching convergence becomes very complex in that case. This is a problem that would be essential to tackle. Furthermore, the demonstrated examples are still very small in system size. It would be interesting to increase the number of polymorphs in the system and go towards more complex systems of a realistic application. This would then allow to test this theoretical framework against experimental results, which finally could open doors to optimized design of technical applications in the field of organic electronics.

Bibliography

[1] J. B. B. Wang and G. W. W. Yang. "Phase transformation between diamond and graphite in preparation of diamonds by pulsed-laser induced liquid-solid interface reaction". In: *J. Phys.: Condens. Matter* 11 (1999), pp. 7089–7094.

[2] N. Koch. "Organic Electronic Devices and Their Functional Interfaces". In: *ChemPhysChem* 8 (10 July 2007), pp. 1438–1455. ISSN: 14394235. DOI: 10.1002/cphc.200700177.

[3] H. Ishii et al. "Energy Level Alignment and Interfacial Electronic Structures at Organic/Metal and Organic/Organic Interfaces". In: *Advanced Materials* 11 (8 June 1999), pp. 605–625. ISSN: 0935-9648. DOI: 10.1002/(SICI)1521-4095(199906)11:8<605::AID-ADMA605>3.0.CO;2-Q.

[4] A. O. F. Jones et al. "Substrate-Induced and Thin-Film Phases: Polymorphism of Organic Materials on Surfaces". In: *Advanced Functional Materials* 26.14 (2016), pp. 2233–2255. DOI: https://doi.org/10.1002/adfm.201503169.

[5] A. Jeindl, L. Hörmann, and O. T. Hofmann. "How much does surface polymorphism influence the work function of organic/metal interfaces?" In: *Applied Surface Science* 575 (Feb. 2022), p. 151687. ISSN: 0169-4332. DOI: 10.1016/J.APSUSC.2021.151687.

[6] A. T. Egger et al. "Charge Transfer into Organic Thin Films: A Deeper Insight through Machine-Learning-Assisted Structure Search". In: *Advanced Science* 7 (15 Aug. 2020), p. 2000992. ISSN: 2198-3844. DOI: 10.1002/advs.202000992.

[7] J Rogal and K Reuter. "Ab Initio Atomistic Thermodynamics for Surfaces: A Primer". In: (2007).

[8] K. Reuter and M. Scheffler. "Composition, structure, and stability of RuO2(110) as a function of oxygen pressure". In: *Physical Review B - Condensed Matter and Materials Physics* 65 (3 Dec. 2002), pp. 1–11. ISSN: 1550235X. DOI: 10.1103/PhysRevB.65.035406.

[9] D. A. McQuarrie. *Statistical Mechanics*. Chemistry Series. Harper & Row, 1975. ISBN: 9780060443665.

[10] H. Eyring. "The Activated Complex in Chemical Reactions". In: *The Journal of Chemical Physics* 3.2 (1935), pp. 107–115. DOI: 10.1063/1.1749604.

[11] G. H. Vineyard. "Frequency factors and isotope effects in solid state rate processes". In: *Journal of Physics and Chemistry of Solids* 3 (1-2 Jan. 1957), pp. 121–127. ISSN: 00223697. DOI: 10.1016/0022-3697(57)90059-8.

[12] L. T. Kong and L. J. Lewis. "Transition state theory of the preexponential factors for self-diffusion on Cu, Ag, and Ni surfaces". In: *Physical Review B - Condensed Matter and Materials Physics* 74 (7 Aug. 2006), p. 073412. ISSN: 10980121. DOI: 10.1103/PHYSREVB.74.073412/FIGURES/1/MEDIUM.

[13] M. J. Hoffmann, S. Matera, and K. Reuter. "kmos: A lattice kinetic Monte Carlo framework". In: *Computer Physics Communications* 185 (7 July 2014), pp. 2138–2150. ISSN: 00104655. DOI: 10.1016/j.cpc.2014.04.003.

[14] M. Andersen, C. Panosetti, and K. Reuter. "A Practical Guide to Surface Kinetic Monte Carlo Simulations". In: *Frontiers in Chemistry* 7 (2019). ISSN: 2296-2646. DOI: 10.3389/fchem.2019.00202.

[15] A. Chatterjee and D. Vlachos. "An overview of spatial microscopic and accelerated kinetic Monte Carlo methods". In: *J. Comput-Aided Mater.* 14 (Jan. 2007), pp. 253–308. DOI: 10.1007/s10820-006-9042-9.

[16] A. Werkovits et al. "Toward Targeted Kinetic Trapping of Organic–Inorganic Interfaces: A Computational Case Study". In: *ACS Physical Chemistry Au* 2 (1 Jan. 2022), pp. 38–46. ISSN: 2694-2445. DOI: 10.1021/acsphyschemau.1c00015.

[17] S. Iyengar and R. Jain. *Numerical Methods*. New Age International (P) Limited, 2009. ISBN: 9788122426106.

[18] D. Kirk. *Optimal Control Theory: An Introduction*. Dover Books on Electrical Engineering Series. Dover Publications, 2004. ISBN: 9780486434841.

[19] I. Gelfand, S. Fomin, and R. Silverman. *Calculus of Variations*. Dover Books on Mathematics. Dover Publications, 2000. ISBN: 9780486414485.

[20] A. Trubiano and M. F. Hagan. "Optimization of non-equilibrium self-assembly protocols using Markov state models". In: *J. Chem. Phys* 157 (2022), p. 244901. DOI: 10.1063/5.0130407.

[21] L. Komzsik. *Applied Calculus of Variations for Engineers*. Taylor & Francis, 2008. ISBN: 9781420086621.

[22] J. Nocedal and S. Wright. *Numerical Optimization*. Springer Series in Operations Research and Financial Engineering. Springer New York, 2006. ISBN: 9780387400655.

[23] C. G. Broyden. "The Convergence of a Class of Double-rank Minimization Algorithms 1. General Considerations". In: *IMA Journal of Applied Mathematics* 6 (1 Mar. 1970), pp. 76–90. ISSN: 0272-4960. DOI: 10.1093/IMAMAT/6.1.76.

[24] R. Fletcher. "A new approach to variable metric algorithms". In: *The Computer Journal* 13 (3 Jan. 1970), pp. 317–322. ISSN: 0010-4620. DOI: 10.1093/COMJNL/13.3.317.

[25] D. Goldfarb. "A family of variable-metric methods derived by variational means". In: *Mathematics of Computation* 24 (109 1970), pp. 23–26. ISSN: 0025-5718. DOI: 10.1090/S0025-5718-1970-0258249-6.

[26] D. F. Shanno. "Conditioning of quasi-Newton methods for function minimization". In: *Mathematics of Computation* 24 (111 1970), pp. 647–656. ISSN: 0025-5718. DOI: 10.1090/S0025-5718-1970-0274029-X.

[27] P. Wolfe. "Convergence Conditions for Ascent Methods". In: *SIAM Review* 11.2 (1969), pp. 226–235. DOI: 10.1137/1011036.

[28] P. Wolfe. "Convergence Conditions for Ascent Methods. II: Some Corrections". In: *SIAM Review* 13.2 (1971), pp. 185–188. DOI: 10.1137/1013035.

[29] R. Descartes. *The Geometry of René Descartes: with a Facsimile of the First Edition*. Dover Books on Mathematics. Dover Publications, 2012. ISBN: 9780486158174.

[30] G. J. O. Jameson. "Counting Zeros of Generalised Polynomials: Descartes' Rule of Signs and Laguerre's Extensions". In: *The Mathematical Gazette* 90.518 (2006), pp. 223–234. ISSN: 00255572.

[31] J. Lagrange and L. Poinsot. *Traité de la résolution des équations numériques de tous les degrés: avec des notes sur plusieurs points de la théorie des équations algébriques*. Bachelier, 1826.

A. Appendix

A.1. Chemical potential of tetracyanoethylene TCNE

For our elevator polymorph example we used the gas phase chemical potential of the tetracyanoethylene (TCNE) molecule (see Figure A.1).

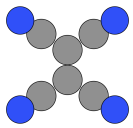

Figure A.1.: Tetracyanoethylene (TCNE) molecule geometry. The blue circles are the Nitrogen atoms, Carbon atoms are the gray circles.

In Chapter 1.3.1 we derived how to approximate the chemical potential of a molecular gas by neglecting all vibrational contributions.

$$\mu_{gas} \approx E_{gas}^{tot} - k_B T \ln\left(\left(\frac{2\pi m}{h^2}\right)^{\frac{3}{2}} \frac{(k_B T)^{\frac{5}{2}}}{p} \frac{\sqrt{\pi \prod_{i=1}^{3} I_i}}{\sigma} \left(\frac{8\pi^2 k_B T}{h^2}\right)^{\frac{3}{2}} J\right) \tag{A.1}$$

The parameters for TCNE are

$m = 2.127 \times 10^{-25}\,\mathrm{kg}$ ... total mass of TCNE molecule

$\sigma = 4$ ... symmetry factor

$J = 1$ ... electronic ground state degeneracy

$I_1 = 5.669 \times 10^{-45}\,\mathrm{kg\,m^2}$

$I_2 = 5.766 \times 10^{-45}\,\mathrm{kg\,m^2}$ ... moments of inertia

$I_3 = 1.144 \times 10^{-44}\,\mathrm{kg\,m^2}$

Here we set the total internal energy E_{gas}^{tot} to zero since we are here only interested in the temperature and pressure behavior of the chemical potential of an ideal molecular gas. The total internal energy would only introduce a constant shift of the chemical potential. In Figure A.2 we can see the chemical potential for different temperatures T and pressure p. One can see that the chemical potential at high temperatures and low pressures is low which means it becomes more favorable for the molecule to be in gas phase with increasing temperature or decreasing pressure.

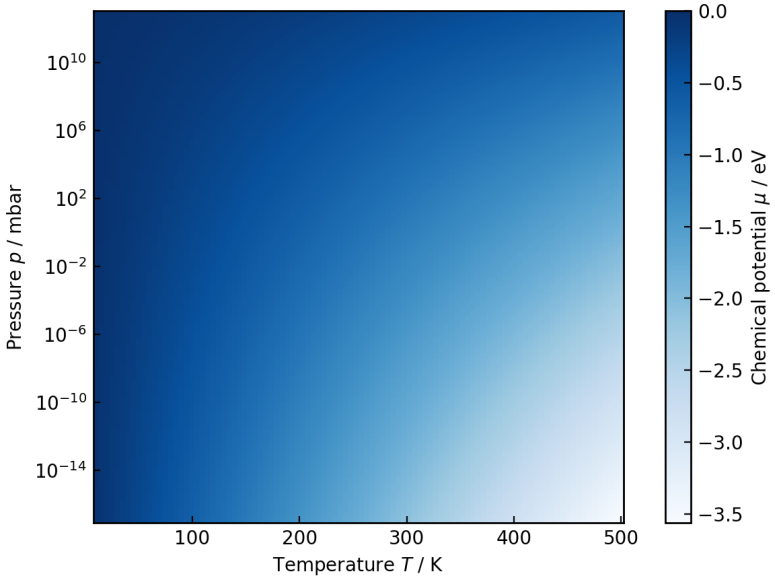

Figure A.2.: Chemical potential of TCNE in the ideal gas approximation without vibrational contributions.

A.2. BFGS update formula

Here we derive the expression 3.54 for updating the inverse Hessian B^{-1} for the BFGS algorithm. To simplify the notation we set $H = B^{-1}$. We need to find a solution to the following equations then

$$\min_{H_{k+1}} \|H_{k+1} - H_k\|_F \tag{A.2}$$

$$H_{k+1}\vec{y}_k = \vec{s}_k \tag{A.3}$$

$$H_{k+1} = (H_{k+1})^T \tag{A.4}$$

Depending on which matrix norm we use another expression for H_{k+1} is found. We actually use a weighted Frobenius norm to find a closed form for the solution. The weighted Frobenius norm looks like this

$$\|A\|_W = \|\underbrace{W^{\frac{1}{2}} A W^{\frac{1}{2}}}_{\hat{A}=\{\hat{a}_{ij}\}}\|_F = \sum_i \sum_j |\hat{a}_{ij}|^2 \tag{A.5}$$

where W is a symmetric matrix which fulfills $W\vec{s_k} = \vec{y_k}$
With this we find

$$\min_{H_{k+1}} \|\underbrace{W^{\frac{1}{2}} H_{k+1} W^{\frac{1}{2}}}_{\hat{H}} - \underbrace{W^{\frac{1}{2}} H_k W^{\frac{1}{2}}}_{\hat{H}_k}\|_F \tag{A.6}$$

Now we do an variable transformation

$$\underbrace{W^{-\frac{1}{2}} W \vec{s_k}}_{\hat{\vec{s}}_k = W^{\frac{1}{2}} \vec{s_k}} = \underbrace{W^{-\frac{1}{2}} \vec{y_k}}_{\hat{\vec{y}}_k} \Rightarrow \hat{\vec{s}}_k = \hat{\vec{y}}_k \tag{A.7}$$

$$\underbrace{W^{\frac{1}{2}} H_{k+1} W^{\frac{1}{2}}}_{\hat{H}} \underbrace{W^{-\frac{1}{2}} \vec{y}_k}_{\hat{\vec{y}}_k} = \underbrace{W^{\frac{1}{2}} \vec{s}_k}_{\hat{\vec{s}}_k} \Rightarrow \hat{H}\hat{\vec{y}}_k = \hat{\vec{s}}_k \Leftrightarrow \hat{H}\hat{\vec{y}}_k = \hat{\vec{y}}_k \tag{A.8}$$

Further we define an orthonormal system of vectors

$$\{\vec{u}_1 = \frac{\hat{\vec{y}}_k}{\|\hat{\vec{y}}_k\|}, \underbrace{\vec{u}_2, \vec{u}_3, \vec{u}_4 ..., \vec{u_n}}_{\text{orthonormal vectors}} \} \tag{A.9}$$

The vector $\vec{u}_{i>1}$ can be any vector which is orthogonal to $\vec{u}_1$.
We combine this orthonormal column vectors $\vec{u}_i$ to a unitary matrix U with

$$\begin{aligned} U &= (\vec{u}_1, \underbrace{\vec{u}_2, ..., \vec{u}_n}_{u_\perp}) = (\vec{u}_1, u_\perp) \\ U^T &= \begin{pmatrix} \vec{u}_1^T \\ \vec{u}_2^T \\ \vdots \\ \vec{u}_n^T \end{pmatrix} = \begin{pmatrix} \vec{u}_1^T \\ u_\perp^T \end{pmatrix} \end{aligned} \tag{A.10}$$

where we defined the $n \times (n-1)$ matrix $u_\perp$.
The matrices U and U^T are unitary matrices which means that $UU^T = U^T U = I$. It can be shown that the Frobenius norm is idependent of a unitary transformation $\|U^T A U\|_F = \|A\|_F$.
First we need the trace representation of the Frobenius norm

$$\mathrm{tr}\big(A^T A\big) = \sum_i \sum_j a_{ij} a_{ij} = \sum_i \sum_j a_{ij}^2 = \|A\|_F^2 \tag{A.11}$$

Then we find

$$\|U^T A U\|_F^2 = \mathrm{tr}\big(U^T A^T U U^T A U\big) = \mathrm{tr}\big(U U^T A^T A\big) = \mathrm{tr}\big(A^T A\big) = \|A\|_F^2 \tag{A.12}$$

where we used the property of the trace, that we can permute the arguments cyclically. This allows us to solve for

$$\min_{H_{k+1}} \|U^T \hat{H} U - U^T \hat{H}_k U\|_F \tag{A.13}$$

First we evaluate the term $U^T \hat{H} U$

$$U^T \hat{H} U = \begin{pmatrix} \vec{u}_1^T \\ u_\perp^T \end{pmatrix} \hat{H} (\vec{u}_1, u_\perp) = \begin{pmatrix} \vec{u}_1^T \hat{H} \vec{u}_1 & \vec{u}_1^T \hat{H} u_\perp \\ u_\perp^T \hat{H} \vec{u}_1 & u_\perp^T \hat{H} u_\perp \end{pmatrix} = \begin{pmatrix} 1 & 0 \\ 0 & u_\perp^T \hat{H} u_\perp \end{pmatrix} \tag{A.14}$$

in the last step we used the fact that the orthonormal vector $\vec{u}_1$ satisfies the secant equation.
The second term reads then

$$U^T \hat{H}_k U = \begin{pmatrix} \vec{u}_1^T \\ u_\perp^T \end{pmatrix} \hat{H}_k(\vec{u}_1, u_\perp) = \begin{pmatrix} \vec{u}_1^T \hat{H}_k \vec{u}_1 & \vec{u}_1^T \hat{H}_k u_\perp \\ u_\perp^T \hat{H}_k \vec{u}_1 & u_\perp^T \hat{H}_k u_\perp \end{pmatrix} \tag{A.15}$$

In combination we find

$$\min_{H_{k+1}} \left\| \begin{pmatrix} 1 - \vec{u}_1^T \hat{H}_k \vec{u}_1 & \vec{u}_1^T \hat{H}_k u_\perp \\ u_\perp^T \hat{H}_k \vec{u}_1 & u_\perp^T \hat{H} u_\perp - u_\perp^T \hat{H}_k u_\perp \end{pmatrix} \right\|_F \tag{A.16}$$

If we look carefully we can see that only the block matrix in the lower right corner of this expression changes with H_{k+1} or $\hat{H}$. This means we need to minimize only this component. The best would be if this term vanishes to zero. This leads to

$$u_\perp^T \hat{H} u_\perp = u_\perp^T \hat{H}_k u_\perp \tag{A.17}$$

We can find that

$$u_\perp^T \hat{H} u_\perp = \underbrace{u_\perp U}_{(0,I)} \begin{pmatrix} 1 & 0 \\ 0 & u_\perp^T \hat{H}_k u_\perp \end{pmatrix} \underbrace{U^T u_\perp}_{\begin{pmatrix} 0 \\ I \end{pmatrix}} \tag{A.18}$$

and extract

$$\hat{H} = U \begin{pmatrix} 1 & 0 \\ 0 & u_\perp^T \hat{H}_k u_\perp \end{pmatrix} U^T = \vec{u}_1 \vec{u}_1^T + u_\perp u_\perp^T \hat{H}_k u_\perp u_\perp^T = \vec{u}_1 \vec{u}_1^T + (I - \vec{u}_1 \vec{u}_1) \hat{H}_k (I - \vec{u}_1 \vec{u}_1) \tag{A.19}$$

where we used $I = UU^T = \vec{u}_1 \vec{u}_1^T + u_\perp u_\perp^T$
We can now transform back all variables and find

$$\|\hat{\vec{y}}_k\|^2 = \hat{\vec{y}}_k^T \hat{\vec{y}}_k = \hat{\vec{y}}_k^T \hat{\vec{s}}_k = \vec{y}_k^T W^{-\frac{1}{2}} W^{\frac{1}{2}} \vec{s}_k = \vec{y}_k^T \vec{s}_k \tag{A.20}$$

$$\vec{u}_1 \vec{u}_1^T = \frac{1}{\vec{y}_k^T \vec{s}_k} \hat{\vec{y}}_k \hat{\vec{y}}_k^T = \frac{1}{\vec{y}_k^T \vec{s}_k} W^{\frac{1}{2}} \vec{s}_k \vec{y}_k^T W^{-\frac{1}{2}} = \frac{1}{\vec{y}_k^T \vec{s}_k} W^{-\frac{1}{2}} \vec{y}_k \vec{s}_k^T W^{\frac{1}{2}} = \frac{1}{\vec{y}_k^T \vec{s}_k} W^{\frac{1}{2}} \vec{s}_k \vec{s}_k^T W^{\frac{1}{2}} \tag{A.21}$$

Bringing all together gives us

$$\begin{aligned} H_{k+1} = W^{-\frac{1}{2}} \hat{H} W^{-\frac{1}{2}} &= \frac{1}{\vec{y}_k^T \vec{s}_k} W^{-\frac{1}{2}} W^{\frac{1}{2}} \vec{s}_k \vec{s}_k^T W^{\frac{1}{2}} W^{-\frac{1}{2}} + \\ &+ W^{-\frac{1}{2}} \left(I - \frac{1}{\vec{y}_k^T \vec{s}_k} W^{\frac{1}{2}} \vec{s}_k \vec{y}_k^T W^{-\frac{1}{2}} \right) W^{\frac{1}{2}} H_k W^{\frac{1}{2}} \left(I - \frac{1}{\vec{y}_k^T \vec{s}_k} W^{-\frac{1}{2}} \vec{y}_k \vec{s}_k^T W^{\frac{1}{2}} \right) W^{-\frac{1}{2}} \end{aligned} \tag{A.22}$$

All the weighting matrices W cancels out and we find the update expression for the approximated inverse Hessian

$$H_{k+1} = \frac{\vec{s}_k \vec{s}_k^T}{\vec{y}_k^T \vec{s}_k} + \left(I - \frac{\vec{s}_k \vec{y}_k^T}{\vec{y}_k^T \vec{s}_k}\right) H_k \left(I - \frac{\vec{y}_k \vec{s}_k^T}{\vec{y}_k^T \vec{s}_k}\right) \tag{A.23}$$

A.3. Two state example: Sufficient condition for a minimum

The found analytical solution of the two state system only satisfies the necessary conditions, which means it can be a minimum, maximum or a saddle point. To actually show which kind of extremum we found we need to find the second derivative of the performance measure $J_{2-state}$ with respect to the control β. If it is positive at the extremum. Then we found a minimum of $J_{2-state}$.

$$\begin{aligned}\frac{\partial^2}{\partial\beta^2} J_{2-state} = f_a \int_0^{t_f} \Bigg(& e^{-\beta\Delta G_{AB}} \left[2\frac{\partial y_A}{\partial\beta}\Delta G_{AB} - \Delta G_{AB}^2 y_A - \frac{\partial^2 y_A}{\partial\beta^2}\right] \\ & - e^{-\beta\Delta G_{BA}} \left[2\frac{\partial y_B}{\partial\beta}\Delta G_{BA} - \Delta G_{BA}^2 y_B - \frac{\partial^2 y_B}{\partial\beta^2}\right]\Bigg) \mathrm{d}t = \\ = & \int_0^{t_f} \frac{\partial^2 j_{2-state}}{\partial\beta^2}\, \mathrm{d}t\end{aligned} \tag{A.24}$$

First we need the derivatives of the states with respect to β but they can only be found if we have a solution to the state equation dependent on β. In the case of the two state equation we can find that

$$\begin{aligned} y_A(t) &= e^{I_1(t)}(y_{A0} + I_2(t)) \\ y_B(t) &= 1 - y_A(t) \end{aligned} \tag{A.25}$$

with

$$\begin{aligned} I_1(t) &= -\int_0^t \left(e^{-\beta(t')\Delta G_{AB}} + e^{-\beta(t')\Delta G_{BA}}\right) \mathrm{d}t' \\ I_2(t) &= \int_0^t e^{-\beta(t')\Delta G_{BA} - I_1(t')} \mathrm{d}t' \end{aligned} \tag{A.26}$$

is a solution to the state equation 5.2 with the initial condition $\vec{y}(0) = \vec{y}_0 = (y_{A0}, 1 - y_{A0})^T$.
With this closed form of the state $\vec{y}(t)$ we can easily calculate the necessary derivatives for our second derivative of the performance measure and find

$$
\begin{aligned}
\frac{\partial y_A}{\partial \beta} &= e^{I_1(t)} \left[\frac{\partial I_1(t)}{\partial \beta} (y_{A0} + I_2(t)) + \frac{\partial I_2(t)}{\partial \beta} \right] \\
\frac{\partial y_B}{\partial \beta} &= -\frac{\partial y_A}{\partial \beta} \\
\frac{\partial I_1}{\partial \beta} &= \int_0^t \left[\Delta G_{AB} e^{-\beta(t')\Delta G_{AB}} + \Delta G_{BA} e^{-\beta(t')\Delta G_{BA}} \right] \mathrm{d}t' \\
\frac{\partial I_2}{\partial \beta} &= -\int_0^t e^{-\beta(t')\Delta G_{BA} - I_1(t')} \left(\Delta G_{BA} + \frac{\partial I_1}{\partial \beta} \right) \mathrm{d}t' \\
\frac{\partial^2 y_A}{\partial \beta^2} &= e^{I_1(t)} \left[\left(\frac{\partial I_1}{\partial \beta} \frac{\partial I_1}{\partial \beta} + \frac{\partial^2 I_1}{\partial \beta^2} \right) (y_{A0} + I_2(t)) + 2 \frac{\partial I_1}{\partial \beta} \frac{\partial I_2}{\partial \beta} + \frac{\partial^2 I_2}{\partial \beta^2} \right] \\
\frac{\partial^2 y_B}{\partial \beta^2} &= -\frac{\partial^2 y_A}{\partial \beta^2} \\
\frac{\partial^2 I_1}{\partial \beta^2} &= -\int_0^t \left[\Delta G_{AB}^2 e^{-\beta(t')\Delta G_{AB}} + \Delta G_{BA}^2 e^{-\beta(t')\Delta G_{BA}} \right] \mathrm{d}t' \\
\frac{\partial^2 I_2}{\partial \beta^2} &= \int_0^t e^{-\beta(t')\Delta G_{BA} - I_1(t')} \left[\left(\Delta G_{BA} + \frac{\partial I_1}{\partial \beta} \right)^2 - \frac{\partial^2 I_1}{\partial \beta^2} \right] \mathrm{d}t'
\end{aligned}
\tag{A.27}
$$

If we evaluate the integral in Equation A.24 and can show that it is positive we found a minimum.

In Figure A.3 $\left| \frac{\partial^2 j_{2-state}}{\partial \beta^2} \right|$ and the integral over the whole time frame is shown for the two state example in Chapter 5.1. One can see that the second derivative is positive and therefor a minimum.

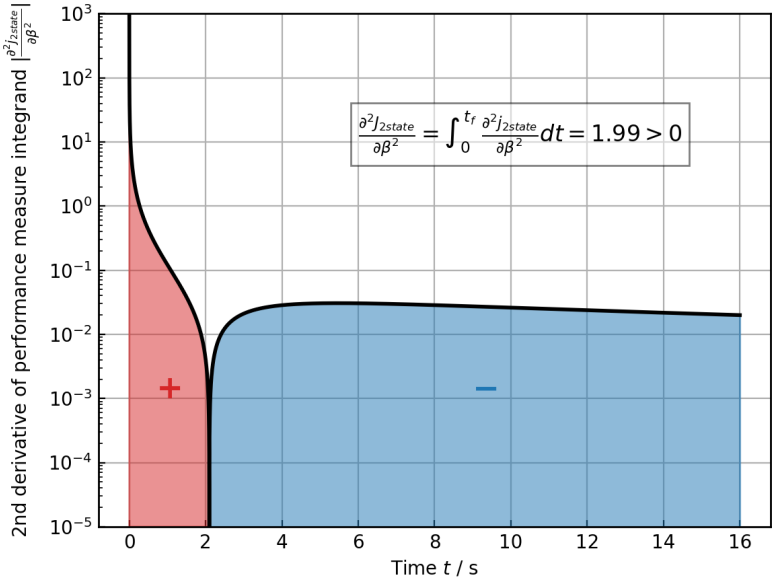

Figure A.3.: Second derivative of the performance measure integrand with respect to β. Here the absolute value of it is plotted. If we perform the integral we get a positive value which means we found a minimum of the performance measure $J_{2-state}$. The red area is bigger than the blue area. Those areas are distorted because of the logarithmic scaling of the y-axis.